Ministero dell'Istruzione, dell'Università e della Ricerca

UNIVERSITY OF SALERNO

Department of Civil Engineering

PhD Course in
Risk and Sustainability in Civil Engineering, Architecture, Environmental Engineering Systems

Cycle XXXII (2016-2019)

TRANSPORT MODELLING AND CONTAMINANT FATE IN UNSATURATED SOILS: ANALYSIS AND PERSPECTIVES

Maria Grazia Stoppiello

Supervisor
Prof. Leonardo Cascini
Prof. Giacomo Viccione

Co-supervisor
Prof. Giusy Lofrano
Dr. Giuseppe Maria Grimaldi

Coordinator
Prof. Fernando Fraternali

Index

Index of figures

Index of tables

Nomenclature list

A	Horizontal source area (m^2)
$A_{uz\text{-}gw}$	Exchange area between the unsaturated zone and the groundwater (m^2)
b	Empirical constant in in Langmuir formulation ($dm^3\ mg^{-1}$)
C	Specific capacity (m^{-1})
C_a	Soil gas concentration ($mg\ m^{-3}$)
C_{NAPL}	Concentration in non-aqueous phase ($mg\ kg^{-1}$)
Cr^g	Grid Courant number
C_s	Concentration of the chemical sorbed by the soil ($mg\ kg^{-1}$)
C_{tot}	Total source concentration ($mg\ kg^{-1}$)
$C_{tot,sat}$	Total source concentration equivalent to saturation conditions ($mg\ kg^{-1}$)
C_w	Dissolved concentration in pore water ($mg\ m^{-3}$)
C_{w0}	Initial dissolved concentration in pore water at the source ($mg\ m^{-3}$)
d	Characteristic length of the porous medium (m)
$\boldsymbol{D'}$	Dispersion tensor of Model II ($m^2\ s^{-1}$)
D'_x	Dispersion parameter of Model II in x-direction ($m^2\ s^{-1}$)
D'_y	Dispersion parameter of Model II in y-direction ($m^2\ s^{-1}$)
D'_z	Dispersion parameter of Model II in z-direction ($m^2\ s^{-1}$)
$\boldsymbol{D_a}$	Diffusion tensor in air ($m^2\ s^{-1}$)
D_a^0	Diffusion coefficient in air ($m^2\ s^{-1}$)
D_a^e	Pore diffusion coefficient in air ($m^2\ s^{-1}$)
$\boldsymbol{D_{diff}}$	Molecular diffusion tensor ($m^2\ s^{-1}$)
D_{eff}	Effective diffusion coefficient according Millington and Quirk relationship ($m^2\ s^{-1}$)
$D_{disp,z}$	Dispersion coefficient in z-direction ($m^2\ s^{-1}$)
$\boldsymbol{D_{sw}}$	Soil water diffusivity ($m^2\ s^{-1}$)
$\boldsymbol{D_w}$	Dispersion tensor in water ($m^2\ s^{-1}$)
D_w^0	Diffusion coefficient in water ($m^2\ s^{-1}$)
D_w^e	Pore diffusion coefficient in water ($m^2\ s^{-1}$)
D_z	Dispersion-diffusion coefficient in water in z-direction ($m^2\ s^{-1}$)
FDM	Finite Difference Method
FEM	Finite Element Method
f_{oc}	Organic carbon fraction
H	Dimensionless Henry's constant
h	Pressure head (m)
h_{cr}	Wetting front suction head (m)

H_w Ponding depth of water surface (m)
I_{eff} Effective infiltration (m s^{-1})
J Mass flux from unsaturated zone to groundwater (m s^{-1})
J_{adv} Advective mass flux (kg m^{-2} s^{-1})
J_{diff} Diffusive mass flux (kg m^{-2} s^{-1})
J_{disp} Dispersion mass flux (kg m^{-2} s^{-1})
$J_{disp\text{-}diff}$ Dispersion-Diffusive mass flux (kg m^{-2} s^{-1})
$\boldsymbol{K}$ Hydraulic conductivity tensor (m s^{-1})
K_d Soil sorbed-water partition coefficient (m^3 kg^{-1})
K_F Freundlich isotherm constant (mg g^{-1}) (dm^3 g^{-1})^n
K_{oc} Organic carbon-water partition coefficient (m^3 kg^{-1})
K_r Relative hydraulic conductivity (m s^{-1})
K_{sat} Saturated hydraulic conductivity (m s^{-1})
$\boldsymbol{K_{sat}}$ Saturated hydraulic conductivity tensor (m s^{-1})
K_{sw} Total soil-water partition coefficient (kg m^{-3})
L_1 Thickness of the contaminant source (m)
L_2 Distance between the top of the source and the water table (m)
L_d Diffusion path length (m)
LDF Leachate-groundwater dilution factor
L_f Distance between the bottom of the source and the water table (m)
LF Leachate factor
m van Genuchten parameter
M_a Contaminant mass in vapour phase (kg)
M_s Contaminant mass sorbed by the soil fraction (kg)
M_{sat} Total contaminant mass equivalent to saturation conditions (kg)
M_{tot} Total contaminant mass (kg)
M_w Contaminant mass in water phase (kg)
n van Genuchten parameter
n_F Adsorption intensity coefficient in Freundlich formulation
Pe^g Grid Peclet number
Q_0 Maximum monolayer coverage capacities in Langmuir formulation (mg g^{-1})
R Retardation coefficient
R' Retardation parameter of Model II
REV Representative Elementary Volume
S Solubility (kg m^{-3})
SAM Soil attenuation model
S_e Effective saturation
S_s Specific storage (m^{-1})
$\boldsymbol{T}$ Tortuosity tensor

t_0 Initial time (s)

t^* Time when the initial source concentration reaches the saturation conditions in Model IV (s)

t_{leach} Time required for the contaminant to reach the underlying water table in Model IV (s)

t_w Time required for infiltrating water to reach the water table in Model IV (s)

t Time (s)

$t_{1/2}$ Contaminant half-time (s)

v' Velocity parameter of Model II (m s^{-1})

v Seepage velocity (m s^{-1})

$\boldsymbol{v}$ Vector of pore-water flow velocity (m s^{-1})

X Length of the contaminant source (m)

x Horizontal spatial coordinate-1 (m)

Y Width of the contaminant source (m)

y Horizontal spatial coordinate-2 (m)

z Vertical spatial coordinate (m)

z_0 Thickness of slug in Model V (m)

z_m Distance from the source to the observation location (m)

α_{dep} Source depletion factor in Model IV

α_l Longitudinal dispersivity in the water phase (m)

α_{leach} Leaching factor in Model IV

α_t Transverse dispersivity in the water phase (m)

α_{vG} van Genuchten parameter (m^{-1})

λ First order degradation constant (s^{-1})

λ' Parameter of Model II (s^{-1})

ξ Tortuosity factor

μ_1 Depletion coefficient in Model III (s^{-1})

μ_2 Depletion coefficient in Model IV (s^{-1})

μ_3 Depletion coefficient in Model VI (s^{-1})

θ Porosity

θ_a Volumetric air content

θ_w Volumetric water content

θ_w^e Effective volumetric water content

θ_w^r Residual volumetric water content

θ_w^s Saturated volumetric water content

ρ_b Soil bulk density (kg m^{-3})

τ Dimensionless time

Ψ^w Total water potential (Pa)

Ψ_m^w	Matric potential (Pa)
Ψ_g^w	Gravitational potential (Pa)
Ψ_p^w	Pressure potential (Pa)
Ψ_o^w	Osmotic potential (Pa)
Ψ_{suct}^w	Soil suction expressed as potential (Pa)
∇	Gradient operator with respect to the spatial coordinates *x*, *y* and *z*

Sommario

Negli ultimi anni, la contaminazione delle acque sotterranee è diventata una problematica ambientale di estrema rilevanza a scala mondiale. Il rilascio improprio di sostanze chimiche da diverse sorgenti di contaminazione (discariche, serbatoi di stoccaggio, etc.) ha fortemente compromesso la qualità delle risorse idriche sotterranee. Molti dei processi di destino e diffusione dei contaminanti avvengono nella zona parzialmente satura, destando grande preoccupazione riguardo la protezione della falda acquifera. Per questo motivo, numerosi studi scientifici sui modelli per la simulazione del trasporto di contaminanti nella zona parzialmente satura sono stati sviluppati. L'applicazione di questi modelli a scala di sito presenta, però, diverse criticità relative ai processi coinvolti e alla caratterizzazione idrogeologica del sito contaminato.

La presente tesi vuole fornire un contributo su questo tema, identificando le caratteristiche e i limiti degli strumenti di modellazione esistenti e sviluppando una metodologia di modellazione finalizzata ad applicazioni ingegneristiche in siti contaminati.

Nello specifico, è stato svolto un confronto quantitativo di alcuni modelli analitici, al fine di identificarne caratteristiche e limiti ed evidenziare le differenze nei risultati di ciascuno di essi. Dal confronto è emersa una significativa variabilità dei risultati rispetto alla variazione dei parametri considerati. Inoltre, l'analisi dei modelli ha consentito di identificare tre gruppi, in base alle ipotesi sulla sorgente di contaminazione e sui meccanismi chimico-fisici che si verificano durante il trasporto. Ciascun gruppo è risultato applicabile ad uno specifico scenario di contaminazione.

Successivamente, è stata proposta una procedura di modellazione basata su una previsione a posteriori, che combina un modello di flusso in condizioni stazionarie con un modello di trasporto di massa. In particolare, gli obiettivi della procedura sono stati la riproduzione delle concentrazioni di contaminante misurate nella falda acquifera all'interno del sito e la costruzione di scenari di contaminazione capaci di fornire informazioni sulle possibili sorgenti di contaminazione primarie. La procedura è stata applicata ad un caso studio molto significativo: il sito contaminato di Taranto. La modellazione sviluppata ha permesso di riprodurre in maniera soddisfacente le concentrazioni di contaminanti misurate in sito e gli scenari di contaminazione ottenuti sono stati ritenuti plausibili e coerenti con la solubilità del contaminante analizzato.

Abstract

In recent years, the contamination of groundwater has become a growing threat at global scale. The improper release of chemicals from numerous and different sources (landfills, leaking storage tanks, etc.) in the subsurface has largely affected the quality of the groundwater resources. Many of the fate and transport processes take place into the unsaturated zone posing a great concern in terms of groundwater protection. Because of that, many scientific studies on models for simulating contaminant transport in the unsaturated zone have been carried out. Application of these models to field scale is a challenging task because of several findings related to the involved processes and the hydrogeological characterization of the site.

The present thesis seeks to contribute to this topic, identifying features and limitations of the existing tools and, thus, developing a modelling approach useful for engineering applications to contaminated sites.

In particular, a quantitative comparison of selected analytical models has been developed, in order to identify features and limitations and highlight the differences in the outcomes of the different models. The comparison highlights a significant variability of the results with respect to the variation of the considered parameters. The analysis of the models makes it possible to identify three groups, according to the assumptions on contaminant source and chemical-physical mechanisms occurring during the transport. Each group appears suitable for a different contamination scenario.

A modelling procedure based on a hindcasting simulation combining a steady-state flow model and a mass transport model has been proposed. Specifically, the objectives of the procedure are to reproduce the contaminant concentration measured in the aquifer within the site, to assess the contaminant concentration of the source and, based on that, to give some insights helping to the identification of the primary sources. The procedure has been applied to a significant case study: the Taranto site The developed modelling has been able to reproduce the measured contaminant concentrations in site and the obtained contamination scenarios have been found plausible and consistent with the solubility of the analysed contaminant.

Acknowledgements

This work would not have been possible without the support of several people. I am most grateful to all for their precious contributions.
First of all, I would like to express my deepest gratitude to Prof. Leonardo Cascini for his strong motivation, understanding, and wise guidance throughout these years. His positive and stimulating attitude has been a source of inspiration for me. Without his effort and patience towards me, I would never have come to this goal.
I owe great thanks to Prof. Giacomo Viccione for his constant support, for providing me valuable and constructive suggestions to carry out this research, but mainly for his infinite helpfulness in every circumstance.
Special thanks to my co-supervisors Prof. Giusy Lofrano for helping me with her expertise, generosity and kindness and Dott. Giuseppe Maria Grimaldi for his useful support and competent advice.
I would like to thank the "Commissario Straordinario for Urgent Interventions of Environmental Requalification of Taranto" Vera Corbelli for providing the data used. This research arose from studies carried out by her working group.
For great collaboration and co-authorship, I would like to thank Prof. Claudio Guarnaccia and Prof. Maurizio Carotenuto.
I am deeply grateful to the geotechnical laboratory and its teaching staff for the help during my PhD. My gratitude also goes to all my past and present colleagues at the laboratory, they have proved to be very good friends, always ready to help or to take a break at any time.
Finally, I am very thankful to all my family members, in particular to my mother and father for their love and support, and my brother for his encouragement and wise advice. Limitless and warm thanks go to Mario for his love, patience and essential support during all this time.
An important person who deserves all my gratitude is Maria Rosaria, I couldn't have handled these years without her constant support and friendship. When I think back to my PhD, she was and she is an anchor in this experience of my life.
Another special thank is to my dear fellow traveller Giuseppe, his example inspired me to do better and his remarks led me on the right track.
Finally, I would like to thank all my friends, especially Mirella, Adele and Nicola who unintentionally "joined" this PhD and made this experience a pleasant journey.

About the author

Maria Grazia Stoppiello graduated in Environmental Engineering at the University of Salerno with 110/110 cum laude, discussing a thesis entitled: "Hydro-mechanical interaction in fine-grained soils under atmospheric conditions". During her PhD programme, she has developed research topics related to the modelling of contaminant fate and transport in unsaturated soils and the application to contaminated sites. To deepen these issues, she undertaken training and research activities at the University of Salerno and attended the postgraduate course "Current topics in flow and transport in geological porous media: modelling and experiments" held by Prof. Brian Berkowitz. She attended also the postgraduate school LARAM (LAndslide Risk Assessment and Mitigation).

Maria Grazia Stoppiello si laurea in Ingegneria per l'Ambiente ed il Territorio, presso l'Università degli Studi di Salerno con la votazione di 110/110 e lode, discutendo una tesi dal titolo: "Hydro-mechanical interaction in fine-grained soils under atmospheric conditions". Durante il corso di dottorato sviluppa tematiche inerenti la modellazione del trasporto di contaminanti nei mezzi parzialmente saturi e le possibili applicazioni nei siti contaminati. Per approfondire tali argomenti, svolge attività di formazione e ricerca presso l'Università di Salerno e frequenta il corso di "Current topics in flow and transport in geological porous media: modelling and experiments" tenuto dal Prof. Brian Berkowitz. Inoltre, frequenta i corsi nell'ambito della scuola di alta formazione LARAM (LAndslide Risk Assessment and Mitigation).

1. Introduction

The contamination of groundwater resources caused by the release of chemicals into soil represents one of the main environmental threat. . Groundwater contamination can damage potable water supply, endangering human health and can affect aquatic ecosystems. (Foster et al., 2002; Whiters et al, 2014; Lehosma et al., 2018). Due to the increasing concern in groundwater protection, scientific literature has displayed a growing interest in models for simulating contaminant transport in the unsaturated zone , which have a key role in groundwater risk assessment and management (Rivett et al., 2011; Berlin et al., 2015).

Application of these models to field scale presents some critical issues. Processes involved in fate and transport of contaminants in the unsaturated zone are complex and interrelated: one or more substances with different physical-chemical properties are carried in two coupled phases, air and water, by several transport mechanisms (advection and dispersion-diffusion) and affected simultaneously by reaction processes (sorption, abiotic transformation, biodegradation, etc...) (Karapanagioti et al., 2003). Furthermore, a successful transport modelling is related to an adequate hydrogeological characterization of the contaminated site (Di Sante et al., 2019), but these sites are often characterized by lack of data and a high degree uncertainty (Thomsen et al., 2016).

In scientific literature diversified approaches are proposed, they range from simple models characterized by a high level of simplification and a limited number of input parameters to more complex models able to reproduce heterogeneous and anisotropic media or multi-contaminant systems which need a large and accurate dataset.

The present thesis is aimed to contribute to this topic, providing new insights about the application of these models to contaminated sites. In particular, the purpose is to identify features and limitations of the existing tools through the development of a review and, thus, define a modelling approach useful for engineering applications to contaminated sites.

The structure of the thesis is as follows. In Chapter 2 the role of fate and transport models in the risk assessment framework is explained and the growing importance of the risk assessment as a result of the large number of contaminated sites and the related environmental problems is highlighted. Chapter 3 focuses on flow in

unsaturated medium, physical-chemical-biological processes ruling fate and transport of contaminants and soil characteristics affecting these processes. Chapter 4 offers an overview of the current literature concerning fate and transport modelling, by presenting a classification based on the model structure, the governing equations used by these models and a selection of the most relevant ones. In Chapter 5 a review of selected analytical models from a quantitative point of view is developed, in order to identify features and limitations and highlight the differences in the outcomes of the different models. Chapter 6 describes in detailed the proposed modelling approach that is based on a hindcasting simulation combining a steady-state flow model and a mass transport model. Chapter 7 presents an application of the approach to a significant case study: the Taranto site. Finally, Chapter 8 summarizes the main conclusions in conjunction with future perspectives.

2. Risk assessment of contaminated sites

This work focuses on models for simulating contaminants fate and transport in the unsaturated zone. In order to clarify the context in which this thesis is developed, this chapter aims to explain the role of these models in the risk assessment framework and highlight the growing importance of the risk assessment as a result of the large number of contaminated sites and the related environmental problems.

2.1 Contaminated sites

The release of contaminants from both point sources (solid waste tips, landfills, leaking storage tanks and leaking sewers) and diffuse sources (agricultural activities and farmyard drainage) and their transport into the environmental compartments is a growing threat to ecosystem and human health (Foster et al., 2002; Shaider et al., 2014; Lehosmaa et al., 2018; Wang and Kelly, 2018). Most of the fate and transport processes take place into the unsaturated zone, commonly known as vadose zone, posing a great concern in terms of environmental preservation and protection (Naidu and Birke, 2015). Many definitions of "contaminated site" are provided by different scientific fields and international regulations. The Joint Research Centre (JRC) defines contaminated site as "a site where hazardous substances, as defined in Article 3 of Regulation (EC) No 1272/2008 (3), are present in a level that pose a significant risk to the environment and human health" (Pérez and Eugenio, 2018).
An indicator of the extent of the problem is the growing number of contaminated sites. It has been assessed that there are more than five million potentially contaminated sites worldwide (CRC-CARE, 2013; Ye et al., 2019). The JRC has considered the possible existence of around 2.8 million sites where polluting activities took or are taking place in the EU-28,about 650 000 are registered in national and regional inventories (Pérez and Eugenio, 2018). The USEPA has assessed a number of hazardous waste sites ranging from 235 000 to 355 000, average 294 000 (USEPA, 2004). The Federal Contaminated Sites Inventory of Canada includes 23 681 contaminated sites, with different priority levels[1]. Similar values are registered in Australia, specifically over 160 000 contaminated sites have

[1] https://www.tbs-sct.gc.ca/fcsi-rscf/classification-eng.aspx (last access: 02/02/2020)

been estimated (Plant et al., 2014). In New Zealand, over 20 000 potential contaminated sites have been registered by the Ministry for the Environment (ME, 2019). Naidu and Birke (2014) report a number of 500 000 potential contaminated sites in Japan. Because of the growing importance of the subject, in recent years the developing countries also have begun to carry out surveys and researches. Although no official inventory or extensive studies have been carried out in most developing countries, several pieces of research stress a significant number of contaminant land, already revealing a serious situation. (Ite et al., 2013; Kocman et al., 2013; Kovalick and Montgomery, 2014, Kuppusamy et al. 2017). According to National Soil Pollution Survey (MEP,2014) in China 1.01 million square kilometres of land do not respect environmental quality standard for soils (Ye et al., 2019) and the China Environment Chamber of Commerce has estimated over 500 000 contaminated sites in China (CECC, 2014). In Brazil, the São Paulo Environmental Sanitation Technology Company (CETESB) has identified an uncompleted list of 5 942 contaminated sites (Thomé et al., 2018). In Colombia, the Ministry of Environment and Sustainable Development (MESD) has carried out a research which identifies 1 843 sites potential contaminated sites (Espana et al., 2018). A map of the geographic distribution of the estimated number of sites in the countries is shown in Figure 2.1. The figure highlights the lack of data concerning most of the world countries.

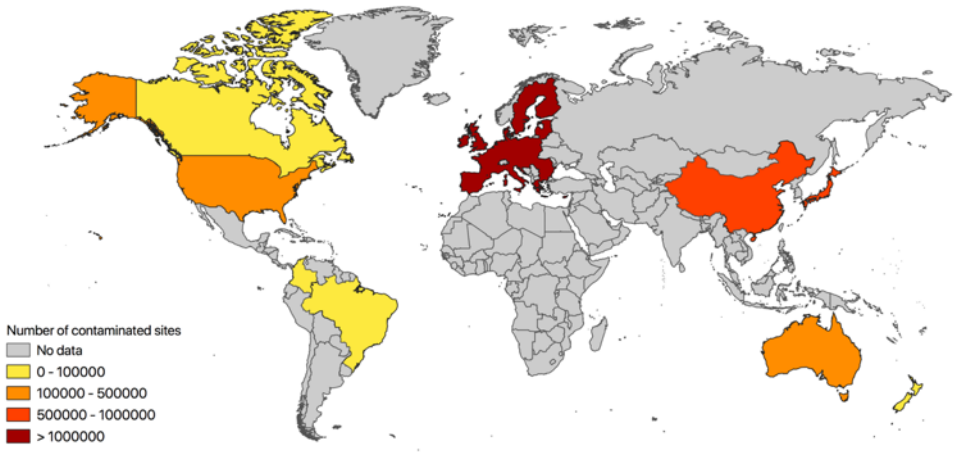

Figure 2.1: Number of estimated contaminated sites in the world.

The leading cause of soil contamination is the high density of industrial and economic activities (Dupuis et al., 2015). Panagos et al. (2013) report the

contaminated site data collected by the European Soil Data Centre (ESDAC). An element of particular interest is the contribution of each category of activities to soil contamination (Figure 2.2). The data collected in 2011-2012 of 22 European countries show that almost 40% of soil contamination comes from waste disposal and treatment, both industrial waste and municipal one. After that, the major sources are industrial and commercial activities (33%), then storage (10%) while the other sector with percentages minor than 10%. Focusing on the industrial/commercial sectors, the industrial sectors having more impact are the metal industry (13.1 %), the chemical industry (8.2 %), and the oil industry (7.4 %); while for the commercial sector, gasoline stations have a key role as source of contamination (15%).
Data collected in 2006 from 16 countries, reported by Panagos et al. (2013), show the occurrence of the different typologies of contaminants in soil and groundwater (Figure 2.3). The percentages in the two environmental compartments are similar, to demonstrate the interrelationship between the two environmental matrices. Heavy metals are the prevalent contaminants, with a percentage higher than 30%, the second major contribution is given by mineral oil, representing more than 20%. As evidenced by the survey's authors, the knowledge of the prevalent contaminants has an important role in the analysis of the contamination and the development of remediation techniques. The properties of a contaminant affect its behaviour in the environment, for this reason is important to recognize characteristics and possible classifications of the several existing chemical substances. This topic will be explored in the following paragraph.

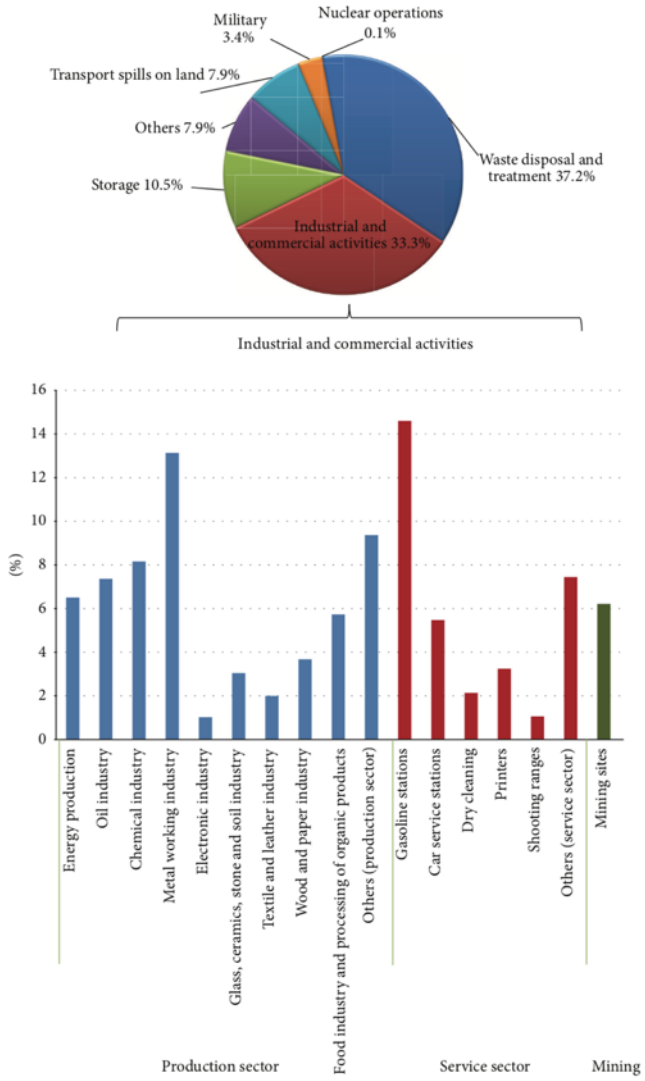

Figure 2.2: Contribution of the different categories of activities to soil contamination in 22 European countries (Panagos et al., 2013).

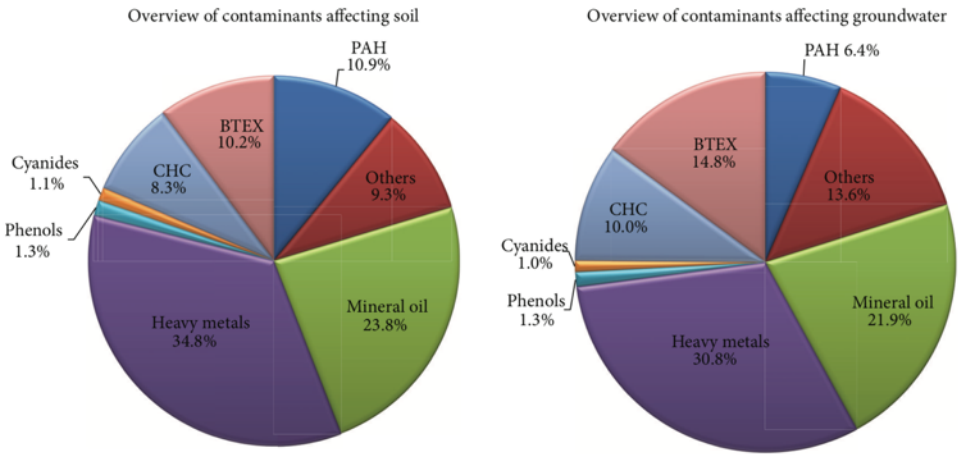

Figure 2.3:Percentages of types of contaminants affecting soil and groundwater in 16 European Countries (Panagos et al., 2013).

2.2 Types of contaminants

During the 19th and 20th centuries, the industrial development, coupled with the improvement of living standard and the continuous growth of consumer demand, have not only intensified exponentially the release of contaminants into the subsurface but also increased the number of substances with a human-made origin. Indeed, many thousands of new compounds have been produced by the industry in recent years (Berkowitz, 2014; Stefanakis and Alexandros, 2015). Given the large number of contaminants, it is important to identify general categories of chemicals with common physical-chemical properties because typically they have similar behaviours. For instance, the propagation mechanisms into the environmental compartments depend on specific characteristics such as the phase state of contaminant, the biodegradability which is related to its molecular structure, the sorption coefficient Kd, the octanol water partition coefficient (log Kow), the organic carbon to water partition coefficient (log K_{OC}) described as the ratio between the sorption coefficient Kd, and the organic carbon content of the sorbent, in units of mass of organic carbon (OC) per mass of soil (g OC/g soil) is commonly used to assess the extent to which an organic chemical is sorbed.

Contaminants characterized by significant values of resistance to degradation, mobility in the environment and toxicity fall into the class of persistent, bioaccumulative and toxic substances (PBTs). Because of the high impact of these substances on human health and environmental ecosystems, their identification is important to regulate their production, use, and release and define specific mitigation

procedures (ECHA, 2017; Cowan-Ellsberry et al., 2009). Another example is the classification of the particulate matter, the mixture of solid and liquid particles in the air, in “coarse particles” (PM2.5–PM10, diameter 2.5–10 m), “fine particles” (PM2.5, diameter <2.5 m), and “ultrafine particles” (UFPs diameter <0.1 m). This classification is particularly used in the analysis of the effects of air pollution on human health (Becker et al. 2009; Polichetti et al., 2009).
As regards contaminants leaching from soil to groundwater, two basic classifications are particularly meaningful: a physical classification based on main phase-state of contaminants in pore water, aqueous-phase, non-aqueous phase liquid and particulate (Cherry and Parker, 2006); and a chemical classification of contaminants based on chemicals properties in organic and inorganic (Berkowitz, 2014).

2.2.1 Physical classification

A contaminant is completely miscible with water when they constitute a homogeneous mixture i.e. components of the mixture are in a single phase and they are no longer physically distinguishable. This thesis focuses on fate and transport of contaminants in this physical state. Substances in solute form are among the most detected in subsurface, their transport is a significant environmental issue because in water phase contaminants are often more available to living organisms and they can move from an environmental matrix to another rapidly (Durães et al., 2018). The contaminant transport is ruled by advection, diffusion and mechanical dispersion. Furthermore, contaminant concentration is affected by partitioning between different phases and different types of biochemical reactions. Regardless of these general considerations, fate and transport of the individual substances are strongly influenced by their specific chemical properties (Cherry and Parker, 2006). Connections between fate and transport mechanisms and chemical properties of contaminants are described in greater detail in Chapter 3.
The contaminants immiscible in water are known as NAPLs (non-aqueous phase liquids). Pure organic compounds and complex mixtures of a large number of compounds, like gasoline, may fall into this category. NAPLs can be divided into two categories: light NAPLs or LNAPLs, that are liquids less dense than water, such as BTEX; dense NAPLs or DNAPLs, that are liquids denser than water (DNAPLs) such as chlorinated solvents, creosote or PCB (Bear and Cheng, 2010). Accidental release from tanks, pipelines and spillages is one of the most common ways for NAPLs to reach the unsaturated zone from the ground surface (Pankow and Cherry,1996; Molins et al, 2010). From the source on the ground surface, NAPLs move and spread out through the unsaturated zone due to gravitational and capillary forces, occupying part of the void space and constituting a multiphase medium with

water, air and soils, the fraction of the pore space occupied by the entrapped phase is called residual saturation. For a significant amount of NAPL, the contamination expands until reaching an underlying water table. When the source is exhausted, part of NAPL remains entrapped in pores by capillary forces, forming residual globules, part dissolves in the aqueous phase and moves with water flow. In fact, a certain quantity of the NAPL may dissolve in the aqueous phase, depending on its water solubility value (František et al., 2003; Bear and Cheng, 2010). Therefore, a NAPL distribution in the unsaturated medium can be considered as a source of dissolved contaminant. In the unsaturated medium (NAPL-water-air system) residual NAPL saturations are generally between 10 and 20%, while in the saturated medium (NAPL-water system) lower saturations occur, ranging from 15 to 50% (Rivett et al., 2011).

Particulates are solid particles in suspension including a wide variety of contaminants. Colloids are among the most significant ones. They can be defined as particles controlled by Brownian forces, the characteristic diameter of these particles varies from 1 nm to 10m (Massoudieh and Ginn, 2010). Colloidal particles include: particles derived from mineral precipitation (e.g. iron, aluminium, calcium or silica precipitates) or rock fragmentation; organic matter derived from plants, wood or coal; biological active particles (e.g. bacteria, viruses or protozoa). Colloids may be contaminant substances or they may transfer contaminants, as hazardous metals or radionuclides, sorbed on colloids surface. The latter process is called colloid-facilitated contaminant transport (Cherry and Parker, 2006). Colloids are transported in the subsurface by the movement of water both in the saturated zone (Sen and Khilar, 2006; Tufenkji, 2007) and in the unsaturated zone (DeNovio et al., 2004; Flury and Qiu, 2008).

The presented classification, based on the phase-state of contaminants in pore water, is summarized in Table 2.1.

Table 2.1: Physical classification of contaminants in pore water

Type		**Examples**
Aqueous phase		Inorganic (primarily ionic); nutrients; trace elements, organic in small quantities according their solubility.
NAPL	LNAPL	Organic like BTEX and other hydrocarbons.
	DNAPL	Organic like chlorinated solvents, TCE, PCE and PCB's; Liquid Hg; creosote; some pesticides.
Particulate		Particles derived from mineral precipitation or rock fragmentation; organic matter derived from plants, wood or coal; biological active particles (e.g. bacteria, viruses or protozoa)

2.2.2 Chemical classification

According to the Encyclopedia Britannica, organic compounds are defined as chemical compounds in which one or more atoms of carbon are connected to atoms of other elements, like hydrogen, oxygen, or nitrogen, by covalent bonds[2]. A few compounds consisting of carbon are not organic, e.g. carbonates. The functional groups which compose the substances are an effective way to classify them and describe their behaviour (Naidu et al., 2008).

Organic contaminants are very diversified in term of characteristics and sources: pesticides, halogenated hydrocarbons, petroleum hydrocarbons and fuel additives, pharmaceuticals and personal care products fall in this category (Berkowitz, 2014).

The European commission define a pesticide as a substance "that prevents, destroys, or controls a harmful organism or disease, or protects plants or plant products during production, storage and transport"[3]. Over 1 800 substances are identified as pesticides[4], subdivided in different categories, among which herbicides, fungicides, insecticides, acaricides, etc.. Their toxicity is a relevant characteristic to be considered because they are developed to be toxic to living organisms, and consequently, they can be potentially hazardous to humans.

Halogenated hydrocarbons (HHCs) come from hydrocarbons and include some halogen atoms within their chemical structure. They include aliphatic, alicyclic, aromatic, polyaromatic, and heterocyclic hydrocarbons and they are commonly used for several decades as non-flammable solvents, unlike kerosene or gasoline (Khan et al., 2008; Gerba, 2019). These compounds are characterized by a low mobility and a significant toxicity respective to conventional hydrocarbons because of the presence of halogen groups (Ramírez-García et al. 2019).

A wide range of complex mixtures of hydrocarbons falls within the category of petroleum hydrocarbons (PHs). As reported by Vorhees et al. (1999) a mixture can be composed of thousands of chemicals, although chemical properties are not well-known for all these substances. BTEX (benzene, toluene, ethylbenzene and xylene) fall within this category, they are small aromatic compounds, often quite volatile and very common in many fuel products. Given the relevance of these compounds, several studies analyse their migration in the vadose zone, e.g. Søvik et al. (2002), Alfnes et al. (2004), Christophersen et al. (2005). Another significant compound is MTBE, it is a gasoline additive with a high solubility, which moves through soil and water matrices with a different velocity than the other gasoline compounds (Berkovitz, 2014), in fact different studies compare the MTBE mass flux with the

[2] https://www.britannica.com/science/organic-compound
[3] https://ec.europa.eu/food/plant/pesticides_en
[4] http://www.alanwood.net/pesticides/index.html (updated 09/01/2020)

mass flux of the other compounds (Lahvis and Rehmann, 1999; Weaver and Charbeneau, 2001).

Pharmaceuticals and personal care products (PPCPs) include products like antibiotics, hormones, cosmetics, etc. In recent years these chemicals have been recognized as contaminants with high persistence or contaminants of emerging concern (CECs) able to threat ecological environment and human health (Liu and Wong, 2013). Few studies analyse the presence in the vadose zone of these compounds, among them Zentner et al. (2015) and Ma et al. (2018).

Inorganic contaminants include several types of contaminant (heavy metals, metalloids, nutrients and salts), which may be found in the environment as dissolved anions and cations (Goldscheider, 2010). Nitrate (NO^{3-}) and phosphate (PO_4^{3-}) are among the main inorganic nutrients used in very large amounts as fertilizers for field crops. Nitrates and phosphates can negatively affect humans and ecosystems. Losses of these compounds from agricultural lands can lead eutrophication in surface waters, Berkowitz (2004) states that this effect can already occur due to few tenth of mg/l of nitrate. Considering the type of source, a lot of research handle the nitrogen and phosphorus flow in the vadose zone, mainly in the root zone (Allaire-Leung et al., 2001; Stenger et al., 2002, Kogovšek and Šebela, S. 2004), but also in the deep vadose zone (Baran et al., 2007; Botros et al., 2011).

Heavy metals are generally defined as metals with a density higher than 5 g/cm^{-3}; among them lead (Pb), cadmium (Cd), mercury (Hg), which are characterized by a high toxicity (Alloway, 2012). Heavy metals and their compounds are naturally found throughout the earth's crust, but over the years a strong increase of their concentration in the soils has occurred, as result of a variety of human activities such as mining, smelting, electroplating, other industrial processes, pesticide use, etc. (Chen et al., 2015; Jing, 2018). They can be found either as separate entities or in combination with other soil components, like exchangeable ions sorbed on the surfaces of inorganic solids, nonexchangeable ions and precipitated or insoluble inorganic metal compounds such as carbonates and phosphates, soluble metal compound, metal complex of organic materials, and metals connected to silicate minerals (Chibuike and Obiora, 2014). Because of their toxicity heavy metal exposure represents a significant threat both to the human health and ecosytems. Metals can be immobile and persistent in the soil because of the sorption mechanisms, however would be more mobile therefore the potential of transfer soil matrix – pore water. Retention and release reactions in soil are ruled by different processes influenced by several soil properties, such as ion exchange, adsorption/ desorption, precipitation/dissolution, which are deepened in the following chapter. These aspects make it difficult to identify a single behaviour for heavy metals in vadose zone and aquifers (Sherene, 2010, Selim, 2012).

The presented classification, based on the chemical properties of contaminants, is summarized in Table 2.2.

Table 2.2: Chemical classification of contaminants

Type	Examples
Organic	Pesticides (herbicides, fungicides, insecticides, acaricides, etc.); halogenated hydrocarbons (aliphatic, alicyclic, aromatic, polyaromatic, and heterocyclic hydrocarbons); petroleum hydrocarbons and fuel additives (BTEX, MTBE, etc.); pharmaceuticals and personal care products (antibiotics, hormones, cosmetics, etc).
Inorganic	Heavy metals and metalloids (lead, cadmium, mercury, nickel, etc.); nutrients (nitrates and phosphates); salts.

2.3 Review of risk assessment methodologies

Contaminated sites pose a serious risk to environmental and human beings for the reasons discussed in the previous paragraphs. For these reasons many countries, both European and non-European have adopted environmental regulations to the manage contaminated sites and define the clean-up objectives of remediation projects (Mazzieri et al., 2016). In all of them, risk assessment is considered as an essential starting point for the subsequent activities, because, as reported by Fergunson et al. (1998), it is able to give "a rational and objective basis for priority setting and decision making". It evaluates the potential exposure to contamination and the severity of the effects for the human beings (Human Health Risk Assessment HHRA) and the ecosystems (Ecological Risk Assessment ERA). Risk assessment of contaminated sites is a complex subject that requires insights into various disciplines like geology, hydrology, chemistry, toxicology, statistics etc..

The ASTM Risk Based Corrective Action (RBCA) standards for evaluating petroleum sites (E 1739-95) and chemical release sites (E 2081-00) are among the first technical standard introduced in this discipline and constitute a starting point for the scientific references and environmental regulations (Mazzieri et al., 2016).

The ASTM RBCA consist of a tiered approach to risk and exposure assessment, where each level is characterized by a higher level of complexity. From Tier 1 to Tier 3 the amount of needed data increase and a more detailed description of the physical and chemical mechanisms ruling fate and transport of contaminants is developed, as shown in Figure 2.4. As a general rule, Tier 1 of the RBCA process involves an initial assessment and classification of the site based on conservative risk-based screening levels (RBSLs) that are not site-specific. Tiers 2 and 3 involve

evaluating the site using more site-specific information (e.g., depth to groundwater, infiltration rate, etc.) and/or evaluating off-site point of exposure. Tier 2 is based on a reasonably detailed site assessment and simple and easy-to-use models, while Tier 3 involve more complex analysis such as more detailed site assessment, probabilistic evaluations, and sophisticated fate and transport models (Spence and Walden, 2001).

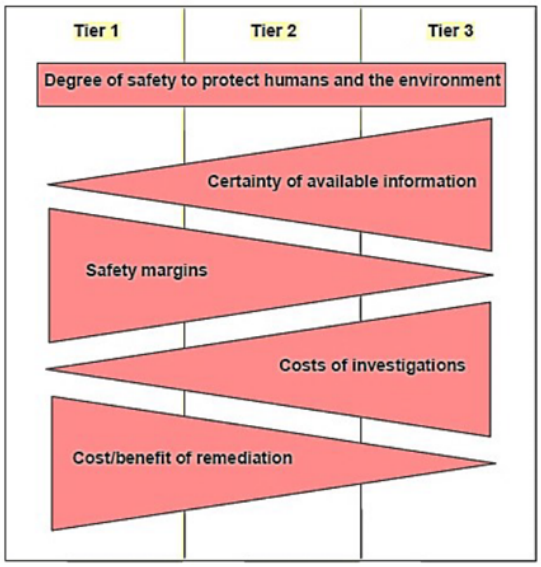

Figure 2.4: Tiered risk assessment characterization (Karkush and Altaher,2016).

Risk assessment procedure is based on the development of a conceptual site model (CSM) that describes the possible contamination pathways, it is usually composed by three module: source, pathway, receptor (Fergunson et al., 1998), as reported in Fig. 2.5.

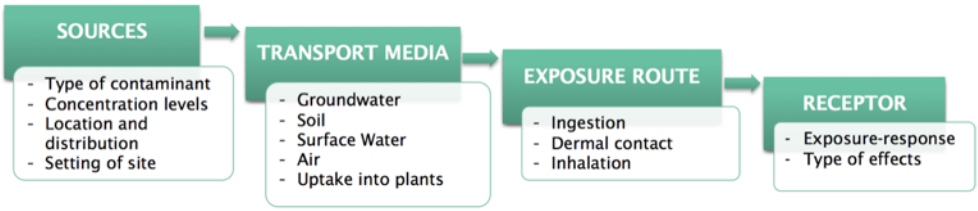

Figure 2.5: Source-pathway-receptor model for risk assessment (modified from Troldborg et al. 2010).

In the procedure the source is represented by the secondary source i.e. the contaminated medium that release contaminants in the other media, while the primary source i.e. the entity or the action that releases contaminants into the

environment is not directly considered (Suter et al., 2000). For example, considering a tank leaking into surface soil, the considered source is the contaminated surface soil not the tank. The development of the CSM includes the identification of all contaminant sources, modes of transport through the different environmental matrices (the contaminant of concern can be carried to the receptor contact point in e.g. groundwater, air and/or soil), potential receptors of concern and the effects of exposure for each one, and the potential exposure pathway routes (e.g. the contaminant can reach a human being through ingestion, inhalation or dermal contact).

In this framework, models for simulating contaminants fate and transport in the unsaturated medium fall within the models needed to the evaluation of the contaminant pathways, specifically for subsurface-groundwater pathways. They evaluate the concentration of the chemicals at the point of exposure on the basis of source concentration located on the ground surface on in the subsurface, allowing to define part of the risk assessment scheme.

3. Fate and transport mechanisms in unsaturated soils

The accurate knowledge of the processes ruling fate and transport of soil pollutants and the proper definitions of parameters (e.g., diffusion coefficients, velocity of advective flow, and distribution coefficients) describing the contaminants and the soils allow to improve the prediction of contaminant concentrations in soil and water (Balseiro-Romero et al., 2018). For this reason, Chapter 3 focuses on these processes. Particularly, the unsaturated medium and the driving forces of porewater flow are described; the physical, chemical and biological mechanisms involved in solute transport are deepened with particular reference to the literature parameters used to describe the main properties of chemicals and soil involved in these phenomena; finally, a review of studies on soil characteristics affecting these processes is provided.

3.1 Unsaturated flow

3.1.1 Vadose zone

The vadose zone, also called unsaturated zone or zone of aeration, is the area between the land surface and the water table; in presence of perched groundwater, the limit of this zone is the lowest water table (Nimmo, 2009). It plays a significant role in the processes of water infiltration and pollutants transmission to groundwater, it may represent both a contamination source, as contaminated soil, and a pathway, through leaching. The depths of this zone vary widely, from less than 1 m to more hundreds meter (Holden and Fierer, 2005), giving different levels of protection to the aquifer below, the transport mechanisms are also influenced by the soil properties (Pepper and Brusseau, 2019). The physical properties of the vadose zone are not uniform, but vary along the depth, saturated zones may intermittently appear.
Regarding to the saturation degree, Bear and Cheng (2010) report a subdivision in three parts: soil water zone, intermediate zone and capillary fringe. The soil water zone is the area in contact with the ground surface, it is also called root zone because it is delimited by the presence of plant roots. The thickness of this area is very variable, depending on the climate and vegetation, normally it is around some

meters. The water circulation is always vertical and can follow two directions: upward for the processes of evaporation and plant transpiration and downward for infiltration. The saturation in this area varies considerably because of the occurring physical processes.

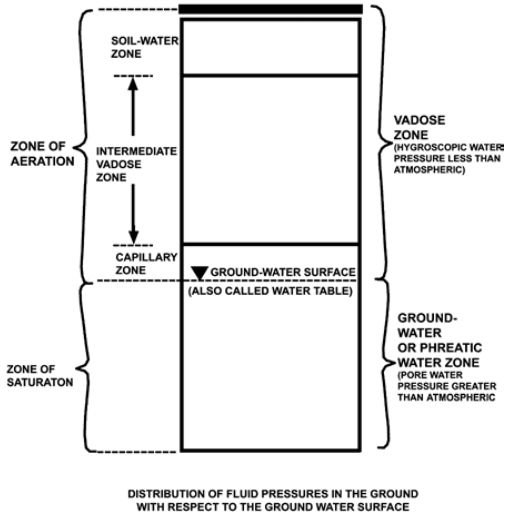

Figure 3.1:Subdivision of vadose zone (Boulding and Ginn, 2004).

The transition zone is at the centre of the unsaturated area; in this area, the waters circulate only towards the aquifer as a result of gravitational forces. This area has no hydraulic connection with the saturated area. It is characterized by low organic content, usually lower than 0.1% (Pepper and Brusseau, 2019). The transition zone may not occur depending on the distance between water table and ground surface, e.g. when the distance is very large or otherwise when the capillary fringe reaches the soil-water zone (Bear 1979).

The capillary fringe is the area immediately above and tightly bond the saturated zone and , the movement of the waters is vertical and bidirectional according to the movements of the aquifer. Its presence is due to the movement of water by capillarity in a porous medium. The capillary rise depends on the soil properties in particular, the size of the pores that ranges from a value of zero for coarse soil to more than 3 meters for fine soils (Bear, 1979). The water content decreases gradually with distance from the water table. Some authors report average values to characterize the capillary fringe, e.g. Bear (1979) suggests an average water content value of 0.75, while Fredlund and Rahardjo (1993) report 0.85-0.90 as the minimum.

3.1.2 Driving forces

The unsaturated medium constitute a multiphase system where the pores of solid matrix are filled with air and water, as Figure 3.2 illustrates, but other fluids can sometimes occur, like NAPLs. The downward water flow towards the water table can transport dissolved contaminants to groundwater, thus movements of contaminant through the medium are strictly related to the water flow.

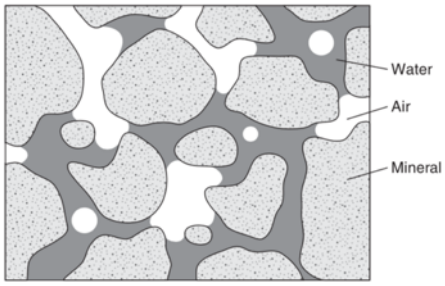

Figure 3.2:Pore space of a hypothetical unsaturated medium (Nimmo et al,2009).

Theory about flow in the unsaturated flow is extensively addressed in several studies and books, e.g. Bear (1979), Zhang (2002), Hillel (2003), Nimmo (2006), Bear and Cheng (2010), Hopmans (2011), Hemond and Fechner (2015).
As presented in Bear and Cheng (2010), the water flux is governed by the energy state of the fluid, which can be expressed as the gradient of the total water potential and depends on the medium properties. The total water potential (Ψ^w) is composed by the contributions of the different forces acting on the fluid; the more significant for the water flow are the matric potential (Ψ_m^w), gravitational potential (Ψ_g^w), pressure potential (Ψ_p^w) and osmotic or solute potential (Ψ_o^w). As a result, the total water potential can be expressed as:

$$\Psi^w = \Psi_m^w + \Psi_o^w + \Psi_g^w + \Psi_p^w \tag{3.1}$$

Matric potential is the attraction of water to soil surfaces, it is caused by two processes: the surface tension across the water-air interfaces and the attraction of water molecules to the solid surface. The osmotic potential is the effect of the concentration of dissolved chemicals in water, which reduces both the surface tension and the forces that attract water molecules to solid surfaces. The gravity potential is related to the difference of the potential energy associated with the elevation of the considered point regarding to a reference point. The pressure potential is related to mechanical pressure. The osmotic potential and the matric potential are negative and represent the driving forces in the unsaturated flow, while

gravitation potential is a positive potential and it is the dominant forces in saturated flow.
There are different way to define a potential. Typically, in engineering application water potential is usually expressed either as a pressure or as an equivalent height of a column of water. The sum of osmotic and matric pressure represents the soil suction (Eq. (3.2)), which represents the driving force in unsaturated flow (Fredlund, 2006).

$$\Psi^w_{suct} = \Psi^w_m + \Psi^w_o \tag{3.2}$$

Osmotic pressure occurs only in the presence of solute, in fact, different studies state that it can be ignored in most engineering applications, like geotechnical engineering (Fredlund et al., 2001). According to Richards (1967), osmotic pressure can be neglected in the absence of solute and for steady concentration. When a significant level of salt in soil occurs, osmotic suction must be considered, like analysis of soils affected by saline infiltrations (Garakani et al, 2018) or contaminant transport where high solute concentrations exist (Scanlon et al., 1997).

3.1.3 Soil water characteristic curve

The relation between the volume of water retained by the soil Θ_w and the negative pore water pressure (or the soil suction, usually presented as a positive quantity) in an unsaturated medium is an important element to understand the unsaturated soil behaviour, this relation is usually called soil-water characteristic curve (SWCC) or water retention function (WTC) (Dane and Hopmans, 2002). The suction forces, governing the pore water pressures, increase when the pore water content reduces; for a fixed soil the size of the water-filled pores can decrease because of drainage, water uptake by plant roots, or soil evaporation. For the same pore water content in different soils, suction values are higher in the fine soils than coarse soil because of the higher ratios of the circumference to the area (Hemond and Fechner, 2015).
The elements which contribute to suction forces values are several: pore-size distribution, specific surface area, type of physical-chemical interactions at the solid-liquid interfaces. For this reason, the SWCC is specific for each soil and highly nonlinear (Hopmans, 2011). Generally, the SWCC is S-shaped and contain some associate variables providing information about the soil, as shown in Figure 3.3.

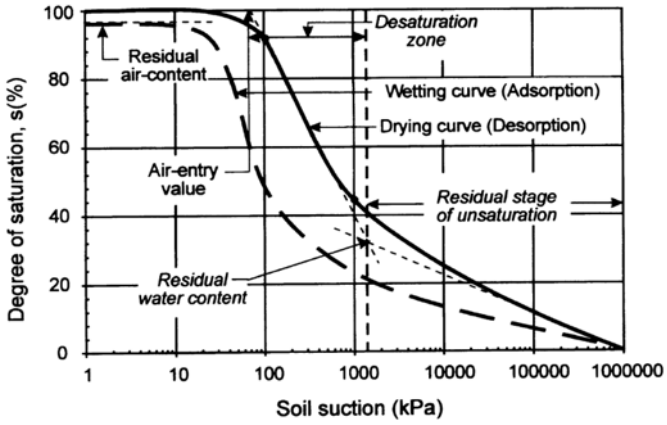

Figure 3.3: A general SWWC and its associated variables (Frendlund et al. 2001).

The curve exhibits hysteresis, that means the wetting paths (during the infiltration) is different from the drying paths (during the drainage). A value derivable from the SWCC is the air-entry value (AEV) or bubbling pressure (Brooks and Corey, 1964), that is the suction value at which the largest pores in the soil begins to drain and air enters the pores in the soil (Frendlund et al. 2001) and correspond to the value, along the drying paths, for which the water content begin to decrease (Hopmans, 2011). A second significant value is the residual water content θ_w^r, that correspond to the amount of water considered immobile, like water in the smallest pores or adsorbed water films (Hopmans, 2011).
The SWWC of a soil is obtained by measured soil water retention data adapted to a mathematical model. In the scientific literature, different empirical models are presented, such as the van Genuchten (1980) and Brooks and Corey (1964) models, an exhaustive review of them is developed by Kosugi et al. (2002).

3.2 Solute transport processes

3.2.1 Advection

In the framework of mass transport in the porous media, advection is the process by which solute particles are carried along the mean direction of fluid flow with a movement rate equal to the average interstitial fluid velocity. The advective component can represent the prevalent one in the mass movement, depending on the type of soil, and reach very high velocity, for this reason advective mass transport can cover long distances in the environment (Brusseau et al., 2019).

According to Bear and Cheng (2010), the advective flux J_{adv} of the contaminant can be calculated as:

$$J_{adv} = \theta_w^e \boldsymbol{v} C_w \tag{3.3}$$

where θ_w^e is the effective volumetric water content, i.e. the water content corrected by subtracting the residual water content θ_r, $\boldsymbol{v}$ is the vector of average interstitial water velocity and C_w is the concentration of the contaminant (expressed as mass of contaminant per unit phase volume).

In unsaturated porous media, assuming the hypothesis of the absence of air movement in the soil and the constant density, the average velocity can be expressed as (Bear, 1979):

$$\vec{v} = -\frac{\boldsymbol{K}(\theta_w^e)}{\theta_w^e} \cdot \nabla h \tag{3.4}$$

where $\boldsymbol{K}(\theta_w)$ is the unsaturated hydraulic conductivity tensor for medium, which is a function of θ_w and ∇h is the gradient in head (equal to dh/dx_i, the change in head per unit distance along the x_i-axis for uniform flow along the x_i-axis).

3.2.2 Dispersion

The solute particles, not only move along the direction of fluid flow, but also are spread with different velocity through the three directions because of dispersion. Dispersion is composed of two physical processes: molecular diffusion and hydromechanical dispersion.

Molecular diffusion is related to the Brownian motion of particle caused by thermal agitation and molecular collisions. Brownian motion results in movement from positions with a higher concentration of solute to positions with lower concentrations, in order to dissipate the concentration gradients. Molecular diffusion is described by Fick's law. In a one-dimensional porous medium the diffusive flux can be expressed, as reported by Vanclooster et al. (2005):

$$J_{diff} = -D_w^e \frac{\partial C_w}{\partial x_i} = -D_w^0 \xi_i(\theta_w) \frac{\partial C_w}{\partial x_i} \tag{3.5}$$

where D_w^e is the diffusion coefficient of the porous medium composed by D_w^0 and ξ_i, which are the Brownian diffusion coefficient and the tortuosity factor, respectively.

In a three-dimensional medium the diffusive flux can be described as (Bear and Cheng, 2010):

$$J_{dif} = -\boldsymbol{D_{diff}}(\theta_w) \cdot \nabla C_w = -D_w^0 \boldsymbol{T}(\theta_w) \cdot \nabla C_w \tag{3.6}$$

where $\boldsymbol{D_{diff}}$ and $\mathbf{T}$ are second rank symmetric tensors and represent the coefficients of molecular diffusion and tortuosity of the porous medium.

The tortuosity factor regards the effective distance that a solute particle covers to dissipate the concentration gradient along a direction. The soil type affects the

tortuosity characteristics and the air phase increases the distance covered, therefore, ξ decreases when θ_w increases. Moldrup et al. (2001) show the relation between soil characteristics, specifically the volumetric surface area (SA), and the tortuosity factor (Figure 3.4).

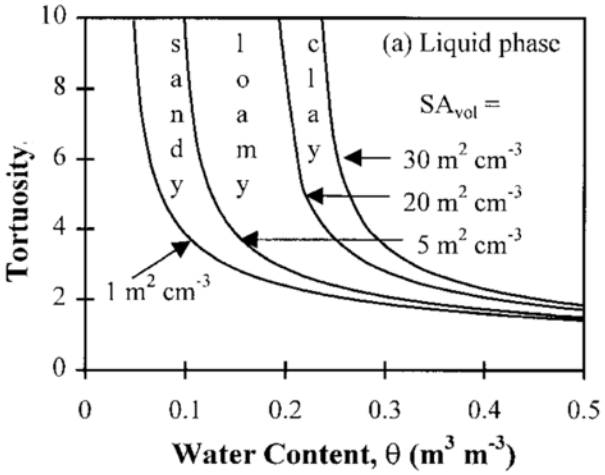

Figure 3.4:Relation between water content and tortuosity for soils with different surface area (SA_{vol}) (Moldrup et al., 2001).

Hydromechanical dispersion is caused by a non-uniform flow field within the Representative Elementary Volume (REV). Flow velocity vectors differ in modulus and direction from the mean advection velocity, depending on physical properties of the porous medium. At the pore scale, this is caused by three processes (Brusseau et al., 2019). The first is related to the friction on the pore walls because the velocity field in a single pore has a parabolic distribution, with a maximum value in the middle of the pore and a zero value on the walls; the second is due to the heterogeneous distribution of the diameter pores that results in different velocities, higher in the larger pores; the third is related to the contaminants paths that have different lengths in relation to tortuosity of the medium.

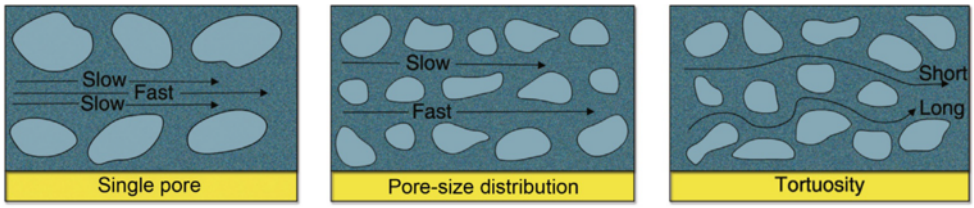

Figure 3.5:The three processes causing hydromechanical dispersion (Brusseau et al. 2019).

The described processes lead to a behaviour similar to the molecular diffusion, for this reason hydrodynamical dispersion can be expressed by the Fick's law. For a one-dimensional problem, Eq. (3.7) relate contaminant flux to concentration gradient through a hydrodynamic dispersion coefficient D_z (Vanclooster et al., 2005):

$$J_{disp} = -D_{disp,z}\theta_w \frac{\partial C_w}{\partial x_i} \tag{3.7}$$

The dispersion coefficient is related to the advective velocity. In one-dimensional systems this relation can be assumed directly proportional (Biggar and Nielsen, 1967):

$$D_{disp,z} = \alpha_l v_z \tag{3.8}$$

where α_l is the longitudinal dispersivity. Three-dimensional problems need the development of a dispersion tensor $\mathbf{D_{disp}}$, which, for an isotropic porous medium, depend on two independent components: longitudinal and transverse dispersivities (α_l, α_t) (Bear and Cheng, 2010). The flux is expressed according to the following equation:

$$J_{md} = -\boldsymbol{D_{disp}}(\alpha_l, \alpha_t) \cdot \nabla C_w \tag{3.9}$$

The values of dispersivity can not be assessed by using theoretical consideration but through experimental measurements. Studies (Gelhar et al. 1985, Gelhar et al. 1992, Beven et al. 1993) relate these values to the length of the contaminant path, showing that dispersivity values vary from one or more centimetres for laboratory soil columns to hundreds of meters for a regional spatial scale. Several later studies confirm this relation both for saturated medium (e.g. Gelhar et al., 1992; Haggerty et al. 2004,) and for unsaturated one (e.g. Forrer et al., 1999 Javaux & Vanclooster, 2004; Vanderborght and Vereecken, 2007). This happens because dispersion, as described above, is a consequence of the heterogeneity of the medium. The longer the distance, the more heterogeneities along the paths hence under the same advective velocity mechanical dispersion increases. In scientific literature, several relations between dispersivity and travel distance (z_m) are proposed. Neuman (1990) developed the following empirical relations (Equations (3.10) and (3.11)) for saturated medium, plotted in Figure 3.6 (on the left) based on data from Gelhar et al. (1992).

$$\alpha_L = 0.017 z_m^{1.5};\ \ z_m \leq 100m \tag{3.10}$$

$$\alpha_L = 0.32 z_m^{0.83};\ \ z_m > 100m \tag{3.11}$$

Vanderborght and Vereecken (2007) suggest two relationships: a linear model (Equation (3.13)) and a power-law model (Equations (3.12)), interpolated from experimental data in unsaturated soils at three scales: core-scale (< 30 cm), column scale (>30 cm), and field scale, shown in Figure 3.6 (on the right).

$$\alpha_L = 0.33 z_m^{0.62} \tag{3.12}$$

$$\alpha_L = 0.046 z_m + 1.23 \tag{3.13}$$

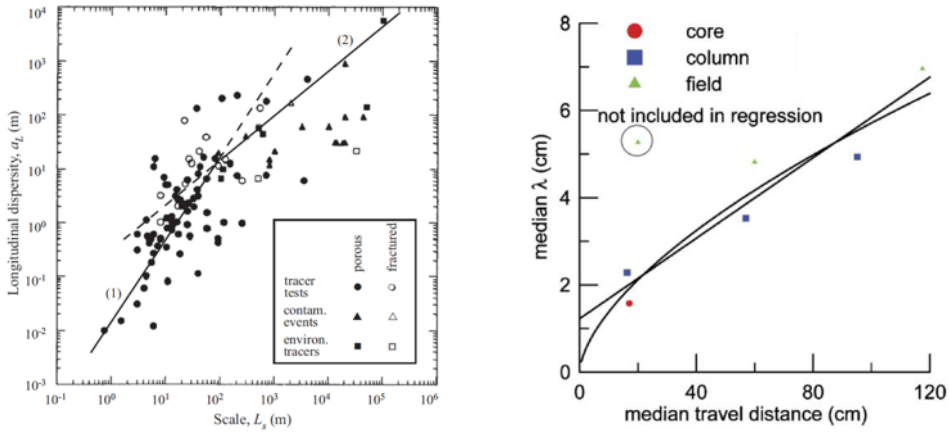

Figure 3.6: (on the left) Longitudinal dispersivity versus travel distance for various types of observations and media and Neuman's relationship (Bear and Cheng, 2010) - (on the right) Median values of longitudinal dispersivity versus median values of travel distance for various types of experimental data in unsaturated soils (Vanderboght et al., 2007).

Transverse dispersivity assumes smaller values than longitudinal one, literature data usually report values in the range of a few millimetres (Klenk and Grathwohl, 2002). Different authors relate these values to the medium characteristics like pore size distribution, hydraulic conductivity, heterogeneity etc. (Perkins and Johnston, 1963; Olsson and Grathwohl, 2007; Chiogna et al., 2010; Carey et al., 2018). In the first instance, longitudinal and transverse dispersivity can be assumed 1/10 and 1/100 of the travel distance, respectively. To obtain more accurate values a calibration procedure based on experimental data is needed.

Adding the two mechanisms (mechanical dispersion and diffusion), it is possible to write:

$$J_{disp-diff} = -D_z\theta_w \frac{\partial C}{\partial x_i} == -(\alpha_l v_z + D_w^e)\theta_w \frac{\partial C}{\partial x_i} \tag{3.14}$$

There are many cases of contaminant transport in subsurface where the molecular diffusion can be assumed negligible with regard to mechanical dispersion, it can be prevalent when the advective velocity is low, e.g. in saturated clay units. An indicator of prevalent mechanisms can be provided by the Peclet number, that is the ratio between the advective component and the diffusive component:

$$Pe = \frac{v_z d}{D_w^e} \tag{3.15}$$

d is the characteristic length of the porous medium. Different studies express the ratio between dispersion coefficient and diffusion coefficient as a function of Peclet number (e.g. Perkins and Johnston, 1963; Nezhad et al., 2019) and highlights that for large Peclet numbers (Pe > 10) the advection is prevalent, for low Peclet numbers

(Pe<0.02) the diffusion is prevalent and the contaminant behaviour is independent from advective velocity.

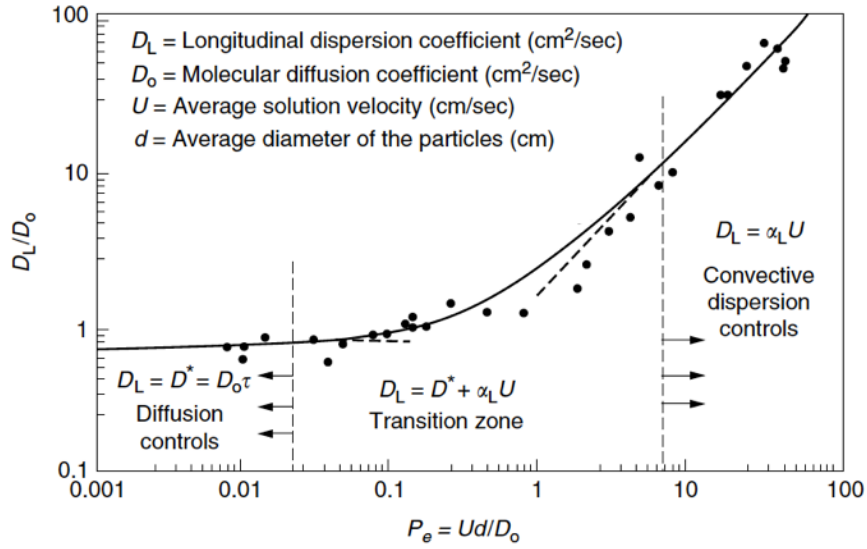

Figure 3.7: Ratio between dispersion coefficient and diffusion coefficien versus the Peclet number (Batu, 2005).

3.2.3 Sorption

Sorption can be defined as a reversible transfer process of contaminant particles between solid and aqueous or gaseous phase and it is one of the main process influencing the transport and fate of contaminant in subsurface. Interaction processes involved can be several (London–van der Waals forces, hydrophobic reactions, hydrogen bonding and charge transfer, ligand and ion exchange, chemisorption …) and their occurrence depend on the surface soil properties, the organic matter content, the chemical characteristics of the porewater, and physical–chemical properties of the contaminants (Mulligan et al. 2004; Balseiro-Romero et al., 2018). In a general and non-exhaustive manner, it is possible identifies different behaviours between inorganic and organic chemicals. Inorganic contaminants in aqueous solution are often ionic or charged substances, hence can be attracted by opposite charged sites occurring on soil particle surfaces. For this reason, the most significant characteristics are: mineralogy and surface area, as regards the soil particles, and the pH, as regards the porewater. For example, the presence of clays, that are characterized by a high surface area and negative charged sites, can increase the sorption behaviour, or the pH water can influence the metals speciation.

Many organic contaminants are nonpolar substances, these compounds interact mainly with the soil organic matter. Nonpolar compounds are characterized by hydrophobic behaviour which increase their affinity for other nonpolar substances (Brusseau and Chorover, 2019). A larger molecule size and an higher chlorine content, in the case of chlorinated organics, increase the hydrophobicity of these compounds (Wauchope et al., 2002).

The partitioning between solid and aqueous phase is usually described by the sorption isotherm i.e. the concentration of contaminant sorbed by the soil C_s expressed as a function of the concentration of the contaminant in aqueous phase C_w. Many equilibrium isotherm models with different degree of approximation have been developed over the years, some of them are shown in Table 3.1, several reviews can also be found in the scientific literature, such as Šimunek and van Genuchten (2016) and Foo and Hamed (2010).

Table 3.1: Sorption isotherms models (modified from Foo and Hamed,2010)

Isotherm	Nonlinear form	Reference
Langmuir	$C_s = \frac{Q_0 b C_w}{1 + bC_w}$	Langmuir,1916
Freundlich	$C_s = K_f C_w^{1/n_F}$	Freundlich,1906
Dubinin–Radushkevich	$C_s = (q_s)\exp(-k_{ad}\varepsilon^2)$	Dubinin and Radushkevich,1947
Tempkin	$C_s = \frac{RT}{b_T} lnA_T C_w$	Tempkin and Pyzhev, 1940
Redlich-Peterson	$C_s = \frac{K_R C_w}{1 + a_R} C_w^g$	Redlich and Peterson, 1959
Sips	$C_s = \frac{K_S C_w^{\beta_s}}{1 + a_s C_w^{\beta_s}}$	Sips, 1948
Toth	$C_s = \frac{K_T C_w}{(a_T + C_w)^{1/t}}$	Toth, 1971
Radke-Pausnitz	$C_s = \frac{a_{RP} r_R C_w^{\beta_r}}{a_{RP} + r_R C_w^{\beta_r - 1}}$	Vijayaraghavan et al.,2006

* a_R Redlich–Peterson isotherm constant (1/mg); a_{RP} Radke–Prausnitz isotherm model constant; a_S Sips isotherm model constant (L/mg); a_T Toth isotherm constant (L/mg); A_T Tempkin isotherm equilibrium binding constant (L/g); b Langmuir isotherm constant (dm^3/mg); b_T Tempkin isotherm constant; C_w equilibrium concentration (mg/L); ε Dubinin–Radushkevich isotherm constant; g Redlich– Peterson isotherm exponent; KF Freundlich isotherm constant (mg/g) $(dm^3/g)^{nF}$ related to adsorption capacity; Langmuir isotherm constant (L/mg); K_R Redlich–Peterson isotherm constant (L/g); K_s Sips isotherm model constant (L/g); K_T Toth isotherm constant (mg/g); n_F adsorption intensity; q_s theoretical isotherm saturation capacity (mg/g); Q_o maximum monolayer coverage capacities (mg/g); r_R Radke–Prausnitz isotherm model constant; t Toth isotherm constant; β_R Radke–Prausnitz isotherm model exponent; β_R Sips isotherm model exponent.

The simplest relation is linear sorption isotherm, which S is directly proportional to C_w, through the distribution coefficient K_d:

$$C_s = K_d C_w \tag{3.16}$$

Several nonpolar organic contaminants have a linear or close to linear sorption behaviour (Brusseau and Chorover, 2019). Furthermore, a commonly assumption for organic contaminant is that sorption occur only with organic material (Allen - King et al., 2002) and, therefore, the distribution coefficient K_d is given by Equation (3.17):

$$K_d = f_{oc} K_{oc} \tag{3.17}$$

where f_{oc} is the organic carbon fraction and K_{oc} is the organic carbon-water partition coefficient. This latter is expressed as a function of octanol–water partition coefficient K_{ow}.

In linear isotherm model the potential sorbed concentration by the solid phase is unlimited, but the actual sorption reach a maximum limit, for this reason linear isotherms are suitable for low solute concentration and non-linear isotherms can be more appropriate in many contaminant scenarios (Mulligan and Yong, 2004).

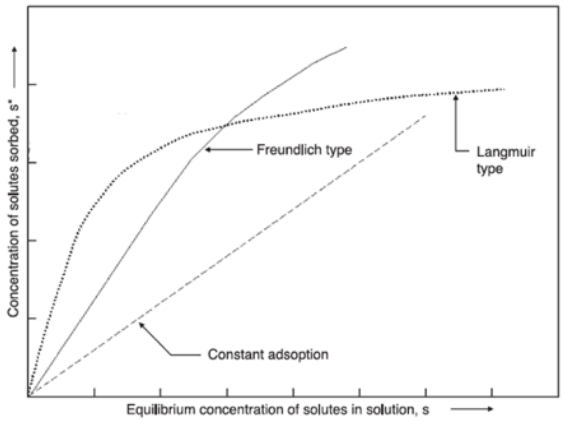

Figure 3.8: Types of adsorption isotherms (modified from Mulligan and Yong, 2004).

Langmuir and Freundlich isotherms are among the most used non-linear models. Langmuir empirical model describes a monolayer adsorption process on a homogeneous surface with a finite and fixed number of binding sites with the same adsorption energy (Foo and Hamed, 2011). Langmuir formulation is given by:

$$C_s = \frac{Q_0 b C_w}{1 + b C_w} \tag{3.18}$$

where b (dm^3/mg) is an empirical constant and Q_0 is the maximum monolayer coverage capacities (mg/g).

Freundlich formulation is suitable when more substances occur. This model describes a multilayer adsorption on a heterogeneous surface with non-uniform

binding sites: the first sites have the greatest adsorption energy, in the other ones energy decreases until to zero in a exponentially way (Foo and Hamed, 2011). Freundlich formulation is given by:

$$C_s = K_f C_w^{1/n_F} \tag{3.19}$$

where K_f (mg/g) $(dm^3/g)^{nF}$ and n_F are coefficients in the Freundlich isotherm.

3.2.4 Other processes

Fate of contaminant in soil can be affected by several processes, such as volatilization, precipitation and dissolution, chemical reaction, biological degradation and radioactive decay, which can be more or less significant with regard to the type of contaminant and the soil characteristics.

Several experimental and modelling studies analyse the importance of volatilization process, i.e. the transfer of contaminant from water to gas phase, highlighting the considerable effect on fate of VOCs, such as aromatic hydrocarbons or some pesticides, in vadose zone (Mendoza and Frind, 1990; Jury et al., 1990; Höhener et al., 2006; Molins et al. 2010; Cryer et al. 2015). The volatilization depends on many factors: physico-chemical properties of the substance as solubility and vapour pressure and environmental variables as temperature. In fate and transport problem volatilization is usually expressed by a linear instantaneous equilibrium between water and gas phase:

$$C_w = HC_a \tag{3.20}$$

where C_a is the concentration in the gas phase (ML^{-3}), C_w is the concentration in the water phase (ML^{-3}) and H is Henry's Constant (dimensionless). As a first approximation, Mulligan and Yong (2004) suggest that volatilization should be taken into account when Henry's constant is greater than 0.05. Furthermore, this process can be more significant in the analysis of the source, while can be negligible in the transport modelling through the unsaturated zone.

Chemical reactions can play a key role in the fate of a specific type of contaminants, but it is difficult to draw general consideration because the processes which can influence these processes are numerous and diverse. Some of the more relevant reactions are hydrolysis and redox reactions. Hydrolysis is a reaction in which the bonds of a substance break down by water molecules, leading to more polar molecules. In most cases hydrolysis products are more biodegradable than the starting substances (Vogel et al., 1987). This process has an important role in the fate of some dissolved organic compounds, e.g. monohaloalkanes, chloroethane, tetrachloroethane (Vogel et al., 1987; Butler and Barker, 1996). It is influenced by the charge properties of the contaminant and the pH (Brusseau and Chorover, 2019).

Redox reactions consist in transfer of electrons between two compounds that are transformed into new chemical species, with different solubility, biodegradability and toxicity (Francisca et al., 2012). Redox reactions involve both organic and inorganic, i.e. metals, nutrients, salts, and chlorinated organic solvents (Ferrey et al., 2004; Shenker et al., 2005; Borch et al. 2010; Violante et al., 2010), and affect mobility and bioavailability of these elements into the environments. For example, under oxidizing conditions phosphorous can be converted in ferro-phosphate complex that is biologically unavailable. In the presence of reducing conditions, phosphorous break down with iron and become biologically available (Brusseau and Chorover, 2019).

Biodegradation is a transformation process of chemical species, in solution or adsorbed on the solid surface, into other products through microbial activity (Bear and Cheng, 2010). Biochemical reactions are triggered by the presence of specific soil microorganisms, carbon sources, oxygen or other electron acceptors, and nutrients; therefore certain conditions of moisture, pH and temperature can inhibit or promote these reactions (Rivett et al., 2011). In most cases, biodegradation represents the predominant attenuation mechanism for dissolved organics. Biodegradation of an organic substance consists of a sequence of degradation steps, each of them takes place through a specific catalyst or enzyme (Maier et al., 2019); intermediate compounds can be more toxic than parents compound, i.e. in anaerobic system TCE can biodegrade in VC, which is an intermediate more toxic and persistent than TCE (Nelson et al., 1993; Shukla et al., 2014). The sequence of degradation steps can end with the mineralization of the parent compound, i.e. the oxidation of the starting organic compound into its inorganic constituents (Maier et al., 2019). Biochemical reactions have a higher biodegradation rate for organics in liquid and NAPL phases than organics sorbed on surface soil, indeed sorbed molecules are usually characterized by low bioavailability. For this reason, on the one hand, soil sorption reduces the contaminant concentration in aqueous phase retarding the transport, but, on the other, it hinders biodegradation and therefore contaminant attenuation (Balseiro-Romero et al., 2018).

Biological and chemical processes occurring in subsurface can be numerous, complex and interrelated, for example different abiotic and biotic pathways can lead to the same products. Therefore, it can be difficult to discriminate abiotic and biotic reaction contributions and define them individually (Cox et al. 2010). In fate and transport modelling, abiotic and biotic degradation is considered ruled by a first-order kinetic (Mulligan and Yong, 2004; Francisca et al., 2012). According to this kinetic the concentration rate due degradation process is given :

$$\frac{dC_w}{dt} = -\lambda C_w \tag{3.21}$$

where λ [T^{-1}] is the first-order reaction constant. Taking into account only biochemical degradation and neglecting advection, diffusion and adsorption processes, the concentration trend with time is described by the following equation:

$$C_w = C_w e^{-\lambda t} \tag{3.22}$$

The reaction constant can be calculated from the contaminant half-life $t_{1/2}$ [T], i.e. the time needed to reduce by half the initial concentration value, according to the equation (3.23):

$$\lambda = \frac{\ln 2}{t_{1/2}} \tag{3.23}$$

The contaminants half-life is evaluated experimentally and is influenced by several elements: measurement methods, possible biotic contributions, use of laboratory or field measurement and environmental conditions, e.g., moisture, pH, temperature and simultaneous occurrence of more chemicals (Rivett et al., 2011). Several authors suggest experimental values of half-life for different contaminants, including Washington (1995), Butler and Barker (1996), Schwab et al. (2006), Tardiff and Katzman (2007), Farlin et al. (2013), Howard et al. (2017).

The most important transport and transformation processes, described in the paragraph 3.2, are presented in Figure 3.9.

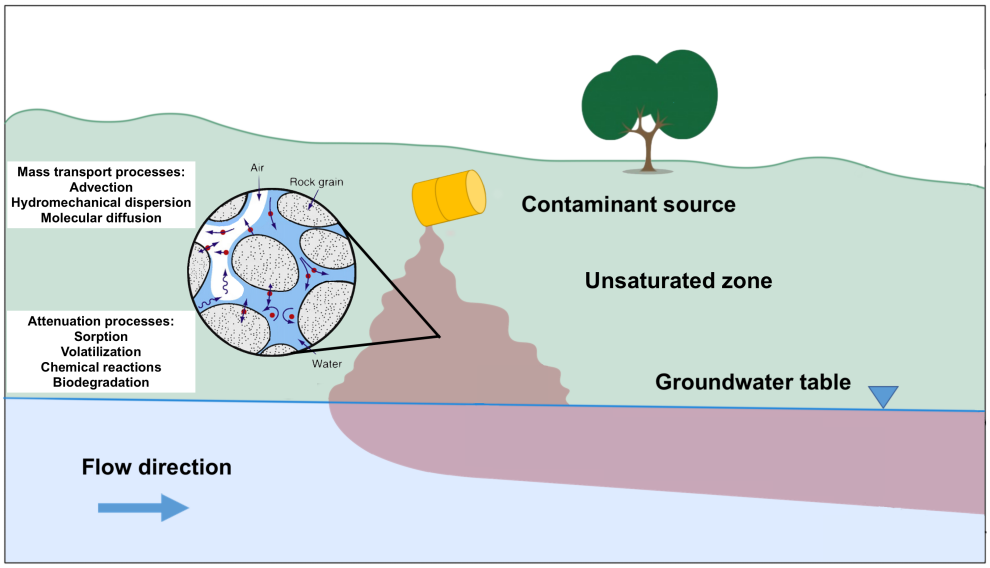

Figure 3.9: A sketch of the conceptual model of the main transport and transformation processes.

3.3 Soil properties affecting fate and transport mechanisms

Soil characteristics have significant effects on contaminant fate and transport behaviour, but their analysis and quantification are a challenging task because of their complexity and interdependency. Soil properties influence hydrological and physical-chemical and biological processes.

The first aspect to assess is the hydrogeological properties and texture of the soil and their effects on the flow occurring in the medium, and consequently the advective velocity. A correct hydrogeological characterization of the soil, assumed as homogenous medium, make it possible to evaluate the soil parameters of the REV: saturated hydraulic conductivity, porosity, water content, characteristic curves, etc.. The assumption of homogeneous medium can lead to a misjudgement in the analysis of flow and solute concentration, because of heterogeneities occurring at different spatial scales that lead to non-uniformly water flow (Fig. 3.10).

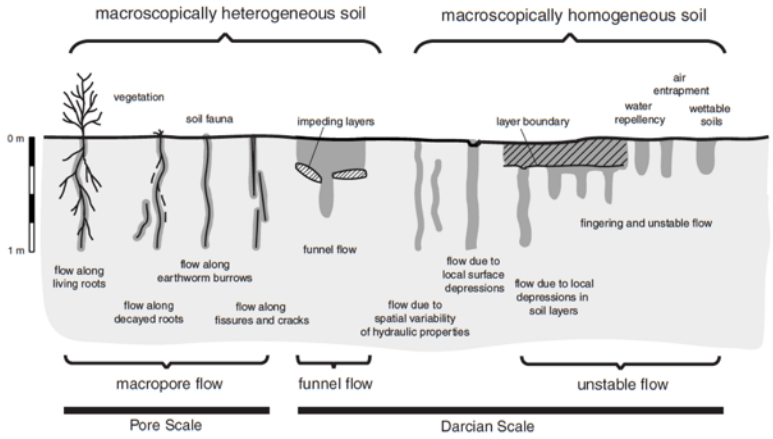

Figure 3.10: Schematic showing different preferential flow mechanisms observed at pore and Darcian scales (Hendrick and Flury, 2001).

Heterogeneities, as inter-aggregate pores and macro-pores, root channels, earthworm burrows, fissures or cracks generate preferential pathways at pore scale which mainly characterize fine-textured soils; while textural layering, water repellence, air entrapment, continuous non-ponding infiltration and funnel flow cause pathways at the darcian scale, which mainly occur coarse-textured materials (Hendrick and Flury, 2001).

As a result of these configurations, solute concentrations are distributed through flow pathways, as shown in Figures 3.11 and 3.12 (e.g., Flury and Wai, 2003; Sander and Gerke, 2007). The breakthrough curve is characterized by a high peak concentration that occurs earlier than uniform flow conditions and a long tail that is exhausted very

slowly; furthermore, the plume spreading mechanism is greater than uniform flow with respect to time and space (Garré et al., 2010). Another consequence of the heterogeneity concerns contaminant degradation because some biochemical reactions are affected by local concentrations, which can greatly vary respect to the homogeneous medium (Javaux et al., 2006; Vanderborght et al.,2006).

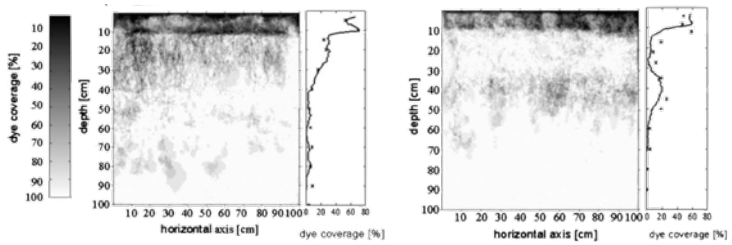

Figure 3.11: Spatial distribution of dye tracer in two-dimensional vertical cross-sections (Sanders and Gerke,2007).

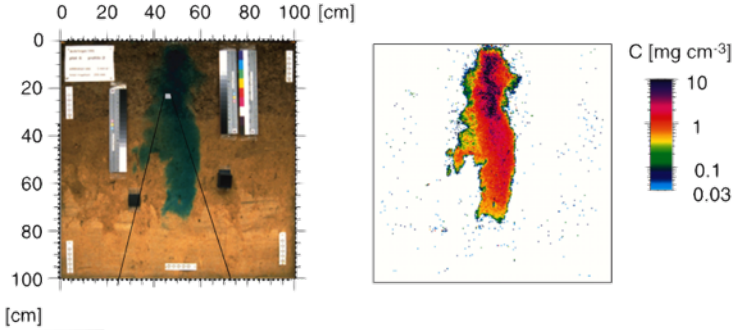

Figure 3.12: Tracer concentrations obtained from color images in a heterogeneous medium (Flury et al.,2003).

As outlined in the previous paragraphs, solute dispersion is caused by non-uniform flow field and hence it is strongly related to heterogeneities occurring in the soil. Vanderborght and Vereecken (2007) review 635 dispersivity values derived from 57 leaching studies in soils, differentiating them with regard to several factors, including soil texture and scale of the experiment. Although analysis of the dispersivity values aggregated by soil texture and travel distance show smaller values for coarse soils than fine soils (Fig. 3.13), the authors highlight this relationship is linked to interactive effects of soil texture and scale of the experiment. In fact, evaluating dispersivity values grouped by these two factors, it is noted that only for core and column experiments dispersivity values are lower in coarse soils, while for field experiment coarse and fine soils have the same values. According to the authors, this

consideration points out that the lateral water flow is very significant for spreading in coarse textured soils. Core and column experiments do not allow to consider this mechanism and for this reason dispersivity could be underestimate.

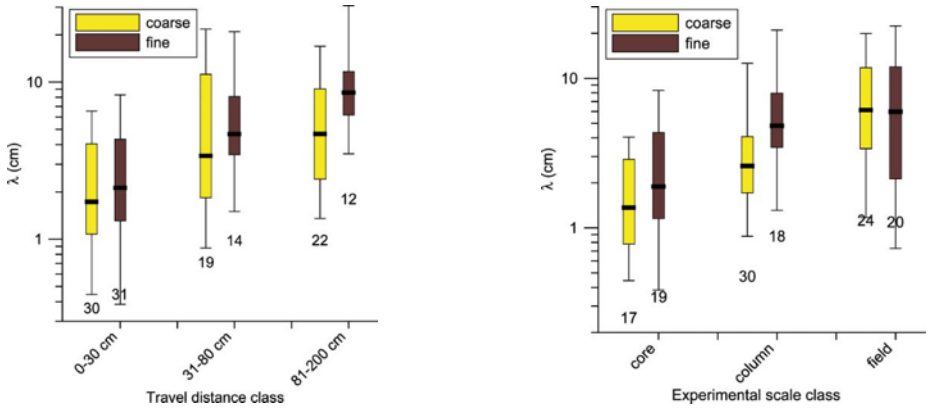

Figure 3.13: (on the left) Effect of transport distance and texture on the dispersivity; (on the right) Effect of the scale of the experiment and texture on the dispersivity. (Vanderborght and Vereecken, 2007).

Unlike hydrological processes, natural attenuation processes as sorption and biochemical degradation are strongly affected by chemical and mineralogical composition of the soil. As set out above, it is possible to consider two different categories of contaminant as regards sorption behaviours: on the one hand charged chemicals, which may be anionic (negatively charged) or cationic (positively charged), and polar chemicals; on the other uncharged chemicals. For the first category, layer silicate clays are the soil component mainly involved in the sorption process. They are usually negatively charged and characterized by a strong affinity for metal cations due to their high cation exchange capacity, high surface area, and pore volume (Uddin, 2017). Different studies (Aşçı et al., 2008; Goyne et al., 2008; Yuan et al., 2013) show that the higher percentages of clay in the soil can increase the sorbed concentration of specific contaminants, as shown in Fig. 3.14 for phosphorus.

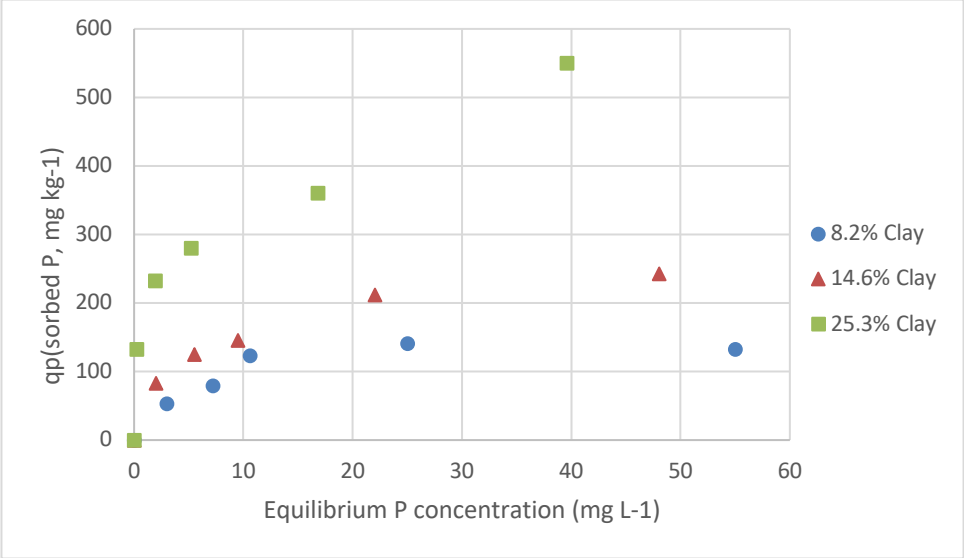

Figure 3.14: Adsorption isotherms illustrating phosphorus (P) sorption to soils with different clay content in absence of dissolved organic matter (data from Goyne et al.,2008).

Clays can be composed by different mixtures of fine-grained clay minerals and in a smaller percentage other minerals and metal oxides. According their chemical composition and structural properties, clays can be classified into groups (Uddin, 2017). One of the more popular classification is proposed by Grim (1962): kaolinite, montmorillonite, and illite are among the main groups of this classification, most of clays are composed by components of these three groups. Several studies analyse the effect of the mineralogy on the sorption capability for single contaminants (Feng et al. 2005; Uddin, 2017; Ren, 2018), but given the wide diversity and number of mechanisms ruling the sorption of metal ions by clay minerals, it is not possible carry out general consideration (Swift and McLaren, 1991).

Another component of the soil involved in sorption are metal oxides, which can be assume anionic, neutral, or cationic form and react with organic and inorganic contaminants (Berkowitz et al., 2014). These minerals become positively charged with low pH conditions and negatively charged with high pH conditions (Qafoku et al. 2004). Fe- and Al-(oxy)hydroxides are among the more widespread compounds in subsurface and their high sorption capacity, especially for metals, is reported by different studies (Sipos et al., 2008; Yaghi and Hartikainen, 2013, Sipos et al. 2018).

A third component particularly important for organic sorption is soil organic matter (SOM), that is partially decayed non-living material generated by microbial transformation of organic residues with a plant or animal origin (Berkowitz et al., 2014). As highlighted in paragraph 3.4, sorption of less polar and nonpolar organic

compounds is mainly caused by SOM content, there is a substantial evidence that the increase of the organic fraction improves the sorption capacity regarding organic compounds, an example is provided in Fig.3.15.

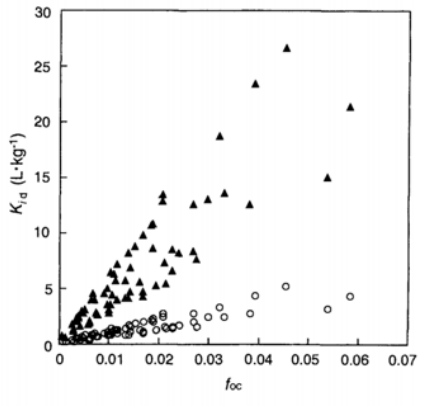

Figure 3.15: Solid-water distribution ratios for the apolar compounds, tetrachloromethane (o) and 1,2-dichlorobenzene (◢) with increasing organic matter content of the solids for 32 soils and 36 sediments. (Schwarzenbach et al., 2016).

For this reason, to a first approximation, distribution coefficient is considered directly proportional to total organic fraction, for any given organic contaminant. Actually, SOM is composed by different compounds (as humic and fulvic acids, proteins, fats, lignin, polysaccharides, kerogen and black carbon) characterized by different chemical compositions, structures, conformations and by specific sorption affinity for organics therefore the same percentages of SOM can result in different values of sorbed contaminant (Mechlińska et al., 2009). The sorption affinity of these compounds for hydrophobic organic contaminants has been widely studied, for example Wen et al. (2007) show that high heterogeneities in the structure and conformation of SOM fractions result in nonlinear sorption processes
or Liu et al. (2010) identify different K_{OC} of phenanthrene for humic acid and fulvic acid.
Contaminant transport, retention, and persistence processes interact with the subsurface environment and may irreversibly alter natural hydrogeological conditions of the soil: not only soil properties affect fate and transport mechanisms, but also these mechanisms can lead long-term changes in soil (Berkowitz et al., 2014). Yaron et al. (2008), (2010) review studies about irreversible changes in properties of the soil induced by contaminant in vadose and aquifer zone. Nachtegal and Sparks (2003) demonstrate that humic substances covering clay minerals may hinder metal adsorption on mineral surface through experiments on nickel sequestration in a kaolinite–humic acid complex.

Different studies focus on the effect of contamination on geotechnical properties (Soule and Burns, 2001; Roque and Didier, 2006; Sunil et al., 2006, Vitone et al, 2016, Sollecito et al., 2019). Ouhadi et al. (2006) analyse the effect of heavy metals on clay properties, showing that the increase of metal cations in pore water entails the decrease of Atterberg liquid limits (LL) and the plasticity index (PI) of soil–bentonite, as a consequence of osmotic consolidation that occur in specific pH conditions. Khamehchiyan et al. (2005) carried out laboratory test to evaluate the effects of crude oil contamination on geotechnical properties of samples of SM (silty sand), SP (poorly graded sand) and CL (lean clay). Some of the finding obtained are shown in Fig. 3.16: Atterberg limits decrease with increasing oil contamination in CL because the presence of a non-polar fluid alters the force of attraction between clay particles and adsorbed water, modifying clays plastic properties; permeability decrease due to the oil content, mainly for low porosity soil, this reduction is caused by the reduction of pore volume due to trapped oil; finally, shear strength parameters decrease with oil contamination for all the soil samples.

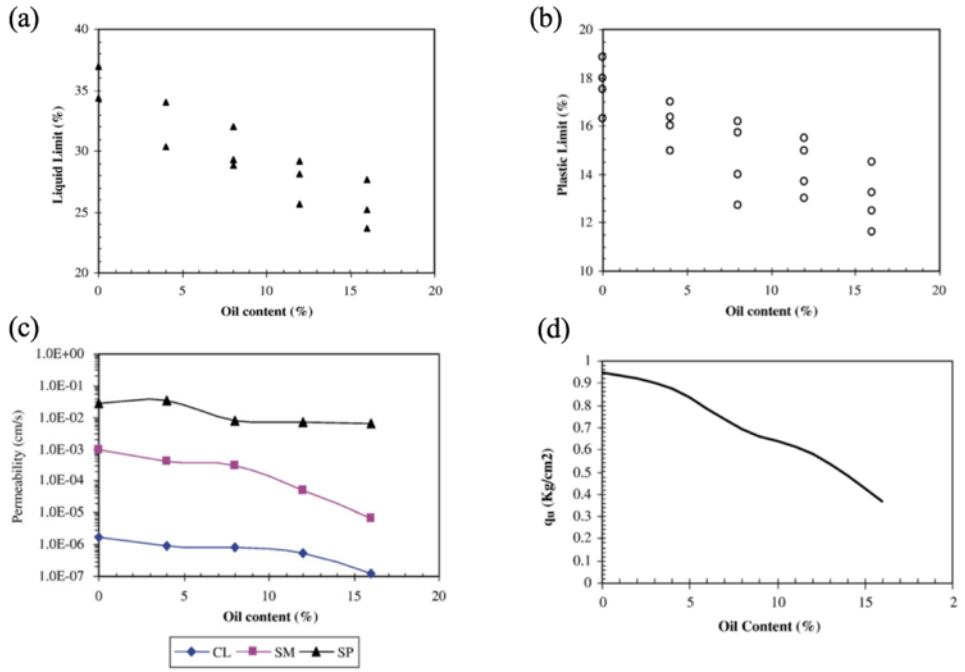

Figure 3.16: Influence of oil content on: (a) Liquid Limit of CL samples; (b) Plastic Limit of CL samples; (c) permeability coefficient of soil samples; (d) Uniaxial compressive strength of SM samples (Khamehchiyan et al., 2005).

Also Nasehi et al. (2016) reached similar results, they evaluate the effect of gas oil contamination on the geotechnical properties of specimens of poorly graded sand (SP), low plasticity clay and silt (CL, ML) demonstrating a decrease in the friction angle and an increase in the cohesion of the soils with the increase of gas oil content, as shown in Figure 3.17.

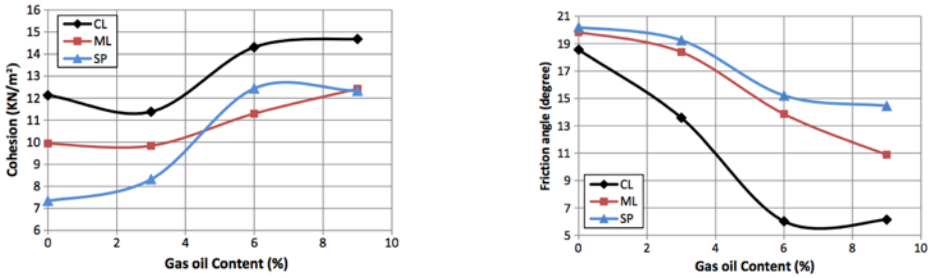

Figure 3.17: Influence of gas oil content on cohesion and friction angle of soil samples (Nasehi et al. 2016).

4. Modelling fate and transport

Chapter 4 offers an overview of the research state concerning fate and transport models, in order to give a contribution to the understanding of the wide range of modelling approaches. First of all, a classification based on the model structure is provided, a subgroup suitable for the selected purposes is identified and the initial assumptions of this subgroup are described. Governing equations ruling unsaturated flow and migration and reaction processes are analysed referring to different possible mathematical descriptions of the phenomena. Finally, a selection of some relevant models is presented, analysing both analytical and numerical models.

4.1 Classification of fate and transport models

In paragraph 2.3 the importance of fate and transport models in the risk assessment framework has been described, highlighting their role in the evaluation of the contaminant concentration at the point of exposure based on source concentration. Among the numerous potential contaminant pathways, this work focuses on solute leaching to groundwater through the unsaturated medium. The variety of approaches to model this phenomenon are countless (Yaron et al., 1996), differing on the purpose of the model, the number of simulated mechanisms, the mathematical representation of the processes and site-features etc.. For this reason, it is necessary to classify the models and narrow down the analysis to a subgroup suitable for the chosen purpose. A general soil pollution models classification, reported by several authors (Addiscott and Wagenet, 1985; Bear and Cheng, 2010; Anderson et al, 2015) is based on a first distinction in deterministic and stochastic models (Figure 4.1).

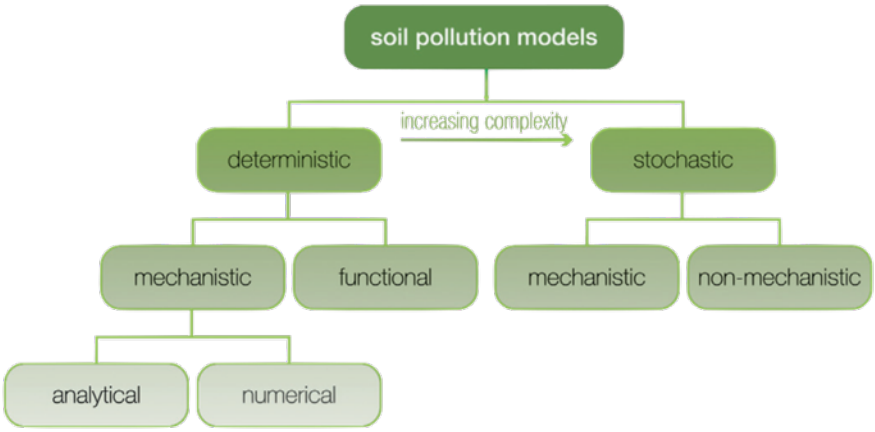

Figure 4.1: Classification of soil pollution models according to the structure of the models (Duraes et al., 2018).

In stochastic models, some hydraulic parameters having a probability distribution that results in all output having a probability distribution. On the contrary, the deterministic models all input data are single value (best estimate value) thus, also the outputs are characterized by a single set of results (Ohio EPA, 2007). Another distinction is between functional models, called also data-driven or "black-box" models, and mechanistic models, called also process-based or physically-based models. The first ones use empirical relationships evaluated from historical data to connect an unknown variable (e.g., head at the water table) to an accessible variable, easy to measure (e.g., precipitation). The second ones consider the main physical-chemical processes. For this reason, mechanistic models are based on one or more governing equations reproducing the specific processes within the problem domain (Anderson et al, 2015). This thesis focuses on this group of models, which can also be distinguished in analytical and numerical, according to the mathematical procedure used to solve the governing equations (Duraes et al., 2018). Analytical models are based on exact solutions of differential equations, while numerical models use numerical time-stepping procedures to obtain the solution (e.g. finite-difference or finite-element method). This latter classification is deepened in the following paragraphs.

As explained in paragraph 3.3, unsaturated flow through the vadose zone is commonly characterized by spatial variability and preferential pathways due to the occurrence of macropores, fractures, other structural voids or biological channels (Šimůnek and van Genuchten, 2016). To describe the wide range of medium configurations different approaches have been developed in literature: some of them describe the medium as a continuum; others assume a discrete medium considering the single fractures, this approach is more complex and used for specific cases like

the analysis of disposal of nuclear waste in unsaturated fractured rocks or the evaluation of an equivalent macroscopic permeability of limestones (Liu et al., 2001; Roels et al., 2003; Li et al., 2020). Focusing on continuum medium, Mallants et al. (2011) report a classification of models in different approaches: single-porosity, mobile-immobile regions, dual-porosity, dual-permeability, multi-porosity, multi-permeability models, the first four are shown in Figure 4.2. Some applications of these approaches are present in Gerke and Van Genuchten (1993), Gwo et al. (1995), Jarvis et al. (1998), Mallants et al. (1997); Brouyère (2006), Frey et al. (2016).

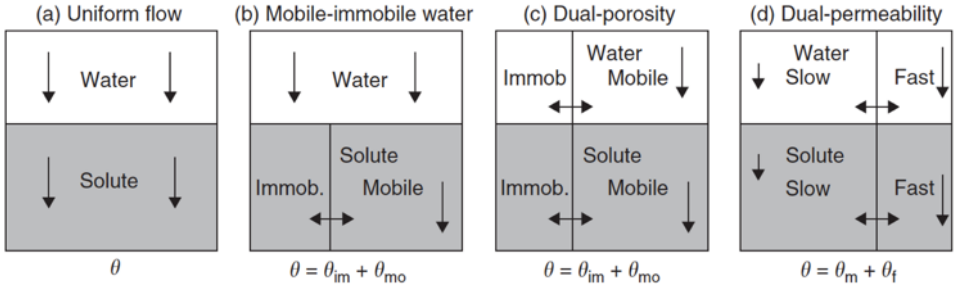

Figure 4.2: Single-porosity, mobile-immobile regions, dual-porosity, dual-permeability models. θ is the water content, θ_{mo} and θ_{im} in (b) and (c) are water contents in the mobile and immobile flow regions and θ_m and θ_f in (d) are water contents in the matrix and macropore (fracture) regions (Šimůnek and van Genuchten, 2016).

The single-porosity (Figure 4.2a) models simulate a single pore system in which water and contaminant can move. For the models based on mobile–immobile flow regions (Figure 4.2b), the flow problem is solved in the same way as a single-porosity model while, only for the solute transport, liquid phase is divided in a mobile and an immobile fraction and contaminant can move only in the mobile fraction and between the two regions. Dual-porosity models (Figure 4.2c) consider two continuum media: the first one is characterized by a macroporosity simulating inter-aggregate, macropore, or fracture system; the second one consist of the micropores or the rock matrix; in these two regions water and contaminant can move only in the macroporosity continuum and between the two regions. Dual-permeability(Figure 4-2d) models are based on the same subdivision of the medium but water and contaminant can move within the matrix. In most of the engineering applications in risk assessment of contaminated sites, single porosity models are used because more complex approaches require an extensive set of laboratory and field data and high-performance computational software. For these reasons models based on an equivalent continuous porous medium are considered in this thesis.
The latter initial assumption concern the physical state of the contaminant, as pointed out in paragraph 2.2.1 a third fluid phase (NAPL) may occupy part of the void space

in the unsaturated zones. This work focuses only on dissolved contaminants carried by the water, neglecting the movement of NAPL as a separate component.

4.2 Governing Equations

4.2.1 Unsaturated flow

Modelling of flow in unsaturated zone is a complicated task, more complex than modelling in the saturated one because water flow occurs only in the pore spaces filled with water, which are highly variable in space and time (Hemond and Fechner, 2015). Furthermore, water flow and wetting and drying paths induce deformation in the solid matrix, making the vadose zone a deformable porous medium (Song and Borja, 2013). Although many simplifications can be assumed on the medium and the two phases, the constitutive relations used to describe the variables involved are highly nonlinear. For this reason, the governing equations usually remain in a non-analytical form and are solved through a numerical solution, rather than make further simplifications or linearization (Bear and Cheng, 2010). The formulation commonly used to describe the unsaturated flow is the Richards' equation (Richards, 1931), that assumes the hypothesis of constant air pressure equal to the atmospheric pressure. In this equation two primary physical variables are unknown, the saturation (or the corresponding water content) and the pressure in the water phase. Depending on how the variables are expressed and which is chosen as dependent variable, three main forms of the Richards' equation can be written, saturation-based (or moisture-based), pressure-based, or mixed (Pop, 2002).
As reported by Kavetski et al. (2000) the three forms are:

$$\frac{\partial \theta_w}{\partial t} - \nabla \cdot \boldsymbol{D_{sw}}(\theta_w)\nabla\theta_w + \frac{\partial K_z(\theta_w)}{\partial z} = 0 \tag{4.1}$$

(saturation, or moisture-based form)

$$\left[C(h) + \frac{\theta_w}{\theta} S_s\right]\frac{\partial h}{\partial t} - \nabla \cdot \boldsymbol{K}(h)\nabla h + \frac{\partial K_z(h)}{\partial z} = 0 \tag{4.2}$$

(pressure-based form)

$$\frac{\partial \theta_w}{\partial t} + \frac{\theta_w}{\theta} S_s \frac{\partial h}{\partial t} - \nabla \cdot \boldsymbol{K}(h)\nabla h + \frac{\partial K_z(h)}{\partial z} = 0 \tag{4.3}$$

(mixed, or coupled form)

where h is the pressure head [L], θ_w is the volumetric water content, t is time [T], z is the (positive down-ward) depth [L], θ is the porosity, S_s is the specific storage [L^{-1}], ∇ is the gradient operator with respect to the spatial coordinates x, y and z. $\boldsymbol{K(h)}$ is the hydraulic conductivity tensor [L T^{-1}], $C(h)$ is equal to $d\theta_w/dh$ and it is the specific capacity [L^{-1}], $\boldsymbol{D_{sw}}(\theta_w)$ is equal to $\boldsymbol{K}(\theta_w)/C(\theta_w)$ is the soil water diffusivity [L^2T^{-1}]. It is necessary to specify that the hydraulic conductivity tensor $\boldsymbol{K}$ can be

expressed as the product of the saturated hydraulic conductivity tensor $\boldsymbol{K}_{sat}$ [LT^{-1}] and the dimensionless relative hydraulic conductivity K_r (Zhang et al., 2003):

$$\boldsymbol{K}(h) = \boldsymbol{K}_{sat} K_r(h) \tag{4.4}$$

The hydrological behaviour of the unsaturated medium can be described by the constitutive relationships between θ_w, h and K_r, i.e. the water retention function (θ_w-h relation) and the conductivity function (K_r-h relation) which allow to solve the Equations (4.1), (4.2), (4.3). As pointed out in paragraph 3.1.3, these relations, strongly non-linear, are expressed by several empirical models. The van Genuchten formulation is one of the widely used, because it give a good description of the soil-water characteristic curve under most circumstances (Song et al, 2013):

$$\theta = \theta_w^r + S_e(\theta_w^s - \theta_w^r) \tag{4.5}$$

$$S_e = [1 + |\alpha_{vG} h|^n]^{-m} \tag{4.6}$$

$$C = \frac{\alpha m}{1-m}(\theta_w^s - \theta_w^r) S_e^{\frac{1}{m}} \left(1 - S_e^{\frac{1}{m}}\right)^m \tag{4.7}$$

$$Kr = S_e^{1/2} \left[1 - \left(1 - S_e^{1/m}\right)^m\right]^2 \tag{4.8}$$

where S_e is the effective saturation, θ_w^r and θ_w^s are the residual and saturated volumetric water content, respectively, α_{vG} [L^{-1}] is a positive parameter to scale the pressure head, depending on the mean pore size and related to the inverse of the air-entry value (Li et al., 2016), and both n and m are dimensionless parameters, m constant is equal to 1-1/n.

For their non-linear characteristics, Richards equations can be solved using analytical and semi-analytical solution only for few problems with simplified boundary conditions, while for the most cases they must be solved numerically. In some applications, the use of analytical models is required, e.g. the evaluation of the accuracy of a numerical solution or the use in combination with an analytical transport model (Alastal et al., 2019). An exhaustive review of analytical infiltration models is carried out by Morbidelli et al. (2018). Among the many existing models, the Green-Ampt model (Green and Ampt, 1911) is one of the most simplified and widely used in different scientific fields, furthermore, a number of its applications in contaminant transport modelling exist in literature (Hussein et al., 2002; Yan et al., 2006; Verginelli et al., 2013). It reproduces water infiltration under ponded conditions in a homogeneous soil profile: a moving wetting front separates an upper saturated zone and a lower unsaturated zone, where the water content is equal to the initial soil water content. The hydraulic conductivity and water content of the soil profile remain constant and the flow is ruled by a constant suction (front suction) that is a parameter of the soil not depending on other factors like the boundary conditions (Chen and Young, 2006; Alastal et al., 2019).

4.2.2 Advection-dispersion-reaction equation (ADRE)

The fate and transport of a conservative solute in a porous medium are evaluated by the combined advection-dispersion equation (ADE) for a single species, presented in its most general form in Equation (4.9):

$$\frac{\partial C_w}{\partial t} + \nabla \cdot (-\boldsymbol{D_w} \cdot \nabla C_w) + \nabla \cdot (\boldsymbol{v} C_w) = 0 \tag{4.9}$$

In some cases, velocity and dispersion functions can depend upon the contaminant concentration C_w e.g. density-driven flow as saltwater intrusion in coastal aquifers. In the most application in risk assessment, the effect of contaminant concentration on this function is negligible and velocity and diffusivity only depend on space and time (Zamani and Bombardelli, 2014).

The equation (4.9) considers only hydrological phenomena, advection and dispersion, however, as pointed out in Chapter 3, other physical and biochemical processes have an important effect on contaminant transport (an example is shown in Figure 4.3).

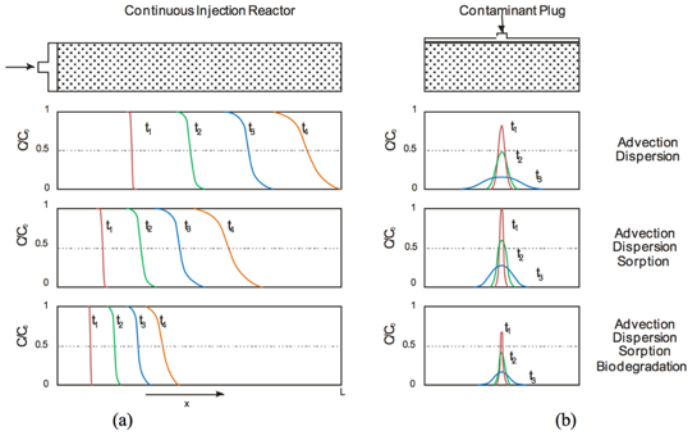

Figure 4.3: Breakthrough curves for different processes for (a) continuous injection and (b) plug injection of contaminant (Francisca et al. 2012).

For this reason, sorption and biological or chemical degradation are usually included in the governing equation, using some mathematical steps. A linear sorption isotherm, described in Equation (3.16) is assumed and a coefficient, called retardation factor, is defined as:

$$R = 1 + \frac{\rho_B}{\theta_w} K_d \tag{4.10}$$

where ρ_B is the soil bulk density (ML^{-3}); furthermore, biological or chemical degradation is considered according to first-order kinetics, described in Equation (3.21).

Considering the equations (4.9), (3.16), (4.10) and (3.21) the general equation governing the transport of non-conservative contaminants is obtained:

$$R\frac{\partial C_w}{\partial t} + \nabla \cdot (-\boldsymbol{D_w} \cdot \nabla C_w) + \nabla \cdot (\boldsymbol{v} C_w) + \lambda C_w = 0 \quad (4.11)$$

For a detailed description of the mathematical steps, Wexler (1992) and Di Molfetta et al. (2010) may be consulted.

The advection-dispersion equation can be solved by either analytical or numerically methods. A brief review of the main analytical and numerical models in unsaturated media is provided in the following two paragraphs.

4.3 Analytical models

Analytical models are based on exact solutions of differential equations, thus they require a high level of simplification of the hydrogeological setting and the chemical-physical processes to reach a closed-form solution. Usually, they assume homogeneous soils, simple geometries of the domain, constant or highly simplified initial and boundary conditions and transport of a single component (Anderson et al., 2015). These models are characterised by ease of use and a limited number of input parameters; these peculiarities make them especially suitable for Tier II risk assessment (Mazzieri et al., 2016; Paladino et al., 2018). On the other hand, their simplicity does not allow to simulate the complexity of site-features, like a heterogeneous and anisotropic medium or a multi-contaminant system. Furthermore, most of the analytical solutions are based on PDE with constant coefficients (Zamani and Bombardelli, 2014), except few solutions like Smiles et al. (1981) and Wilson and Gelhar (1981). Consequently, velocity field and dispersion tensor are assumed uniform and steady and the water content remains constant over space and time (Šimůnek & van Genuchten, 2016), this is an important limitation to the modelling. Numerous analytical solutions of the Equation (4.9) for conservative solute and (4.11) for non-conservative solute have been developed during the last years, initially for purely scientific purposes, then for analysing laboratory and field measured data and finally for risk assessment applications. Several hydrogeology textbooks and studies propose solutions for a one, two and three-dimensional domain and several boundary conditions (Locatelli et al., 2019). Among the most remarkable it is possible to find: Hunt (1978), van Genuchten (1981), Wexler (1992), Yeh (1981). In order to accurately describe the unsaturated medium, Toride et al. (1993) and Leij et al. (1993) present analytical solutions for vertical transport, that are based on a non-equilibrium solute transport through a medium subdivided in a mobile and an immobile region and take into account advection, dispersion and first-order decay.

Connell (2002) modify the analytical solution of Ogata and Banks (1961) to consider the root zone processes.
Interest in applications of analytical solutions to analyse contaminated sites and to implement software tools is elevated, as highlighted by Rivett et al. (2011). One of the best-known development and application of an analytical model is carried out by Jury et al. (1983, 1984). In the first work, the authors present a one-dimensional solution considering advection, diffusion, equilibrium partitioning between air, solid and aqueous phases and first-order degradation. In the second work, the model is used to analyse the effects of soil conditions and contaminant properties on volatilization and leaching mechanisms. Jury's model is improved by Shan and Stephens (1995) including dispersion processes. Another analytical solution is proposed by Ünlü et al. (1992) and later implemented in the risk assessment tool RISC (Spence and Walden, 2001). Karapanagioti et al. (2003) examined several public domain software for modelling contaminant transport in unsaturated zone, three of them (all developed by US EPA) are based on analytical solution, Hydrocarbon Spill Screening Model HSSM (Weaver et al.,1994), Regulatory and Investigative Treatment Zone RITZ (Nofziger et al. 1988) and PESTAN (Ravi and Johnson,1993). HSSM estimate the effects of LNAPL spill considering transport in different phases, considering also LNAPL dissolved in the water phase. RITZ is a screening model for simulation of unsaturated zone flow and transport of oily wastes during land treatment. The model considers the downward movement of the pollutant with the soil solution, volatilization, and loss to the atmosphere and degradation. Other relevant solutions are presented by Troldborg (2008),(2009) and Verginelli (2013), but these models will be deepened in the following chapter.

4.4 Numerical models

Numerical models solve the system of differential equations discretizing the spatial and temporal domain and calculating the unknown variables at discrete nodes of the domain (Huang et al., 2011). Numerical models are able to handle flow and transport problems that are analytically intractable. They allow simulating contaminant transport for both steady-state and transient groundwater flow, in three dimensional heterogeneous and anisotropic media with complex initial and boundary conditions, and for multi-contaminant systems with different types of reactions (Wu, 2015). This high complexity requires a large number of parameters which are often not available or properly assessed, by reducing the reliability and accuracy of the prediction (Paladino et al., 2018). Numerical modelling has the disadvantages of a greater

complexity of the model preparation and a higher computational costs, which make it unsuitable for many applications.

A numerical model must be characterized by consistency, stability, convergence (Venkateshan and Swaminathan, 2013): the model is consistent if the local truncation error tends to zero as the mesh size tends to zero; it is stable when numerical errors which are generated during the solution of discretized equations are not magnified by roundoff and iterations errors; it is convergent if the numerical solution converges towards the solution of the differential equation when the discretisation steps sizes in space and time tend to zero. Furthermore, to provide a realistic description of the physical system, the numerical solution has to guarantee "conservation", i.e. conservation laws have to be respected on both a local and a global basis, and "boundness", i.e. physically non-negative quantities, like densities or concentrations, should always be positive (Kuzmin and Hämäläinen, 2015).

Numerical solutions of the transport equation, obtained with the different numerical procedures, are affected by two types of numerical problems, numerical dispersion and oscillatory behaviour (Ataie-Ashtiani and Hosseini, 2005). As mentioned by Šimůnek and van Genuchten (2016), these problems can be greater for transport simulation characterized by small dispersivity values.

Several authors (Daus et al., 1985; Yang and Hsu, 1990; Kresic, 2006) show that the numerical accuracy of the numerical solutions can be controlled selecting an appropriate combination of the spatial and temporal discretization. The dimensionless grid Peclet and Courant numbers can be used as criteria for a correct discretization (Huyakorn et al, 1984). The first criterion is related to the grid Peclet number, Pe^g, which defines the predominant type of solute transport (advective or dispersive) in relation to the coarseness of the finite element grid. It is defined by:

$$Pe^g = \frac{v\Delta x}{D} \leq p \tag{4.12}$$

where Δx is the characteristic length of the spatial discretization [L], p is a literature value.

The second criterion is related to the Courant number, Cr^g, that is associated with the time discretization, and it is defined by:

$$Cr^g = \frac{v\Delta t}{\Delta x} \leq c \tag{4.13}$$

where Δt is the time discretization [T], c is a literature value.

Šimůnek and van Genuchten (2016) suggest p and c values equal to 5 and 1, respectively. Comparing equation (4.12) and (4.13), it should be noted that, in some application, a significant computational effort can be required to match both criteria

because a finer grid designed to satisfy the first equation results in a smaller time step required to reduce the Courant number (Kresic, 2006).
Among the many numerical methods (finite-difference method, finite-element method, finite volume method, boundary element method, etc.), the finite-difference method (FDM) and the finite-element method (FEM) are the most commonly used in flow and mass transport modelling (Bear and Cheng, 2010). In the FDM, the domain is divided using a rectangular grid in nodes (Figure 4.4) and the unknown variable is solved at each node of the grid using an approximate form of the governing equation obtained by a Taylor series expansion. In the FEM, the domain is divided into elements that are defined by nodes (Figure 4.5). The unknown variable is defined as a continuous simple basic function, such as polynomials, within elements that may be solved (Anderson et al., 2005).

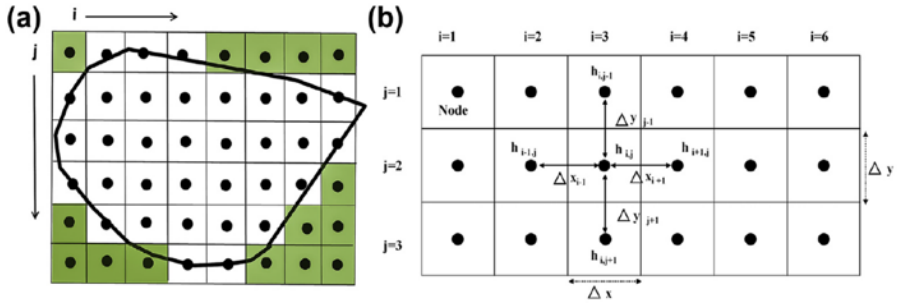

Figure 4.4: Finite-difference (FD) grid: (a) Two-dimensional (2D) horizontal FD grid with uniform nodal spacing (b) group of five nodes comprising the FD computational module centered around node (I,j). (Anderson et al, 2005).

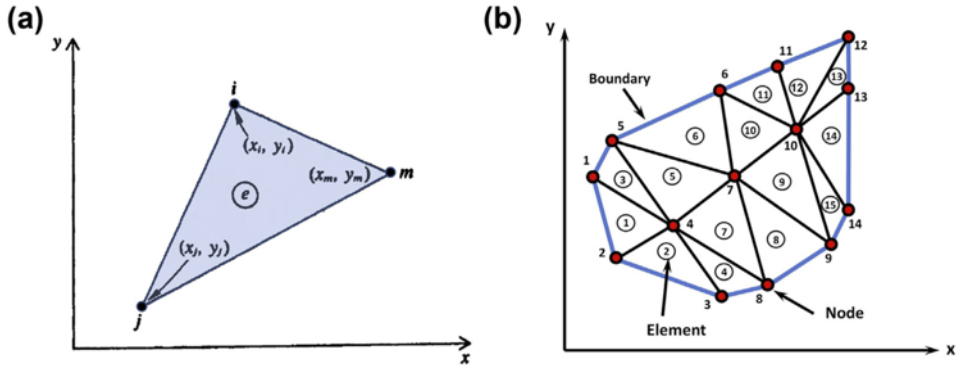

Figure 4.5: Two-dimensional horizontal finite-element mesh with triangular elements and notation. (a) A representative triangular element with nodes I, j, and m; (b) Subdivision of the domain in triangular elements. (Anderson et al, 2005).

The implementation of FDM is simpler and more efficient than FEM in terms of computer memory and computational time, but the rectangular grid has some difficulties to represent irregular boundaries and describe significant zones of the domain with a denser local grid spacing (Gao et al., 2019). FEM, using triangular and various irregularly shaped elements, may have an unstructured mesh. This allows more flexibility to describe irregularly shaped domains and concentrate elements in regions where variations in the considered variable are larger or better accuracy is needed (Bear and Cheng, 2010). The main differences between the two methods are presented in Table 4.1.

Table 4.1: Main Differences between FDM and FEM

	Finite Difference Method (FDM)	**Finite Element Method (FEM)**
Basic principles	Based on the differentiation: the differential equation is converted to a difference equation	- Integration of simple function - Weighted residual (reducing the error)
Advantages	- Easiest method to implement - Taylor series based - Low computational requirements	- Can use irregular grid (suitable to complex geometries and boundaries) - Can be applied to anisotropic media
Disadvantages	- Need to have regular grid (difficulties representing irregular boundaries)	- More complex than to FDM

In the last decades, thanks to the improvements in the software capabilities countless models have been developed to simulate fate and transport processes under different environmental conditions at laboratory and field scales, by researchers and universities, governmental agencies, and commercial companies. (Balseiro-Romero et al.,2018, Bear and Cheng, 2010). Some government agencies, such as the U.S. Geological Survey (USGS) or the U.S. Environmental Protection Agency (USEPA), have been particularly productive, by providing several public domain codes (Bear and Cheng, 2010). Focusing on transport in the unsaturated medium, several reviews of numerical models are available in scientific literature, some review contain model with general application (Vanderborght et al., 2005, Bear and Cheng., 2010; Šimůnek and van Genuchten, 2016; Wilson et al. 2018) others consider only models

suited to more specific purposes (Karapanagioti et al., 2002; Mulligan and Yong, 2004, Rivett et al., 2011).

Given the large number of models, many of them with comparable characteristics, a non-exhaustive list of numerical models is provided based on their widespread use and applicability to risk assessment. R-UNSAT (Lahvis and Baehr, 1997) is a FDM developed by USGS that solves axisymmetric, reactive, multispecies transport in the unsaturated zone. It is able to simulate transport mechanisms (gas diffusion and aqueous advection and dispersion) and reaction mechanisms (sorption and biodegradation). Examples of applications of this model are presented by Lahvis and Rehmann (1999) and Day et al. (2001), which simulate scenarios of transport and fate of MTBE and other fuel components to groundwater, and Peterson et al. (1999), which determine the biodegradation and volatilization of six volatile organic compounds (VOC) in a 150-meter deep vadose zone. SUTRA is a FEM, also developed by USGS, initially released as a 2D code (Voss, 1984) and then improved to a 3D code (Voss and Provost, 2002). SUTRA models flow and transport phenomena under saturated and unsaturated conditions, with conditions of variable density, and, hence, has been widely used for simulating saltwater intrusion. Tsanis (2006) evaluate the leachate contamination of an aquifer coming from a landfill site; Cronkite-Ratcliff et al. (2012) implement a 3-D flow and transport model in a geostatistical model of an alluvial unit to produce a statistical distribution of flow and transport responses to the geologic heterogeneity. MODFLOW-SURFACT (HydroGeoLogic, 1998) is a FDM, based on the MODFLOW groundwater modelling software package of the USGS (McDonald and Harbaugh, 1988) which expands the capability of the code to the unsaturated domain. MODFLOW-SURFACT includes a module for contaminant transport that simulates single-species and multi-component transport, linear or nonlinear retardation, first-order decay and biochemical degradation. Min et al. (2010) use the model to predict leachate levels within a municipal solid waste landfill and evaluate design alternatives for landfill expansion. GEOSTUDIO (GEOSLOPE International Ltd., 2017) is a commercial finite element software composed by different modules for various physical problems. The modules SEEP/W and CTRAN/W are the most useful for fate and transport modelling: the module SEEP/W which computes the water flow velocity, the volumetric water content, and the water flux can be combined with the module CTRAN/W which analyses the contaminant transport in water phase. Allam et al. (2019) use a simple 2D model to assess the abilities of inclined barrier walls to retard the migration of contaminants through porous media. Pratt and Fonstad (2017) assess the impact of leachate arising from carcass disposal burial pits. COMSOL (COMSOL Multiphysics, 2010) is a commercial finite element software package for several physics and engineering applications, that allow

modelling a wide variety of environmental flow (e.g., two-phase flow, fracture flow, flow according to the Darcy, Brinkman or incompressible Navier-Stokes equations) and transport phenomena with a coupled approach. Due to its complexity, it is used mainly for research industrial application, but some applications can be found in water resources management, for example Wissmeier and Barry (2011) present a multi-component solute transport model in two and three-dimensional domains in combination with several geochemical reactions.

Table 4.2:Comparison between the analysed software

Model	Software	Type	Processes	Characteristics
R-UNSAT	Public domain	2D FDM	Advection Dispersion (vapour and aqueous phases) Sorption Decay	Advective - dispersive transport of compounds in the aqueous phase associated with ground-water recharge in the unsaturated medium Gas transport based on Fick's Law of diffusion
SUTRA	Public domain	2D-3D FEM	Advection (with variable density) Dispersion Sorption Decay	Dissolved constituents and immiscible liquids Percolation and flow in the unsaturated medium
MODFLOW-SURFACT	Public domain	2D-3D FDM	Advection Dispersion Sorption Decay	Contaminant transport in aqueous phase in the unsaturated medium Single-species and multi-component transport
GEOSTUDIO (SEEP/W-CTRAN/W)	Commercial	2D FEM	Advection Dispersion Sorption Decay	Contaminant transport in aqueous phase in the unsaturated medium
COMSOL	Commercial	2D-3D FEM	Advection Dispersion Sorption Various chemical reactions	Porous media flows in the laminar and turbulent flow regimes Contaminant transport and heat transfer together with arbitrary chemical kinetics in the unsaturated medium

5. Comparative assessment of analytical transport models

(Based on: *Stoppiello, M.G.; Lofrano, G.; Carotenuto, M.; Viccione, G.; Guarnaccia, C.; Cascini, L. "A Comparative Assessment of Analytical Fate and Transport Models of Organic Contaminants in Unsaturated Soils". Sustainability 2020, 12, 2949*)

In Chapter 5 a review of selected analytical models is developed, in order to identify features and limitations and highlight the differences in the outcomes of the different models. The models have been selected based on their common characteristics. Specifically, all the models reproduce the fate and transport of organic contaminants dissolved in the aqueous phase from unsaturated zone to groundwater, assuming steady-state flow and constant parameters over the time.
Comparative simulations were carried out with five target contaminants (Benzene, Benzo(a)pyrene, Vinyl Chloride, Trichloroethylene, and Aldrin) with different decay's coefficient, three types of soil (sand, loam and clay) and three different thickness of the contaminant source. The analysis of the models allows identifying three groups of models according to the assumptions on contaminant source and physico-chemical mechanisms occurring during the transport.

5.1 Reasoned selected models

Many risk assessment models and analytical solutions exist for simulating contaminant transport in the unsaturated zone. In order to develop a quantitative review, six models have been selected and compared on the base of common characteristics. They are presented in: ASTM (2000); Troldborg et al. (2009); Troldborg et al. (2008), Verginelli and Baciocchi (2013), Enfield et al. (1982), Spence and Walden (2001).
The common features of the selected models listed as I; II; III; IV; V; VI in Table 5.1; are: i) the assessment of the concentration of a single contaminant dissolved in

aqueous phase that moves to the water table from a source located in the unsaturated zone; ii) the neglection of movement of substances in non-aqueous phase; iii) the small number of geometrical; hydrogeological and chemical input data; iv) the use of several simplifying assumptions. These characteristics make them straightforward tools in many applications such as analysis of groundwater vulnerability to pesticides contamination; risk assessment of contaminated sites (Di Sante et al.; 2014; Di Gianfilippo et al.; 2018; Meza et al.; 2010). The selected models can be coupled to models reproducing transport in other media and they can be included in integrated approaches which assess the fate and transport of contaminants between the different environmental media.

Table 5.1: Analytical solutions of the selected models.

Group	Model	Boundary and initial conditions	Solution	Reference
1	I	(-)	$C_w(z = L_f) = SAM \cdot C_{w0}$ $SAM = \frac{L_1}{L_f + L_1}$	*ASTM, 2000*
	II	$C_w(z,x,y,0) = 0 \quad 0 < z < \infty \quad -\infty < x < \infty \quad -\infty < y < \infty$ $C_w(0,x,y,t) = \begin{cases} C_{w0} & -\frac{X}{2} < x < \frac{X}{2}, -\frac{Y}{2} < y < \frac{Y}{2} \\ 0 & otherwise \end{cases}$	$C_w(z,x,y,t) = \frac{C_{w0}}{8} \int_{\tau=0}^{\tau=t} f'_z(z,\tau) f'_x(x,\tau) f'_y(y,\tau)\, d\tau$ $f'_z(z,\tau) = \frac{z}{\sqrt{\pi D'_z}} exp\left(\frac{v'z}{2D'_z}\right) \cdot exp\left[-\tau\left(\frac{(v')^2}{4D'_z} + \lambda'\right) - \frac{z^2}{4D'_z\tau}\right] \cdot \tau^{-3/2}$ $f'_x(x,\tau) = \left\{ erf\left[\frac{x + \frac{X}{2}}{2\sqrt{D'_x t}}\right] - erf\left[\frac{x - \frac{X}{2}}{2\sqrt{D'_x t}}\right] \right\}$ $f'_y(y,\tau) = \left\{ erf\left[\frac{y + \frac{Y}{2}}{2\sqrt{D'_y t}}\right] - erf\left[\frac{y - \frac{Y}{2}}{2\sqrt{D'_y t}}\right] \right\}$	*Troldborg et al., 2009*
2	III	(-)	$C_w(t) = C_{w0} \exp(-\mu_1 t)$ $\mu_1 = \frac{\theta_W}{\theta_W + \rho_b K_d + H\theta_a} \left(\frac{I_{eff}}{L_2 \theta_W} + \lambda\right)$	*Troldborg et al., 2008*
	IV	$C_w(z=0) = C_{w0}$ $\frac{d^2 C_w}{dz^2}(z = L_f) = 0$	$C_w(z,t) = C_{w0} \cdot \alpha_{dep}(t) \cdot \alpha_{leach}$ $\alpha_{dep}(t) = \exp(-\mu_2 \cdot t) \qquad \mu_2 = \frac{I_{eff} \cdot K_{sw}}{R \cdot L_1 \cdot \rho_s} + \frac{\lambda_{source} \cdot \theta_w \cdot K_{sw}}{\rho_s}$ $\alpha_{leach} = \frac{\sigma \cdot \exp(k \cdot z)}{k \cdot \sinh(\sigma \cdot z) + \sigma \cdot \cosh(\sigma \cdot z)} \qquad k = \frac{z}{2 \cdot D \cdot t_{leach}} \qquad \sigma = \sqrt{k^2 + \frac{\lambda \cdot \theta_w}{D}}$	*Verginelli and Baciocchi, 2013*
3	V	$C_w(z,t=0) = \begin{cases} 0 & -\infty < z < -z_0 \\ C_{w0} & -z_0 < z < 0 \\ 0 & 0 < z < \infty \end{cases}$ $\lim_{z \to \infty} \frac{\partial C_w}{\partial z} = 0$	$C_w(z,t) = \frac{C_{w0}}{2} \exp(-\lambda t) \left\{ erf\left[\frac{z + z_0 - \frac{v\,t}{R}}{2\sqrt{\frac{Dt}{R}}}\right] - erf\left[\frac{z - \frac{v\,t}{R}}{2\sqrt{\frac{Dt}{R}}}\right] \right\}$	*Enfield et al., 1982*
	VI	$C_w(z,0) = 0$ $C_w(0,t) = C_{w0} \exp(-\mu_3 t)$ $\frac{\partial C_w}{\partial z}(\infty, t) = 0$	$C_w(z,t) = C_{w0} \exp(-\mu_3 t) \frac{1}{2} exp\left[\frac{(v-w)z}{2D_z}\right] erfc\left[\frac{zR - wt}{2\sqrt{D_z R t}}\right] + \frac{1}{2} exp\left[\frac{(v+w)z}{2D_z}\right] erfc\left[\frac{zR + wt}{2\sqrt{D_z R t}}\right]$ $w = \bar{v} \sqrt{1 + \frac{4D_z R}{v^2}[\lambda - \mu_3]}$ $\mu_3 = \frac{I_{eff} K_{sw}}{L_1 \rho_b} + \frac{D_{eff} H}{\rho_b L_1 L_d}$	*Spence & Walden, 2001*

They differ mainly in their assumptions on the source and in the physical-chemical mechanisms as highlighted in Table 5.2.

Table 5.2: Features of the selected models.

Group	Model	Source				
		On ground surface	**Inner domain**	**Continuous**	**Time-Varying**	**Residual NAPL phase**
1	I		x	x		
	II		x	x		
2	III		x		x	x
	IV		x		x	x
3	V	x			x	
	VI		x		x	x

Group	Model	Chemical-physical mechanisms during the transport					Solve transport equation
		Advection	**Dispersion-diffusion in water**	**Diffusion in gas**	**Sorption**	**Degradation**	
1	I	x			x		
	II	x	x (3D)	x (3D)	x	x	x
2	III	x					
	IV	x	x (1D)		x	x	x (steady state)
3	V	x	x (1D)		x	x	x
	VI	x	x (1D)		x	x	x

The reference scheme assumed by the models is depicted in Figure 5.1. It consists of an unsaturated layer lower bounded by an aquifer. The contaminant source is located in the subsoil or on the ground surface, characterized by a parallelepiped shape with dimensions L_1; X and Y. The position along the z-axis is given by L_f and L_2 with regard to the water table and by L_d as regards the ground surface. The unsaturated zone has homogeneous and isotropic hydrogeological properties θ; θ_w; θ_a; ρ_b; K_{sat}; f_{oc}; I_{eff} are fixed for the unsaturated soil, according to the hypotheses of the models. The physical-chemical behaviours of the contaminants are indicated by H; D_a; D_w; S; K_{oc}. The selected models, except Model I, consider the degradation processes of the contaminant in water phase using a first-order kinetic formulation where λ is the degradation constant.

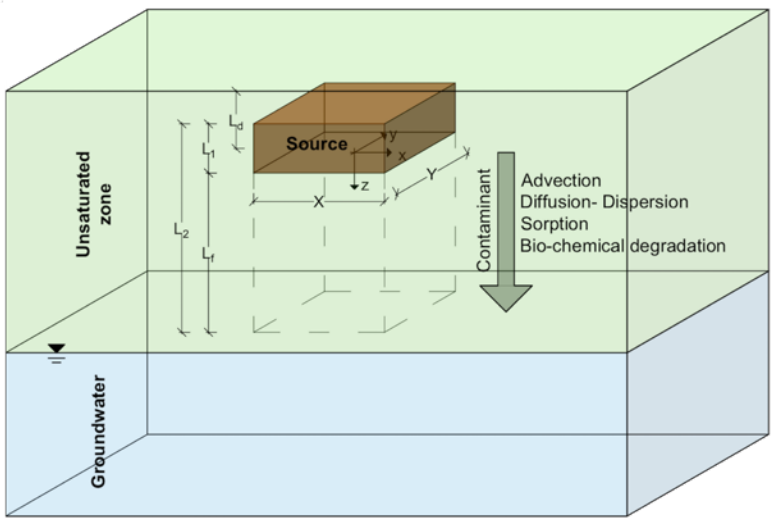

Figure 5.1: Reference scheme

The total concentration of the contaminant is expressed using C_{tot} (Eq. (1)), the total mass of the contaminant upon the mass of the affected soil,

$$C_{tot} = \frac{M_{tot}}{\rho_b V}. \tag{5.1}$$

The concentration of the contaminant in the different phases (water, solid and air) is expressed using:

$$C_w = \frac{M_w}{\theta_w V}, \tag{5.2}$$

the mass of the dissolved contaminant upon the volume of pore water;

$$C_s = \frac{M_s}{\rho_b V}, \tag{5.3}$$

the mass of the contaminant sorbed by the soil fraction upon the mass of the affected soil;

$$C_a = \frac{M_a}{\theta_a V}, \tag{5.4}$$

the mass of contaminant in vapor phase upon the volume of pore air.

In all models, the partitioning of the chemical between these three different phases is expressed by instantaneous linear equilibrium.

When low solute concentration occurs a linear adsorption isotherm can be assumed (Mulligan and Yong, 2004). Thus, the ratio between C_s and C_w is constant and equal to K_d, so

$$C_s = K_d \cdot C_w \tag{5.5}$$

where

$$K_d = f_{oc} \cdot K_{oc} \tag{5.6}$$

for organic contaminants.
The liquid-vapor partition is evaluated through the Henry's Law:

$$C_a = H \cdot C_w \ . \tag{5.7}$$

On the basis of the previous equations, the dissolved concentration in pore water C_w can be evaluated from C_{tot}:

$$C_w = K_{SW} \cdot C_{tot} \tag{5.8}$$

where K_{sw} is expressed in Eq. (9),

$$K_{SW} = \frac{\rho_b}{\theta_W + \rho_b K_d + H\theta_a} \ , \tag{5.9}$$

and represents the dissolution of soil contaminants into infiltrating rainwater according to the hypothesis of instantaneous and linear equilibrium.
The maximum value of C_w is the solubility (*S)* of the contaminant. Therefore, taking into account only air, water and solid phases, the maximum C_{tot} is:

$$C_{tot,sat} = \frac{S}{K_{SW}} \ . \tag{5.10}$$

Some of the selected models (Models III, IV, VI, Table 5.1) take into account the presence of a residual NAPL (Non-Aqueous Phase Liquid) in the source. This allows to consider an initial C_{tot} higher than $C_{tot,sat}$. For these models, when the measured C_{tot} is higher than $C_{tot,sat}$, it is possible to consider C_{tot} as a sum of two components:

$$C_{tot} = C_{tot,sat} + C_{NAPL} \tag{5.11}$$

where C_{NAPL} is the concentration of the contaminant in non-aqueous phase.

The initial dissolved concentration in pore water at the source C_{w0} can be evaluated as follows:

$$C_{w0} = K_{SW} \cdot C_{tot} \qquad for \quad C_{tot} < C_{tot,sat} \tag{5.12}$$

$$C_{w0} = S \qquad for \quad C_{tot} \geq C_{tot,sat} \ . \tag{5.13}$$

In all the analyses developed in this paper, the C_{tot} is assumed less than $C_{tot,sat}$ in order to use the same initial C_{tot} for all the simulations.
Based on the common characteristics the models can be organized into three groups. The first group is composed by models with a continuous source (Models I and II), leading to a constant concentration after a certain period of time. The second group considers a decaying source. In this case, the transport equation is not solved (Models III) or it is solved for a steady state (Model IV). Finally, the third group considers a decaying source and a solution of the transport equation in transient conditions (Models V and VI). Specific features of the models will be carefully described in the following paragraphs.

5.1.1 Model I

Model I has been developed by the ASTM (American Society for Testing and Materials) and described in Appendix 3 of the Standard Guide for Risk-Based Corrective Action (ASTM, 2000). It provides a very basic approach to estimate the dissolved concentration of contaminant at the water table. The model is based on the determination of the contaminant Leachate Factor (LF), which represents the steady ratio between the contaminant concentration in the soil source and the resultant concentration in groundwater. This approach may be applied to both organic and inorganic contaminants and it is adopted by various software for risk assessment, e.g. Risk-Based Corrective Action (RBCA) Tool Kit for Chemical Releases (Connor et al., 2007). Its widespread use is related to its simplicity of use and a limited number of input parameters. The source is assumed uniform and constant, the only considered transport mechanism is the steady leaching from the source to the groundwater table.

The LF is composed by three coefficients: K_{SW}, see Eq. (5.9), SAM (Soil Attenuation Model) and LDF (Leachate-groundwater Dilution Factor). SAM, introduced by Connor et al. (2007), represents the attenuation of contaminant concentration caused by the sorption of chemicals related to the leaching through the clean soil. This coefficient is derived from the principle of mass conservation and it depends only on the geometry of the scheme. In fact, it is defined as a ratio between source thickness L_1 and the distance between the top of the source and the water table L_2. Thus, it is possible to obtain C_w at the water table, as reported in Table 5.1- Model I. LDF evaluates the uniform dilution of the leachate with groundwater within a mixing zone in the aquifer, but this mechanism is not analysed in the paper.

5.1.2 Model II

Model II is presented in Troldborg et al. (2009) and differs from the others because it takes into account combined gas and water phase diffusion in three dimensions. For this reason, the model is particularly suitable when gas phase transport may be prevalent, as for volatile organic compounds. It assumes mono-dimensional advection in water phase and three-dimensional diffusion in gas and water phases. In addition, it considers uniform and constant concentration of the contaminant in the source, neglecting the attenuation processes. Furthermore, soil sorption and first-order degradation take place in the unsaturated zone.

The starting point of the transport equations for water phase and gas phases is:

$$\begin{cases} \frac{\partial R\theta_w C_w}{\partial t} = [\boldsymbol{\nabla} \cdot (\theta_w \boldsymbol{D_w})] \cdot \boldsymbol{\nabla} C_w - I_{eff} \frac{\partial C_w}{\partial z} - \lambda \theta_w C_w \\ \frac{\partial \theta_a C_a}{\partial t} = [\boldsymbol{\nabla} \cdot (\theta_a \boldsymbol{D_a})] \cdot \boldsymbol{\nabla} C_a \end{cases} \tag{5.14}$$

where R is assumed as follows:

$$R = 1 + \frac{\rho_B}{\theta_w} K_d \ . \tag{5.15}$$

From equations (14), Troldborg et al. obtained the following Eq. (16)

$$\frac{\partial C_w}{\partial t} + v' \frac{\partial C_w}{\partial z} - \nabla \boldsymbol{D'} \cdot \nabla C_w + \lambda' C_w = 0 \tag{5.16}$$

where:

$$v' = \frac{I_{eff}}{R'} \ , \tag{5.17}$$

$$\boldsymbol{D'} = \begin{pmatrix} D'_x & 0 & 0 \\ 0 & D'_y & 0 \\ 0 & 0 & D'_z \end{pmatrix}, \tag{5.18}$$

$$\lambda' = \frac{\theta_w \lambda}{R'} \ , \tag{5.19}$$

and the parameter R' is equal to:

$$R' = R\theta_w + H\theta_a. \tag{5.20}$$

The dispersion coefficients of the diagonal tensor **D** are given by:

$$D'_x = D'_y = \frac{(\theta_w D_w^e + \theta_w \alpha_t v + H\theta_a D_a^e)}{R'} \tag{5.21}$$

$$D'_z = \frac{(\theta_w D_w^e + \theta_w \alpha_l v + H\theta_a D_a^e)}{R'} \tag{5.22}$$

where D_w^e and D_a^e are estimated according to Moldrup et al. (2001) and v is calculated according the equation:

$$v = \frac{I_{eff}}{\theta_w} \ . \tag{5.23}$$

The set of initial and boundary conditions is shown in Table 5.1-II. The solution of Eq. (5.16) was developed by Sagar (1982) and Wexler (1992) and has been reported in Table 5.1- Model II.

Troldborg et al. (2009) pointed out that the evaluation of the contaminant dilution in groundwater is more difficult using a three dimensional model because the contaminated area at the water table is bigger than the source area, therefore the dilution water volume has to be evaluated and the concentrations are not spatially constant within this area.

5.1.3 Model III

Model III, presented in Troldborg et al. (2008), is a subset module of a large model, named CatchRisk; this model evaluates the contaminant transport from a point source to the groundwater. In Model III the unsaturated zone is designed like a reactor where the mass flux is governed only by water advection and the other transport mechanisms are neglected, so the transport equation is not solved as in the

Model I. On the opposite, Model III assumes that the dissolved concentration is constant along the depth.

The decay of the source concentration is taken into account. The mass of contaminant within the compartment decreases due to both leaching by water percolating through the unsaturated zone and degradation of the contaminant in water phase. The dissolved concentration over the time can be obtained solving a mass balance in which the variation over the time of the mass of chemical is set equal to the rate of mass depletion due to leaching and degradation. The solution of this mass balance is shown in Table 5.1-Model III.

Furthermore, the model considers the residual non-aqueous phase concentration in the source. If the mass of contaminant is higher than the equilibrium mass, a separate phase is present. At the initial time, Ctot and C_{w0} are described, respectively, by Eq. (5.11) and Eq. (5.13) and the total contaminant mass is equal to:

$$M_{tot} = C_{tot}\, \rho_b\, V\ . \tag{5.24}$$

The mass flux J, leaving the unsaturated zone, described in Eq. (5.25), is constant over the time until the contaminant mass is equal to the mass equivalent to saturation conditions M_{sat}, defined in Eq. (5.26),

$$J = S\, X\, Y\, I_{eff}\ , \tag{5.25}$$

$$M_{sat} = \frac{S}{K_{sw}}\, \rho_b V. \tag{5.26}$$

When M_{tot} is equal to M_{sat}, C_w can be calculated through the solution shown in Table 5.1-Model III.

5.1.4 Model IV

The analytical model proposed in Verginelli and Baciocchi (2013) is composed of three terms: $\alpha_{dep}(t)$, α_{leach} and LDF. $\alpha_{dep}(t)$ considers the source depletion caused by leaching and biodegradation. α_{leach} describes the transport phenomena, taking into account the mechanisms of advection, dispersion-diffusion, sorption and biodegradation. LDF evaluates the dilution of the contaminant with groundwater within a mixing zone in the aquifer, but, as mentioned above, this mechanism is not analysed in the paper.

$\alpha_{dep}(t)$ is defined by an exponential law, obtained from a mass balance that includes the mass losses caused by leaching and biodegradation, reported in Table 5.1-Model IV.

Furthermore, the model includes the presence of a residual phase in the source. In this case, the dissolved concentration in the source over the time is equal to:

$$C_w(t) = \begin{cases} C_{w0}\, \alpha_{dep}(t) & for\ t^* \leq 0 \\ S\, \alpha_{dep}(t) & for\ t^* > 0 \end{cases} \tag{5.27}$$

where

$$\alpha_{dep}(t) = \begin{cases} \exp(-\mu_2 t) & for\ t^* \leq 0 \\ \exp(-\mu_2 (t - t^*)) & t^* > 0,\ for\ t > t^* \\ 1 & t^* > 0,\ for\ 0 < t \leq t^* \end{cases} \quad (5.28)$$

and t^* is the time when the initial source concentration reaches the saturation conditions

$$t^* = \frac{C_{tot} - C_{tot,sat}}{C_{tot,sat}\,\mu_2}. \quad (5.29)$$

α_{leach} is obtained solving the advection-diffusion differential equation for the steady state:

$$D_z \frac{d^2 C_w}{d^2 z} - v_{leach} \frac{dC_w}{dz} - \lambda \theta_w C_w = 0\ . \quad (5.30)$$

The dispersion-diffusion coefficient D_z is calculated as:

$$D_z = \alpha_l v_{leach} + D_w^e \quad (5.31)$$

where D_w^e is calculated as:

$$D_w^e = D_w^0 \frac{\theta_w^{10/3}}{\theta^2}\ . \quad (5.32)$$

Unlike the other models, the seepage velocity is not obtained from the effective infiltration, but from the time required by the contaminant to reach the underlying water table t_{leach}. It is calculated as a linear function of the time required for infiltrating water to reach the water table t_w using the retardation coefficient of the contaminant R:

$$t_{leach} = R\ t_w. \quad (5.33)$$

R is calculated according to the following equation:

$$R = 1 + \frac{\rho_b K_{sw}}{\theta}\ . \quad (5.34)$$

The time t_w is calculated using the Green and Ampt equation (Green and Ampt, 1911):

$$t_w = \frac{\theta_a}{K_{sat}} \left[L_f - (H_w - h_{cr}) \ln \left(\frac{H_w + L_f - h_{cr}}{H_w - h_{cr}} \right) \right] \quad (5.35)$$

where H_w is the ponding depth of water surface, h_{cr} the wetting front suction head.

The set of initial and boundary conditions to be given to the differential equation (5.30) is shown in Table 5.1-Model IV.

The analytical solution proposed by the authors is the following:

$$C_w = \alpha_{leach}\ C_{w0}\ . \quad (5.36)$$

The value of the term α_{leach} is reported in Table 5.1- Model IV as well.

5.1.5 Model V

PESTAN (PESTicide ANalytical) is a software developed by the US EPA (Environmental Protection Agency of United States) to assess the transport of

organic contaminants, mainly pesticides (Ravi and Johnson, 1994). The theoretical model underlying the software PESTAN has been published in Enfield et al. (1982). This model differs from the others mainly for the conceptualization of the source. The source is considered a mass of granular solid contaminant, located on the ground surface, which dissolves in a "slug" of contaminated water infiltrating into the soil. The thickness of the slug z_0 is the equivalent depth of the pore water required to dissolve the total mass of the solid chemical in water.

In order to compare the model with the others, the reference scheme presented above has been adopted and z_0 has been assumed equal to the equivalent depth of the pore water contained in the source (Eq. (5.37)).

$$z_0 = \theta_w L_1 . \tag{5.37}$$

The differential equation underlying the model (Eq. (5.38)) takes into account the following mechanisms: advection and dispersion in the vertical dimension, sorption and biochemical degradation described according to a first order kinetic.

$$R \frac{\partial C_w}{\partial t} = D \frac{\partial^2 C_w}{\partial z^2} - v \frac{\partial C_w}{\partial z} - \lambda C_w, \tag{5.38}$$

where R is reported in Eq. (5.34).

D is evaluated through the relationship of Biggar & Nielsen (1976)

$$D = D_w^e + 2.93 v^{1.11} \tag{5.39}$$

where D and D_w^e are expressed in cm^2 day^{-1} and v in cm day^{-1}.

The initial and boundary condition for the equation (5.38) and the proposed analytical solution are given in Table 5.1- Model V.

5.1.6 Model VI

Model VI is implemented in the risk assessment software RISC$_4$ (Spence and Walden, 2001) upgraded to a newer version RISC$_5$, which incorporates the approach developed in Ünlü et al. (1992). In this model the source depletes with time, due to the simultaneous effect of leaching and volatilization of volatile organic contaminants (VOC), but, unlike the previous model, biological degradation is neglected. The presence of a residual phase in the source is considered, as described above.

The leachate concentration in the source decays exponentially with time. The exponential law is obtained from a mass balance where the variation over the time of the mass of chemical is equal to the rate of mass depletion due to leaching and volatilization. The source depletion law obtained is:

$$C_w(t) = C_{w0} \exp(-\mu_3 t) . \tag{5.40}$$

The coefficient μ_3 is described by the following equation:

$$\mu_3 = \frac{I_{eff} K_{sw}}{L_1 \rho_b} + \frac{D_{eff} H}{\rho_b L_1 L_d} . \tag{5.41}$$

where D_{eff} is the effective diffusion coefficient in soil estimated using the Millington-Quirk relationships (Millington and Quirk, 1961)

$$D_{eff} = D_w^0 \left(\frac{\theta_w^{10/3}}{\theta^2}\right) + D_a^0 \frac{1}{H}\left(\frac{\theta_a^{10/3}}{\theta^2}\right) \quad (5.42)$$

and L_d is the distance from the ground surface to the center of the source.
The Model VI is ruled by the same differential equation of Model V (Eq. (5.38)).
The dispersion coefficient is assumed as a linear function of the seepage velocity (Eq. (5.43)) because the mechanism of molecular diffusion is neglected,

$$D_z = \alpha_l v \quad (5.43)$$

where α_l is calculated using the Gelhar relationship (Gelhar, 1985):

$$ln\alpha_l = -4.933 + 3.811 lnz_m \qquad z_m \leq 2 \quad (5.44)$$

$$ln\alpha_l = -2.727 + 0.584 lnz_m \qquad z_m \geq 2 \quad (5.45)$$

where z_m is the distance from the source to the observation location.
The set of initial and boundary condition and the solution to be given, see (Van Genuchten and Alves, 1982), are reported in Table 5.1- Model VI.

5.2 Comparison methodology

The analysis of the models has been carried out by comparing the solutions of the models for the same scenario and by carrying out simulations with different types of soils, different contaminants and different thickness of the source for each model. These latter simulations make possible to evaluate the outputs with reference to different soil parameters and contaminant properties since the models do not respond in the same way to the variation of the parameters because of the diverse assumptions about the source and the transport mechanisms.
The models have been applied to the reference scheme represented in Figure 5.1. The values of the geometrical parameters of the scheme depicted in Figure 5.1 have been reported in Table 5.3. Three types of soils, that differ mainly in water content and hydraulic conductivity have been chosen: sand, loam and clay. Furthermore, five organic contaminants have been selected for their different mobility and biodegradability characteristics in order to explore a wide range of fate and transport mechanisms. The soil parameter values have been derived from Carsel and Parrish (1988), Connor et al. (1996) and listed in Table 5.4. It is worth nothing that the proposed values of Carsel and Parrish are not strict as in the literature variable ranges can be found for the same soil. The contaminant chemical properties have been derived by USEPA (1996), except for the first order degradation constant λ. The chosen value of λ is the minimum of the range reported in Howard (2017) because it represents the most conservative value. The C_{w0} has been chosen on the basis of

values found in contaminated sites (Hallberg, 1989; Troldborg et al., 2009; Shao et al., 2014; Schiefler et al., 2018). The properties of the selected contaminants have been reported in Table 5.5.

Table 5.3: Values of the geometrical parameters.

Parameter*	Measurement unit	Value
L_1	m	2
X	m	4
Y	m	4
L_f	m	5

Table 5.4: Soil parameters values.

Parameter*	Measurement unit	Value		
		Sand	Loam	Clay
ρ_b	kg/m^3	1700	1700	1700
θ	-	0.385	0.352	0.312
θ_w	-	0.130	0.200	0.304
θ_a	-	0.300	0.230	0.076
h_{cr}	m	-0.0164	-0.178	-0.269
I_{ef}	m/s	5.708E-09	2.854E-09	5.708E-10
K_{sat}	m/s	8.250E-05	2.889E-06	5.556E-07
f_{oc}	-	0.001	0.001	0.001

Table 5.5: Physical-chemical properties values of the selected contaminants.

Parameter*	Measurement Unit	Contaminant				
		Benzene	Benzo(a)pyrene	Vinyl chloride	Trichloroethylene	Aldrin
H	-	2.280E-01	4.630E-05	1.110E+00	4.220E-01	6.970E-03
S	kg/m^3	1.750E+00	1.620E-06	2.760E+00	1.100E+00	1.800E-04
D_a	m^2/s	8.800E-06	4.300E-06	1.060E-05	7.900E-06	1.320E-04
D_w	m^2/s	9.800E-10	9.000E-10	1.230E-10	9.100E-10	4.860E-10
K_{oc}	m^3/kg	6.170E-02	9.690E+02	1.860E-02	9.430E-02	4.870E+01
λ	1/s	1.114E-08	7.567E-09	2.790E-09	4.852E-09	6.778E-09
C_{w0}	µg/dm^3	100	1	100	100	10

The application of fate and transport models is significantly influenced by the high uncertainty of input parameters due to as well as the limited availability of site-specific data. Indeed, for some parameters (e.g. dispersivity coefficient, first-order degradation rate) the values may vary by more than one order of magnitude for the same contaminant and soil type (Vanderborght and Vereecken, 2007; Mulligan and Yong, 2004). Hence, some insights about the response of the models to the variation of parameters could be useful to the selection of a model over another.

5.3 Results and discussions

5.3.1 Predicted concentration according to the different models

In order to provide a first overview of the differences between the solutions of the models, the values of C_w at a given depth have been calculated as a function of time and compared for all the models. The aim is to make explicit the behaviour over the time of the models, fixing a single contaminant (Trichloroethylene, TCE), the soil type (sand) and the source thickness (2 m) and the depth of the water table equal to 5 m.

The results of the ratio between $C_w(t)$ and C_{w0} have been plotted in Figure 5.2. A secondary y-axis has been added to give a clear graphical view of the results since two models (V and VI) provide outputs of different magnitude than the others.

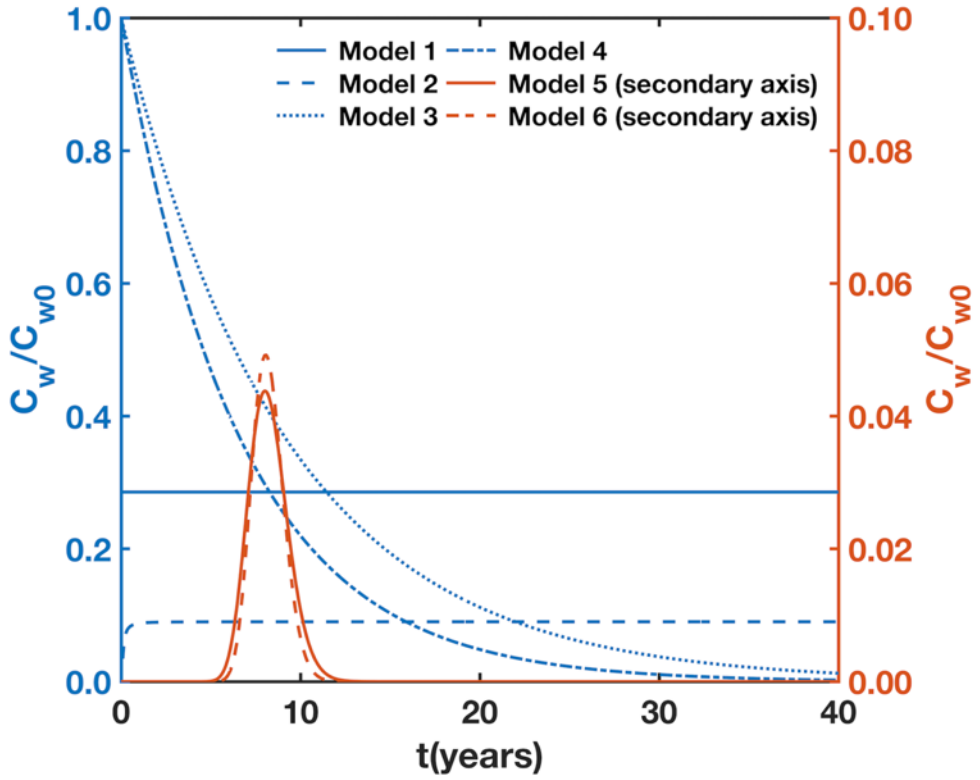

Figure 5.2: Predicted dimensionless concentration C_w/C_{w0} of TCE at z=5 m according to the selected models versus time. Results of model V and VI are scaled by making use of the secondary axis.

As shown in Figure 5.2, the source and the transport mechanisms influence both the value of the initial dimensionless concentration and the shape of the curve. The outputs of the models validate the division into the three groups previously indicated: group 1 (Model I and II) shows a constant concentration over the time (with the exception of an initial transient phase for the latter); group 2 (Model III and IV) shows a decreasing exponential trend and group 3 (Model V and VI) exhibits a bell-shaped curve.

Model I is evidently the most elementary because it neglects the fate and transport mechanisms over the time. Therefore, the normalized concentration remains constant. Conversely, Model II solves the transport equation and considers a constant source, therefore at t equal to zero the value of C_w is zero and, after a transient phase, becomes constant. Although both the models show a similar trend over the time, Model II depends on the spatial coordinates *x*, *y*, and *z*. The models belonging to

group 1 can be used when the reduction processes of the source, like leaching and volatilization losses or biodegradation, are negligible, so the source can be considered constant.
The solutions of the second group are exponential laws that reproduce the depletion processes of the source. Model III assumes instantaneous mixing in the unsaturated zone and it does not consider transport mechanisms. Therefore, C_w is constant over the z axis and it decreases over the time. Instead, in Model IV the exponential law is multiplied by α_{leach}. In this scenario, the value of α_{leach} is approximately equal to 1, because of the selected type of soil and the contaminant. As a consequence, the exponential part is dominant. The depletion coefficients μ_1 and μ_2 are equal to 3.469 E-09 s^{-1} and 4.800 E-09 s^{-1}, respectively. They are indicators of the depletion rate of the contaminant and differ only for the retardation coefficient. Therefore, in these conditions, the results of the two models are very similar. For group 2, the source depletion processes (bio-chemical degradation and leaching losses) are predominant, while the transport mechanisms are less significative.
Models V and VI represent the most complete models because they consider both the source depletion and the transient transport equation. This causes the distinctive bell-shape and a lower concentration over the time than the other models. The solutions contain two parts: a time-dependent exponential law and the space- and time-dependent solution of the transport equation. As regards the first part, Model V takes into account only the biochemical degradation, while Model VI considers leaching and volatilization losses. The second part differs due to the initial and boundary conditions of the transport equation. For these reasons, the peaks of the solutions differ between the two models. In this scenario, for Model V the maximum of the normalized concentration is 4.338E-02 at 8.17 y, while in Model VI the maximum of the normalized concentration corresponds to 4.920 E-02 at 8.08 y. These models represent the fate and transport mechanisms in a more complete way than the other models. For this reason, the obtained concentrations are approximately an order of magnitude lower than the values of the others.
The different output concentrations of the models lead to different amounts of contaminant which reach the water table. In order to determine and compare the mass value reaching the groundwater for the different models, the mass flux (J) from unsaturated zone to groundwater is integrated over the time. J is governed only by water phase advection and it is evaluated as suggested by Troldborg et al. (2009):

$$J = C_w \, A_{uz-gw} \, v_{leach} \tag{5.46}$$

where $A_{uz\text{-}gw}$ is the exchange area between the two zones.
For all the models, except Model II, $A_{uz\text{-}gw}$ is equal to A and the dissolved concentration C_w is constant over the area. In the paper describing Model II

(Troldborg, 2009) $A_{uz\text{-}gw}$ is bigger than A and the concentration is variable with space, hence it is necessary integrate $C(x,y,t)$ over the space and the time.
For the considered contaminant (Trichloroethylene, TCE), soil type (sand) and source thickness (z=2m)), the mass reaching the water table in twenty years and forty years has been calculated starting from an initial source concentration C_{w0} (100 μg/dm^3) reported in Table 5.5. Results are reported in Table 5.6.

Table 5.6: Mass of TCE at the water table in twenty and forty years.

Group	Model	M_w (kg) in 20 years	M_w (kg) in 40 years
1	I	1.272E-02	2.534E-02
	II	2.201E-02	4.443E-02
2	III	1.798E-02	2.000E-02
	IV	1.393E-03	1.460E-02
3	V	2.599E-04	2.599E-04
	VI	2.391E-04	2.391E-04

The results highlight that the third group of models returns a lower contaminant mass than the others. As shown in Table 5.6, after 20 years the exponential models belonging to group 2, Model III and IV present highest results, while by extending the period of time to 40 years Model I shows the maximum value of mass.

5.3.2 Predicted concentration of different contaminants

The physical-chemical parameters values of the contaminant strongly affect its mobility through the unsaturated zone and its evolution over the time, since they are representative of properties like the affinity for the soil, the volatility and the rate of degradation (Weber et al. 1991; Mulligan and Yong, 2004). It is difficult to evaluate the effect of a single parameter on the model results because the involved parameters are several and they change simultaneously for each contaminant. Therefore, in order to highlight in the differences, output of different models with regard to the type of the contaminant, the selected models have been solved using the contaminants listed in Table 5.5. The simulated case is characterized by a thickness of the source equal to 2 m and a sand soil. The values of physical-chemical properties and the C_{w0} of the contaminants are listed in Table 5.5.
The amount of time, in which the transport mechanisms take place, ranges between some orders of magnitude according to the contaminant mobility. Hence, in order to overcome this discrepancy and compare the results, the dimensionless concentration has been plotted versus a dimensionless time τ, calculated as the ration between the physical time and a reference time t_{ref}. This criterion has not been used for Model I

because the results are independent of time and contaminant properties. In this case the t_{ref} has not been considered and the dimensionless concentration has been plotted versus time. The value of the t_{ref} cannot be evaluated in the same way for all the models, since in the models belonging to the groups 2 and 3 the dimensionless concentration goes to zero after a certain period of time depending on contaminants and the medium properties. Therefore, for the models belonging to the groups 2 and 3 the value of the t_{ref} has been set equal to the time when C_w/C_{w0} reaches the 0.1%, while for model II the value of the t_{ref} has been calculated with a different criterion because the results of the model tend to a horizontal asymptote. In this case the t_{ref} has been set equal to the time when the difference between the *i*-th and the previous step is less than a threshold value set at 0.01 μg/dm^3. Hence, for this model the value of t_{ref} also depends on the temporal discretization, which has been set equal to 1 month for Benzene, Vinyl chloride and Trichloroethylene and 1 year for Benzo(a)pyrene and Aldrin.
The values of the t_{ref} are listed in Table 5.7. By comparing the models of the group 2 and 3, it can be observed that Model III has the longest t_{ref} for all the contaminants and, more generally, the models belonging to group 2 show a longer t_{ref} than the other models for the contaminants characterized by a greater mobility (Benzene, Vinyl Chloride, and Trichloroethylene). For Benzo(a)pyrene and Aldrin, the t_{ref} of Model V is not reported because the C_w remains always below the threshold, as explained better below.

Table 5.7: Reference time evaluated for different contaminants and models.

Group	Model	t_{ref} (year)				
		Benzene	**Benzo(a)pyrene**	**Vinyl chloride**	**Trichloroethylene**	**Aldrin**
1	I	-	-	-	-	-
	II	1.75E-00	7.00E+00	1.17E-00	1.67E+00	1.00E+01
2	III	2.93E+01	2.00E+05	9.19E+01	6.33E+01	1.07E+04
	IV	2.18E+01	4.03E+04	6.72E+01	4.57E+01	2.29E+03
3	V	8.67E+00	-	6.83E+00	1.16E+01	-
	VI	9.08E+00	1.58E+05	5.75E+00	1.09E+01	7.73E+03

In Figure 5.3 the results of the comparisons between all the models are reported. For the Model II (Figure 5.3.b) it is possible to observe a marked distinction in the trend concentration between contaminants characterized by a less mobility (Benzo(a)pyrene and Aldrin) and the others (Benzene, Vinyl chloride, Trichloroethylene). The first group of contaminants reaches a steady-state concentration higher than the others: the C_w/C_{w0} ratio is equal to 0.443 for Benzo(a)pyrene and 0.358 for Aldrin. Instead, the second group reaches lower

values, the C_w/C_{w0} ratio is about equal to 0.090 for the three contaminants. The C_w/C_{w0} ratios for Benzo(a)pyrene and Aldrin in the Model II are higher than in Model I (C_w/C_{w0} =0.286). This proves as in some cases, the Model I is not the most conservative approach, as it is typically considered (ASTM, 2000). This result can be related to the fact that in Model I the SAM is assumed simplistically constant for all the contaminants.

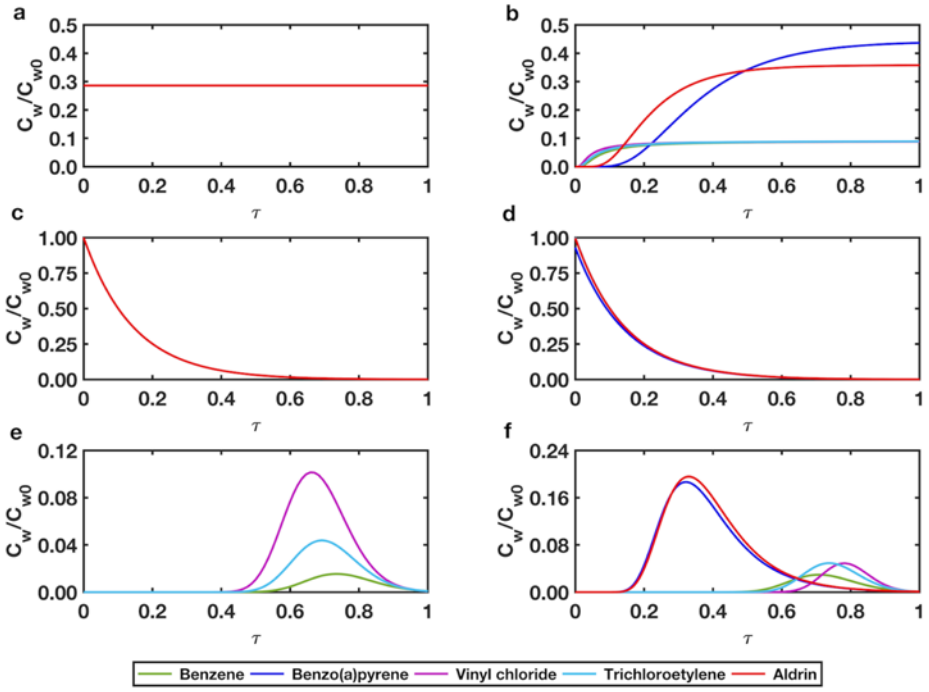

Figure 5.3: Dimensionless concentration C_w/C_{w0} versus dimensionless time τ for different contaminants. (a)Model I, (b) Model II, (c) Model III, (d) Model IV, (e) Model V, (f) Model VI.

In Model III, as can be seen from Figure 5.3.c, the results collapse on the same curve as a consequence of the use of dimensionless time. This occurs to some extent in Model IV. in fact, as explained above, it consists of two terms: α_{dep} and α_{leach}: the former is characterized by scale invariance while the latter is approximately equal to one for all the contaminants in the analysed case. The minimum value of α_{leach} has been obtained for Benzo(a)pyrene and it is 0.930.

In Model V the concentrations of contaminants with low mobility (Benzo(a)pyrene and Aldrin) is closed to zero during the whole interval time. The reason is that the transport mechanisms take place in a wide time interval (10^4-10^5 years), but the exponential part of the model becomes zero using these values of time. Therefore,

the results of this model (Figure 5.3.e) are shown only for the three contaminants Benzene, Vinyl Chloride and Trichloroethylene. Finally, the results of Model VI are shown in Figure 5.3.f, for which it is possible to identify the two groups of contaminants, characterized by low and high mobility, respectively. The contaminants of the first group reach the peak in the first part of the interval time and with a value of Cw/C_{w0} higher than the second group. The same behaviour has been highlighted in Model II.

5.3.3 Comparison between different decay coefficient

The decay coefficient λ takes into account contaminant degradation in the environment, which is simulated in the selected models through a first order kinetics. The contaminant degradation considers both chemical mechanisms (hydrolysis, redox reductions and photodegradations) and biodegradation. The involved mechanisms are several and each of them could be affected by many environmental variables. This large variability makes the assessments of these coefficients highly uncertain (McLachlan et al., 2017). The values of the 1st-order degradation constant λ in a natural porous media could vary more than one order of magnitude for each contaminant (Nham et al., 2016; Greskowiak et al., 2017). For these reasons, the differences in the results of the models achieved by varying λ have been investigated. The comparison has been developed with respect to the Trichloroethylene concentration in the same conditions of the previous sections, that are depth equal to 5 m, source thickness equal to 2 m and the unsaturated zone composed by sand soil. In Howard (2017) the values of λ for this compound in groundwater ranges from 4.852E-09 s^{-1} to 2.499E-08 s^{-1}. Three values have then been chosen for the comparison: the first λ_1 is the minimum value (4.852E-09 s^{-1}), the second λ_2 is the mean of logarithms of the two extremes (1.101E-08 s^{-1}) and the third λ_3 is the maximum value (2.499E-08 s^{-1}). The results of the comparison are shown in Figure 5.4.

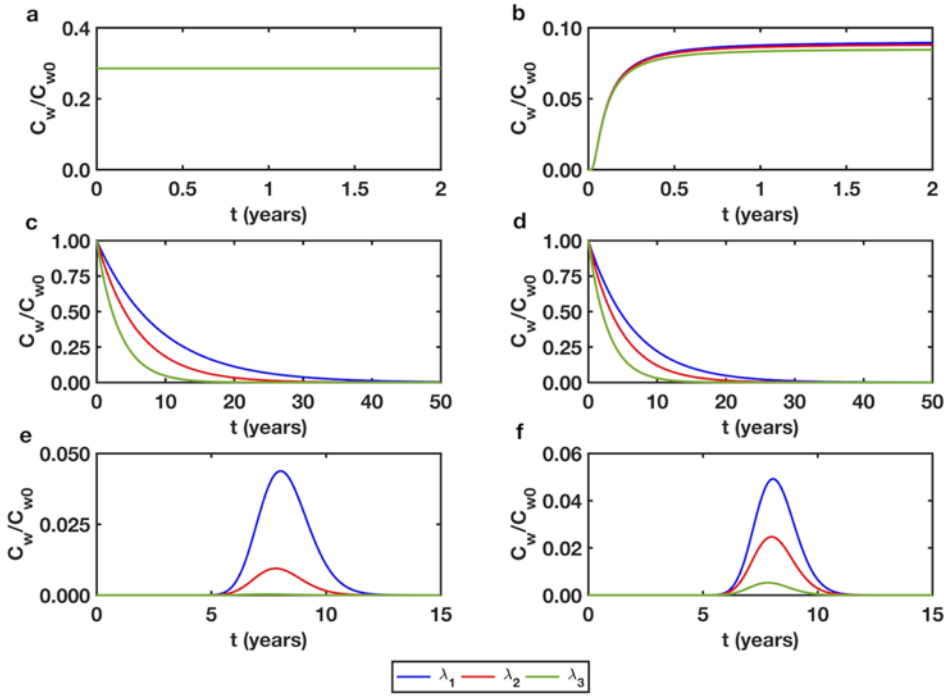

Figure 5.4: Dimensionless concentration C_w/C_{w0} of TCE at z=5 m for different decay coefficients λ. (a) Model I, (b) Model II, (c) Model III, (d) Model IV, (e) Model V, (f) Model VI.

As already highlighted, Model I is independent of contaminant properties, so C_w/C_{w0} is 0.286 for all the values of λ. In the results of Model II (Figure 5.4.b), it can be noted little differences related to the decay coefficients. The stationary C_w/C_{w0} obtained from the model is equal to 0.0901, 0.0884 and 0.0848 for λ_1, λ_2 and λ_3, respectively. The reason of observing these similar values can be found in the small time to reach the steady state.

In the models III and IV (Figures 5.4.c and 5.4.d), the λ coefficients play the same role in the exponential decay, affecting the depletion coefficients μ_1 and μ_2 , see Table 5.1.

Regarding the third group (Figures 5.4.e and 5.4.f), the variation of λ affects Model V more than Model VI, because they represent the coefficient of the exponential part in the analytical solution. It affects the height of the peak as well as the time when it occurs. In both models, the higher is the value of λ the earlier and lower is the peak. In the results of Model V, the peaks are equal to 0.0438 observed at 8 y, 0.0094 observed at 7.83 y, 0.00033 observed at 7.42 y for the three values of λ respectively,

whereas in Model VI the peaks are equal to 0.0492 observed at 8.08 y, 0.0247 observed at 7.92 y and 0.0053 observed at 7.83 y, for λ_1, λ_2 and λ_3, respectively.

5.3.4 Comparison between different soils

The type of soil, i.e. its physical properties, represents a further element that affects the fate and transport mechanisms, in particular the mobility of the contaminant. The properties of the soil affect mainly two aspects: the sorption capacity relating to the organic carbon fraction and the advective velocity of the contaminant which depends on the water content, the hydraulic conductivity and the infiltration rate. With regard to the first point, simulations with three different soils (sand, loam, clay) have been carried out, in order to evaluate the differences in the contaminant behaviour. The three types of soils are characterised by different grain size and, consequently, different water content, hydraulic conductivity and infiltration rate, instead the same organic carbon fraction is used for the three types of soils. The comparison has been developed with respect to the concentration of Trichloroethylene at same conditions depicted in the previous section. The soil parameters values are listed in Table 5.4.
As previously seen, Model I is independent of the soil parameters. In the graph of Model II (Figure 5.5.b), it is possible to see a similar behaviour in sand and loam. For sand and loam steady C_w/C_{w0} ratios are 0.0902 and 0.0836, respectively for times 1.67 y and 2.42 y. On the other hand, the main differences are evident for clay, in which a less mobility takes place. In this case the steady concentration reached at t=7.67 y is 0.0538. Hence, the leaching velocity has a greater impact compared to the sorption capacity.

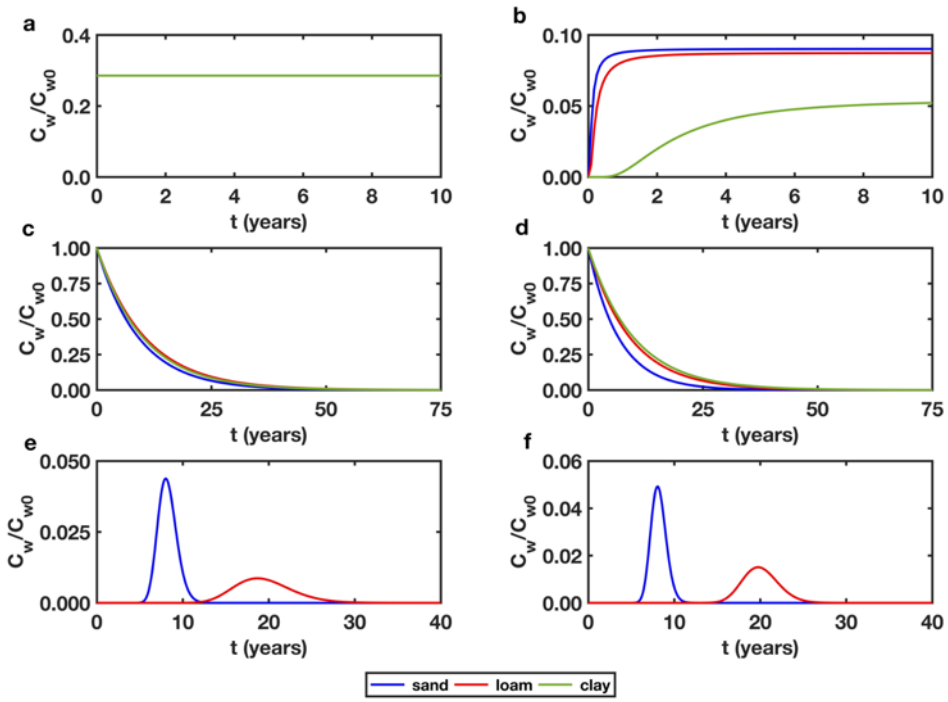

Figure 5.5: Dimensionless concentration C_w/C_{w0} of TCE at z=5 m for different soils: (a) Model I, (b) Model II, (c) Model III, (d) Model IV, (e) Model V, (f) Model VI

The Model III and Model IV, give similar trends, as shown in Figures 5.5.c and 5.5.d. Using Model III, the time needed to reach the 0.1% of the initial concentration, is equal to 63.17 y, 72.67 y, 69.83 y whereas, using Model IV the time needed to reach the 0.1% of the initial concentration is equal to 45.67 y, 63.00 y and 68.58 y for sand, clay and loam, respectively.

The third group of models is the most influenced by the soil parameters, affecting both the time at which the maximum concentration occurs as well as the related values. As concerning the application of Model V for clay, time related to the transport mechanisms is extremely long, hence the concentrations is so extremely low and therefore undetectable. The peak are equal to 4.380E-02 at 8 y and 8.651E-03 at 18.67 y in sand and loam, respectively. In Model VI the peaks are of the same order of magnitude for sand and loam, whereas is negligible for clay. For this model the peaks are equal to 4.920E-02 at 8.08 y, 1.509E-02 at 19.75 y in sand and loam, respectively.

5.3.5 Comparison between different source thickness

The last analysed parameter is the thickness of the source. As can be seen in Table 5.1-I, this value determines the soil attenuation model (SAM) of the contaminant in the Model I and the time needed to deplete the source in the models composed of an exponential part, i.e. from III to VI. Model II is not influenced by the change of source thickness because it does not take into account the source depletion and soil attenuation. The simulations have been carried out for the reference scheme described in Figure 5.1 with three different source depths: 1 m, 2 m and 4 m, using sand as type of soil and Trichloroethylene as contaminant. The concentration of Trichloroethylene has been calculated at a depth z =5 m.

The concentrations calculated with Model I (Figure 5.6.a) shows a significant variation in relation to the source thickness, C_w/C_{w0} is equal to 0.167, 0.286 and 0.444, for L_1 equal to 1 m, 2 m, 4 m respectively.

In the two exponential models III and IV (Figures 5.6.c and 5.6.d) the source thickness has a different effect, in particular the Model IV is more sensible by its variation. The depletion coefficients μ_1 and μ_2 may be used as an indicator of the contaminant depletion velocity. In the model III and IV, the source thickness affects the depletion coefficients μ_1 and μ_2, in accordance with Table 5.1-I. The time needed to reach the 0.1% of the initial concentration increases with thickness, reaching the values of 58, 64 and 73 years in the model III. In Model IV the time needed to reach the 0.1% of the initial concentration is equal to 27, 46 and 70 years for the three values of L_1.

In the Model V an increased thickness of the source determines a higher peak delayed. In facts, the dimensionless concentration C_w/C_{w0} is 2.25E-02 (t=7.92 y), 4.38E-02 (t= 8.00 y) and 8.24E-02 (t=8.25 y) for L_1 equal to 1 m, 2 m, 4 m respectively.

In Model VI, the increasing of the thickness lead to higher but earlier peaks. For this model, the peaks are equal to 3.19E-02 observed at 8.08 y, 4.92E-02 observed at 8.08 y and 7.93E-02 observed at 8.00 y, for L_1 equal to 1 m, 2 m, 4 m respectively.

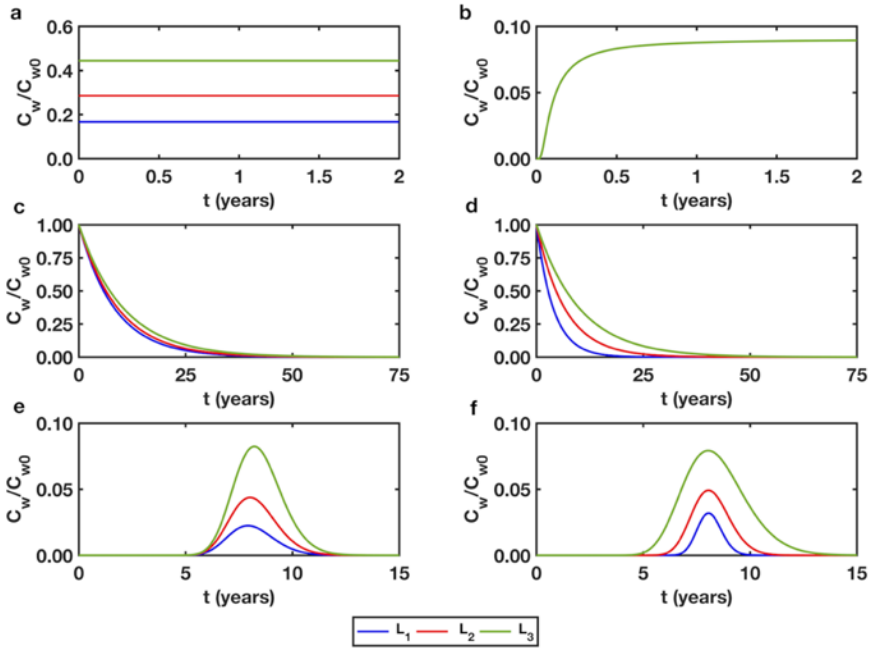

Figure 5.6: Dimensionless concentration C_w/C_{w0} of TCE at z=5 m for different source thickness L1. (a) Model I, (b) Model II, (c) Model III, (d) Model IV, (e) Model V, (f) Model VI.

5.4 Final remarks

The use of fate and transport models may give a considerable support to tackle with environmental problems involving chemical leaching through the unsaturated zone of soils. Analytical models are frequently used in many of these applications, especially in the risk assessment.

The models belonging to the first group are suited for contamination scenarios where the source may be assumed constant, e.g. in the case of continuous chemicals leakage. Those belonging to the second group are particularly appropriate when the depletion processes are predominant and the travel distance of the chemical is low, e.g. a localized spill of biodegradable organic contaminant near the water table. Finally the models belonging to the third group describes more comprehensively all the processes occurring during the transport. Simulations being carried out, showed that models belonging to the third group yielded lowest values of contaminant concentration with respect to the other models, giving the less conservative results. When a more conservative approach is needed, Models I to IV should be preferred instead.

6. Proposed modelling approach

In the current literature, as already discussed in chapter 4, contaminant leaching in the unsaturated zone is investigated with different aims, applying several approaches. In some cases, they allow to obtain the contaminant concentration over the time in a specific point (at the water table, etc.) starting from either the known or assessed-by-data contaminant at the source. This approach is certainly useful when reliable data at the source are available. In case of the data unavailability or in the presence of multiple contaminant sources it may not be applied instead.
For this reason, a modelling procedure based on a hindcasting simulation combining a steady-state flow model and a mass transport model is proposed. Specifically, the objectives of the procedure consist into reproduce the contaminant concentration measured in the aquifer within the site, assess the contaminant concentration of the source through a history matching with the concentration measurements and, based on that, give some insights helping to the identification of the primary sources.
The application of this approach to different sites is possible as it may deal with different types of contaminants, including the main significant physical processes, while, at the same time, it does not require a large set of input parameters. The application of the described procedure with reference to a well-monitored case study, the Taranto site, is reported in the next chapter.

6.1 The reference framework

The proposed modelling procedure consists of the steps listed in Figure 6.1. The reference framework starts from the understanding of the physical reference system as well as all the significant physical and biochemical processes. Consequently, it is at this stage defined the conceptual model. The latter has the key role to give a proper representation of the site and the occurring processes, and support decisions during the modelling process, like the definition of the boundary conditions or the selection of the calibration parameters.
The choice of an appropriate mathematical model, on the basis of both the aim of the analysis and the conceptual model defined at the previous stage has been carried out in second step of the procedure. The mathematical model should include all the processes hypothesized in the conceptual model, remaining with a low level of

complexity, hence reducing as much as possible, the input parameters. Two models matches this need: one of analytical type and one of numerical type. A comparison between the two modelling types has been carried out.
In the third step the geological, hydraulic and chemical parameters' values are assessed according to literature studies on the area, available databases, laboratory test and in situ investigations. The appropriate assessment of the parameters, of paramount importance to provide consistent modelling results, comes from a detailed analysis of the available data coupled with a proper conceptual model.
The next step consists of model calibration, which is fundamental because this stage allows to apply the model to a specific case study. It is based on the estimation of some selected input parameters (calibration parameters) by means of history matching, that is by reducing the differences between field observations and computed values, tuning the calibration parameters until measured and computed values are sufficiently comparable.
Data modelling and individuation of a contamination scenario is finally developed. The model is used not only to reproduce the contaminant measurements but also to reconstruct past contaminant source conditions in a hindcasting simulation. Obtained results have been compared with the solubility in water of the analysed contaminant, as a preliminary check.
In the last step the analysis of the results and the comparison between the two models is performed. This comparison has the additional purpose to highlight the difference between the selected analytical and numerical models.

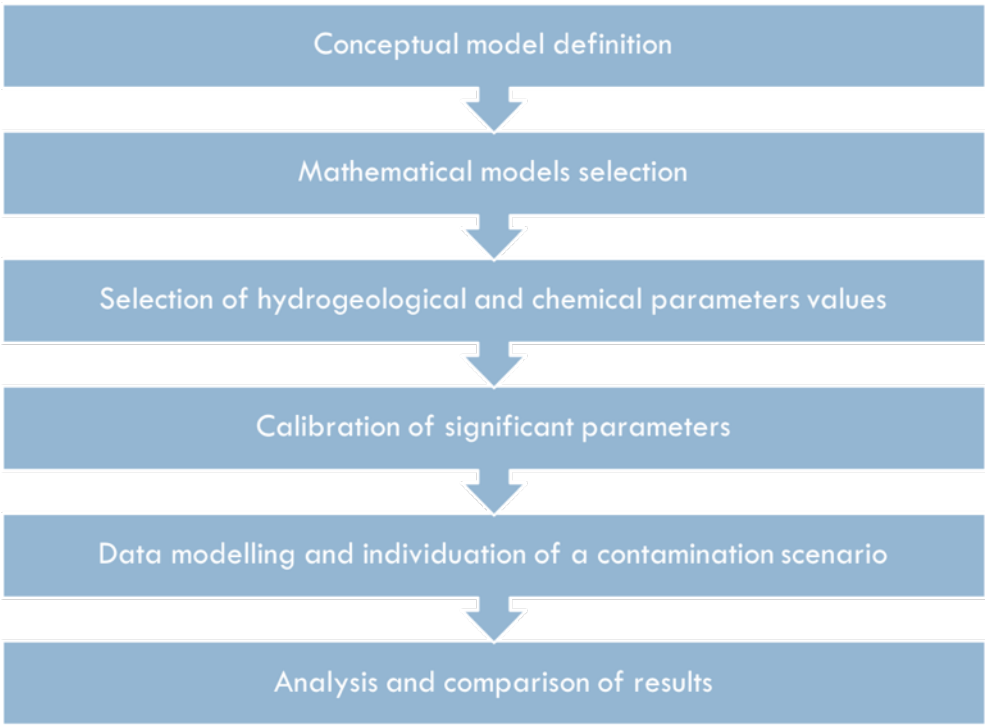

Figure 6.1:Proposed approach to modelling field case study.

6.2 Conceptual model

The conceptual model allows a straightforward representation of flow and transport processes occurring in the selected site using simplified assumptions, based on the integration of all the relevant hydrogeological and chemical information coming from the available studies. The general reference scheme assumed by the models need to be checked and adapted to the specific case study, it is depicted in Figure 6.2.

The analysed subsoil consists of an upper unsaturated layer lower bounded by a saturated zone. The contaminant source is located on the ground surface, it is a thin layer of contaminant with dimensions of L_1, X and Y for the analytical model, and it is assumed as a boundary condition for the numerical model. From the source, the contaminant is transported to the water table located at a depth L_2 from ground level. The unsaturated zone is assumed homogeneous, isotropic, with an uniform thickness and hydrogeological properties constant over the time. Steady-state flow conditions are assumed and the mass flux is governed solely by vertical driving forces. The significant transport processes are advection, longitudinal dispersion and sorption

according to a linear isotherm, other more specific fate and transport mechanisms, like evaporation or precipitation, are neglected.

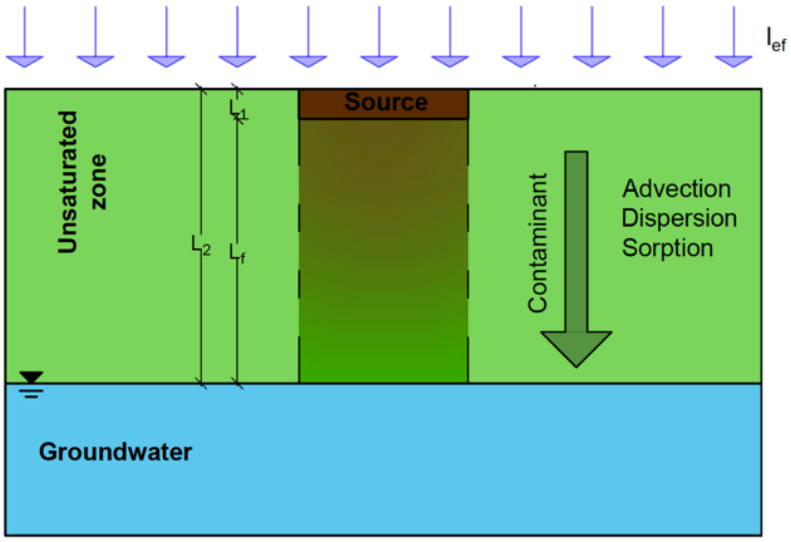

Figure 6.2: Reference scheme of the proposed modelling.

6.3 Selection of the analytical and numerical model

6.3.1 The analytical model

The analytical model of Spence and Walden (2001) is chosen by means of the review of the analytical models being carried out in chapter 5. The selected one-dimensional (vertical) model assumes steady-state flow conditions and constant water velocity along the vertical direction. It reproduces the advective, dispersive transport and the adsorption processes according to a linear isotherm. Biochemical degradation has been neglected in the source and during the transport, because for the considered cases the transport time compared with the half degradation time are low enough. The source depletes with time, due to the simultaneous effect of leaching and volatilization, hence the source concentration is described by a decreasing exponential trend with time. For further detail see paragraph 5.1.6.
This model has been selected because is the most pertinent to the developed conceptual model, it is able to consider both depletion processes of the source and transport mechanisms, describing more comprehensively the all processes occurring during the transport.

6.3.2 The numerical model

The numerical model has been implemented in the FEM code Geoslope, using the SEEP/W and CTRAN/W modules, presented in paragraph 4.4, through an uncoupled approach: pore water pressure variations are not influenced by solute concentration. The SEEP/W module has been used to simulate the flow of water through unsaturated porous media, the considered governing equation is a two-dimensional form of (4.3). Additionally, the CTRAN/W module has been used to simulate solute transfer by advection and dispersion, for this module the governing equation is a two-dimensional form of (4.11). Due to the very high value of the hydraulic conductivity of the porous media it is possible to associate the solute migration into the saturated/unsaturated media only to the advection phenomenon neglecting the diffusion term. This porous media behaviour also justify the adopted uncoupled approach. The governing equations have been solved using the implicit Backward Difference approximation method (BDA) to reduce spurious numerical noise in the solution.

The domain of the implemented model consists of a column of soil with a depth equal to the distance between the ground surface and the water table, generated using an axisymmetric geometry. Meshing is performed by setting up quadrilateral elements. Different mesh dimensions are tested, ranging from 0.1 m to 0.01 m, to evaluate the convergence of the results. From the analysis, the dimension of 0.05 m is selected to achieve the accuracy of the results and reduce the computation time.

As regards to flow system, the properties of the partially saturated medium are expressed through the use of the characteristic curves described according to the Van Genucthen formulation; steady-state flow conditions are assumed; the top boundary condition is assumed of Neumann type, specifically, a constant inflow is set while the bottom boundary condition is set equal to atmospheric pressure head to simulate the groundwater table.

Advective, dispersion and sorption processes are considered: the dispersion is reproduced using coefficients of longitudinal dispersivity while the sorption using a linear isotherm. At the initial time, the soil domain is assumed uncontaminated hence the initial liquid phase concentration is zero. The source concentration is described using a stepwise function with a step of 100 days; this time interval is evaluated through a preliminary calibration with respect to the measured concentration values. The contaminant is assumed non-volatile and non-reacting, therefore the degradation kinetic rate is equal to zero.

6.4 Model parameters

The assessment of parameters' values depends on several factors and it is strongly related to the specific case study. In this perspective, the paragraph provides both general indications and specific evaluations carried out relating to the case study discussed in the following chapter.
Hydraulic parameters of the porous media and chemical ones of the specific solute can be estimate separately because of the uncoupled adopted approach. As for the first ones, porosity, vertical and horizontal saturated hydraulic conductivities and the shape of the characteristic curves can be assessed by both field measurements and laboratory tests. If few information is available, lithological and stratigraphical interpretation can be used in conjunction with soil map information.
The diffusion coefficient (as stated neglected in the analyses performed), the dispersion coefficient, chemical reaction parameters (i.e. chemical decay) or porous media adsorption can be estimated by laboratory tests, by inverse analyses on well-known simplified schemes or by using literature data.
It should be stressed that both hydraulic and chemical parameters are typically scale-dependent, hence these values can vary with the different scales of the different type of measurement because different REVs (Reference Element Volumes) are considered.
In the assessment of parameters values, the differences between the scale of the field or laboratory measurements and the domain of the mathematical model must be considered. The calibration phase described in the following paragraph can help to adjust the parameter value in order to consider this discrepancy.
As stated above, attempts have made to develop a modelling approach with a small number of parameters. The input parameters are presented in Table 6.1 and 6.2. Furthermore, the Van Genuchten parameters related to the soil characteristics curve are required in the numerical model.

Table 6.1: Physical and hydrological parameters of the soil

Symbol	Parameter	Measurement unit
ρs	Soil Density	kg/m3
θ	Porosity	-
θw	Volumetric water content	-
Ksat	Saturated hydraulic conductivity	m/s
foc	Organic carbon fraction	-
Ief	Effective infiltration	m/s

Table 6.2: Physical-chemical parameters of the contaminant

Symbol	Parameter	Measurement unit
S	Solubility	mg/l
Kd/koc	Soil-water partition coefficient	dm^3 /kg

6.5 Model calibration and data modelling

A calibration procedure of the significant parameters has been carried out. The volumetric water content, saturated hydraulic conductivity, organic carbon fraction, the effective infiltration and the soil-water partition coefficient are assumed as fixed data evaluated from the available information, while the hydraulic conductivity and the longitudinal dispersivity are calibrated within the analysis.
In this procedure, the modelling is developed as an inverse problem: the output, consisting of the contaminant concentration at the water table is used to determine the initial boundary condition (the contaminant source) by history matching. The contaminant source has a shape defined by the conceptual model while its intensity is evaluated through subsequent adjustments that produce a more satisfactory match to field observations.
Anderson et al. (2015) present two main groups of history matching, manual trial-and-error and automated trial-and-error, comparing their characteristics. They state that although the manual trial-and-error is labour intensive and subjective, it allows the modeller to guide the elaboration with its insight and "hydrologic-sense", this can not fully replaced by the advanced methods. For this reason, a manual trial-and-error has been chosen in this procedure. Starting from a trial source, the calibration is developed through subsequent attempts. At each attempt, the difference between the measured and observed concentrations is evaluated and an adjustments to the source is introduced to minimize the discrepancy.

7. Application of the model to the case study of Taranto

An application of the proposed approach to a significant case study in Taranto contaminated site has been presented. The site is part of a sensitive environmental area that requires remediation of the soil, subsoil, surface water, and groundwater. For this reason, several scientific studies have been carried out over the years and a wide monitoring campaign, from which some of the used data come, has been recently performed by the "Commissario Straordinario for Urgent Interventions of Environmental Requalification of Taranto". The available database and the analysed monitoring wells network are presented.
The modelling concentration and the contamination scenarios obtained for the monitoring wells are shown. Furthermore, the analytical and numerical models have been compared. Lastly, an indicator of the effectiveness of the results has been compared to the hydraulic gradients of the underlying groundwater, in order to evaluate the influence of the gradients on the modelling.

7.1 The case study of Taranto

7.1.1 Site location and description

The proposed approach has been tested in a study area located in Taranto, city of Southern Italy characterised by environmental problems of extreme scientific value for the complexity of the involved factors.
Since the 1960s Taranto has experienced an intense industrialization process, which has led to the development of a large industrial settlement on the western side of the city. The area presents a significant number of industrial activities with a high environmental impact, including the largest steel plant in Europe extending over 15 square kilometres, an important oil refinery, a cement factory, military and shipbuilding activities, two thermoelectric power stations and other various industrial plants (Vitone et al., 2016; Lai et al., 2019). Furthermore, other sources of pollution with lower environmental impact are widely distributed throughout the territory. This has resulted in high levels of contamination involving all

environmental matrices (air, surface water, soil and groundwater). The identified types of contaminants are several: heavy metals, aliphatic compounds, polycyclic aromatic hydrocarbons (PAHs), polychlorinated biphenyls (PCBs) and dioxins (Cardellicchio and Costiero, 2013).

Given the severity of the health and ecological risks, an area of 564 km^2 in Taranto has been declared "area at high risk of environmental crisis' by the National Law No. 349/1986; afterwards, a more limited area has been recognised as Site of National Interest (National Law No.426/1998). More specifically, the Taranto SIN consists of the Sea SIN (a sea area that extends on a surface of 70 km^2, including the two inlets of Mar Piccolo, Mar Grande and the western area of Mar Grande) and the Land SIN (a land area that extends on a surface of 43 km^2, including the industrial district, a saltworks called "Salina Grande" and some landfills and disused quarries). An aerial view of the Taranto Site is shown in Figure 7.1(a), with particular reference to the area at high risk of environmental crisis and the SIN. In this geographical framework, a specific area of the industrial district has been analysed (Figure 7.1(b)). This area, which is covered by the oil refinery and extends about 5.4 km^2, has been chosen due to its hydrogeological characteristics and the available hydrological and chemical data. The overall topographical surface of the area has been evaluated by means of a Digital Terrain Model (DTM) with a grid resolution of 10 m (Figure 7.2). Two distinct morphological zones can be noticed, a zone next to the cost with altitude lower than 5 m a.m.s.l. and a zone with higher altitude that range from about 15 a.m.s.l. to 25 a.m.s.l., which are separated by a cliff of a few meters.

Figure 7.1: (a) Geographical framework of the Taranto Site, area at high risk of environmental crisis and Land SIN and Sea SIN (b) Close-up on the study area.

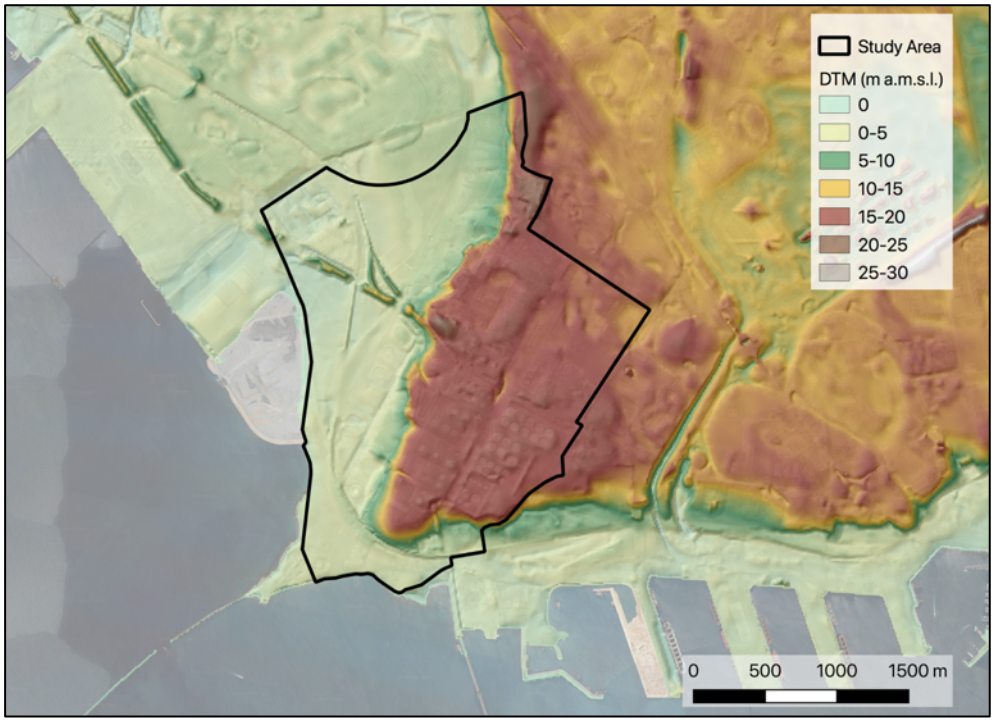

Figure 7.2: DTM map of the study area overlaid with a hillshade model obtained from the DTM.

7.1.2 Geological and hydrogeological setting

From a geological perspective, the area of Taranto is placed in the south-western sector of the Apulian foreland and it is characterized by a Cretaceous limestone formation topped by a number of more recent geological units (Martinis and Robba, 1971). More specifically, the stratigraphic succession of the area consists of (from the bottom to the top): Cretaceous limestone (Altamura limestone), Upper Pliocene-Lower Pleistocene calcarenites (Gravina calcarenite), Lower Pleistocene clays (Subappenine clays), Middle-Upper Pleistocene calcarenites and sands (terraced marine deposits), Holocene alluvial deposits and coastal deposits.

The mainly hydrogeological complex is represented by the deep aquifer located in the Cretaceous limestone characterised by high permeability caused by fracturing and karstic processes, which contain an important groundwater reservoir. In the formations of Pleistocene sequence, local shallow aquifers of limited extension can occur, when these overlie impermeable clays formations (Zuffianò et al. 2016).

The lithological map of the area study obtained by the hydro-geomorphological map of the Apulia region (Scale 1:25 000) is shown in Figure 7.3.

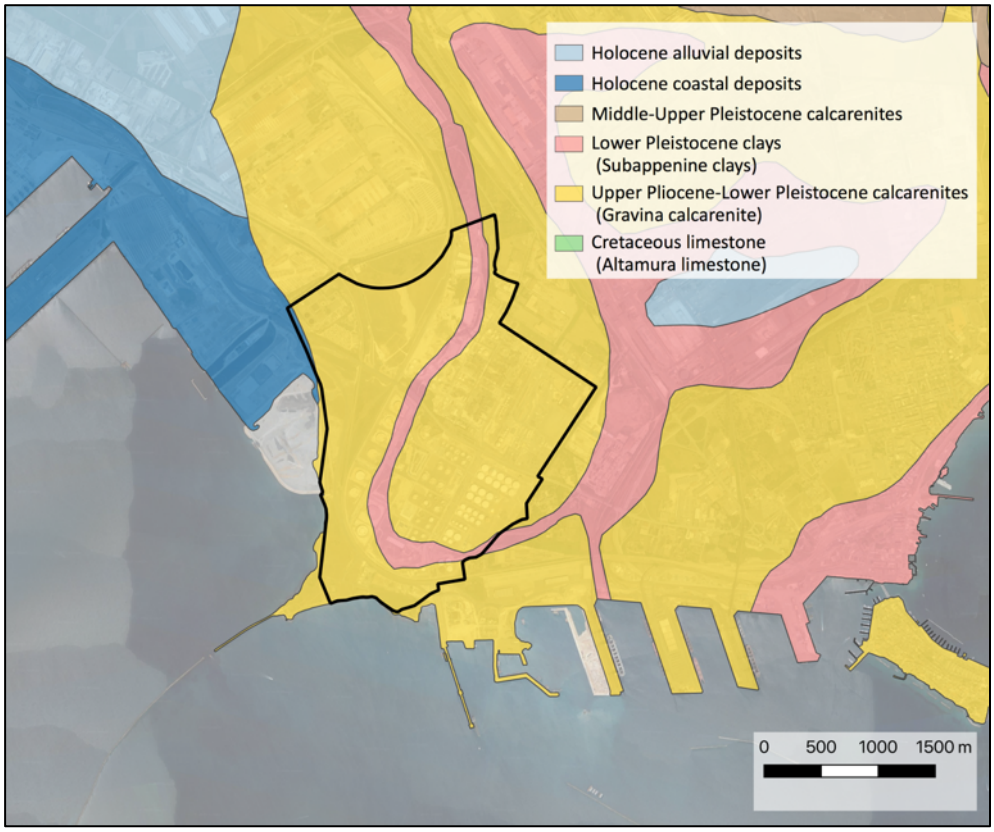

Figure 7.3: The lithological map of the area study obtained by the hydro-geomorphological map of the Apulia region (Scale 1:25 000).

The study area is covered by porous and permeable lithostratigraphic units with some clay outcropping in correspondence of the morphological scarp, groundwater contained in the shallow aquifers are strongly conditioned by several human interventions carried out over time. The clay layer separates the surface layers from the deep stratum present in the lower limestone layers.

7.1.3 The available database

In the area a network consisting of 120 wells (Figure 7.4) is installed, which provide hydrogeological and hydro-chemical measurements of shallow groundwater. For the most wells measurements cover a period from 2008 to 2018.
The water table and the hydro-chemical measurements are detected every month and every six months. The hydro-chemical measured parameters are: pH, electrical conductivity, total organic carbon, chlorides fluorides, sulphates, lead, cadmium,

copper, zinc, vanadium, total chromium, arsenic, selenium, mercury, nickel, iron, manganese, hexavalent chromium, boron, PCB, total hydrocarbons, (expressed as n-hexane), light and heavy hydrocarbons (<C12, C12-C25,> C25), MTBE, BTEXS, IPA, phenols.

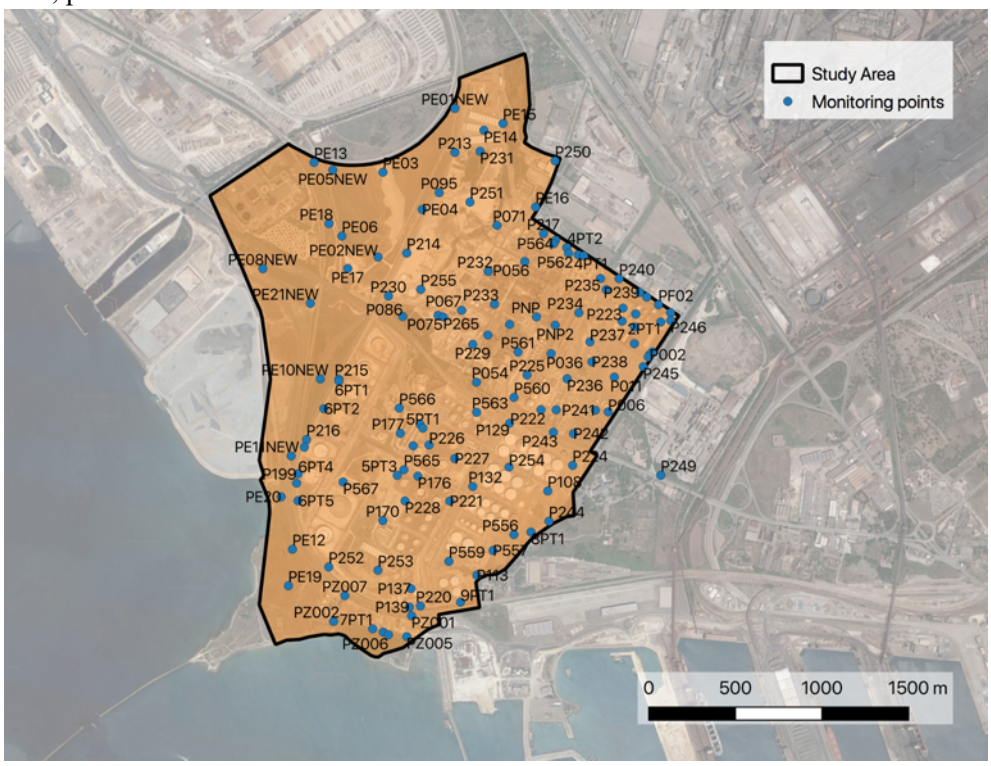

Figure 7.4: Monitoring points in the study area.

7.2 Results and discussions

7.2.1 Selected monitoring points

The modelling approach has been applied to 9 monitoring points. They have been selected because the measured concentrations of the reference contaminant (Nickel or MTBE) far exceed the threshold values defined for groundwater by the Italian law (D.Lgs. 152/06). Seven of these are affected by Nickel contamination (PE17, PE13, P086, P252, PZ002, P214, P255) and two by MTBE contamination (P245, P227). Afterwards, other 5 monitoring points (P052, P222, P225, P232, P243) with significant concentration of n-hexane exceeding the threshold value have been used

for numerical modelling that has been carried out for the analysis on the effects of the hydraulic gradient of groundwater presented in paragraph 6.3.4. All the modelling points with the considered contaminants are shown in Figure 7.5.

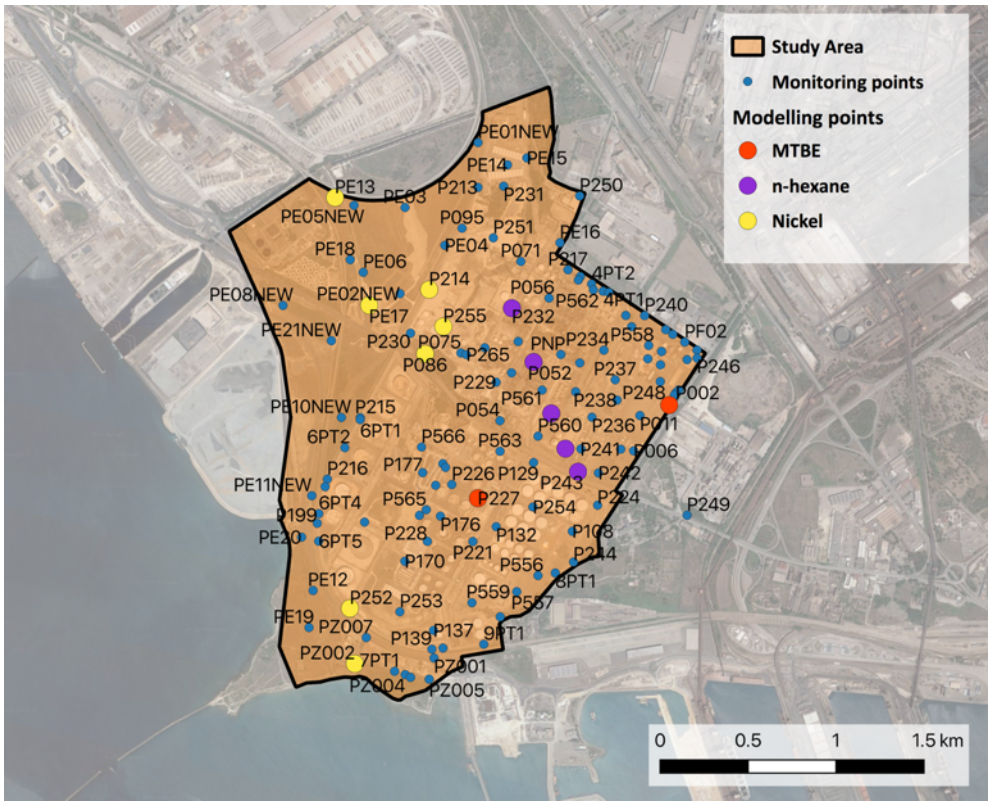

Figure 7.5: Location of modelling points with the considered contaminant in the study area

7.2.2 Model parameters

The hydrogeological parameters has been derived from the hydrogeological studies of the area and they are presented in Table 7.1. The chemical parameters of the selected contaminants has been evaluated from scientific literature references and they are presented in Table 7.2.

Table 7.1: Selected soil parameter values

Symbol	Parameter	Value	Measurement unit
ρs	Soil Density	1700	kg/m3
θ	Porosity	0.5	-
θw	Volumetric water content	0.3	-
Ksat	Saturated hydraulic conductivity	10-6	m/s
foc	Organic carbon fraction	0.001	-
Ief	Effective infiltration	$2.1*10^{-8}$	m/s

Table 7.2: Selected physical chemical properties values of the contaminants

Parameter*		Value			Measurement unit
		MTBE	n-hexane	Nickel	
S	Solubility	48000	76000	422000	mg/l
Kd/koc	Soil-water partition coefficient	1.2	0.4	0.4	dm3 /kg

The values of the position of the groundwater table have been obtained using the average value of the measured values in the monitored wells in the second semester of 2017.

7.2.3 Calibration

A calibration phase has been carried out and the longitudinal dispersion coefficient has been chosen as the calibration parameter. The calibration has been carried out with reference of the well PE17, the results are shown in Figures 7.6 and 7.7. From the calibration phase the same value, equal to 0.1 has been obtained for both the analytical model and the numerical model.

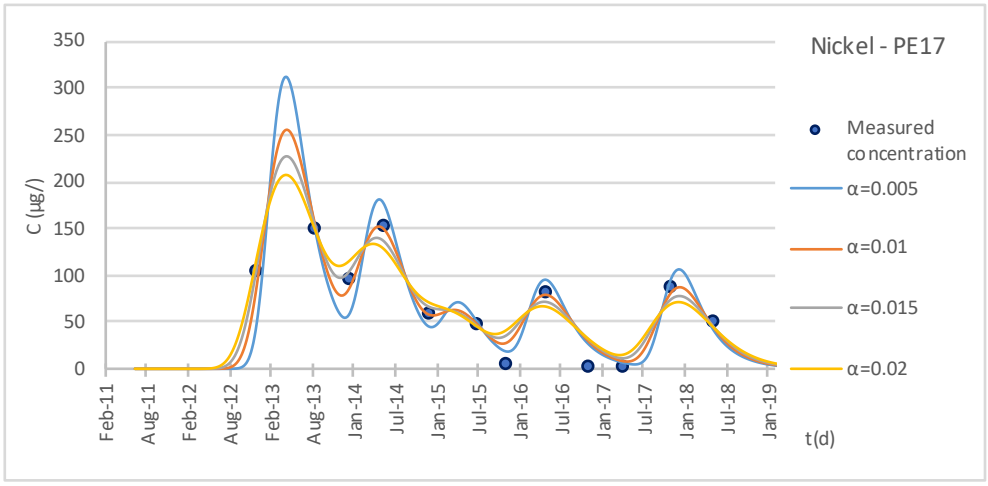

Figure 7.6: Calibration of longitudinal dispersivity for the analytical model

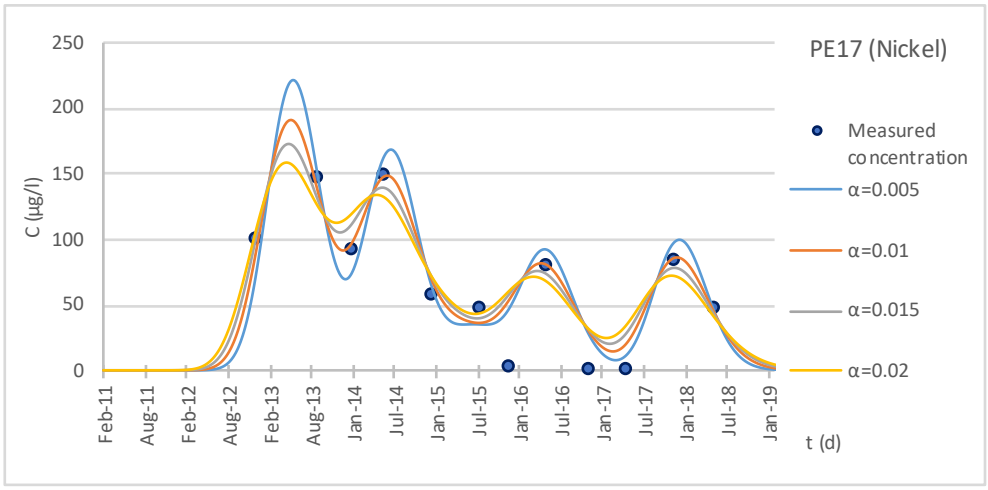

Figure 7.7: Calibration of longitudinal dispersivity for the numerical model.

7.2.4 Results on Nickel modelling

For the seven points (PE17, PE13, P086, P252, PZ002, P214, P255) analytical and numerical models have been applied to reproduce the measured concentrations furthermore contaminant source has been assessed for each models by means of a back-analysis procedure. In Table 7.3 the depth from the ground surface of the modelling points is reported. The results of analytical and numerical have been compared. Results are shown in Figures from 7.8 to 7.28.

Table 7.3: Depth from the ground surface (m)of the modelling points

Monitoring well	Depth from the ground surface (m)
PE17	1.32
PE13	1.84
P086	2.66
P252	4.81
PZ002	2.72
P214	0.85
P255	2.96

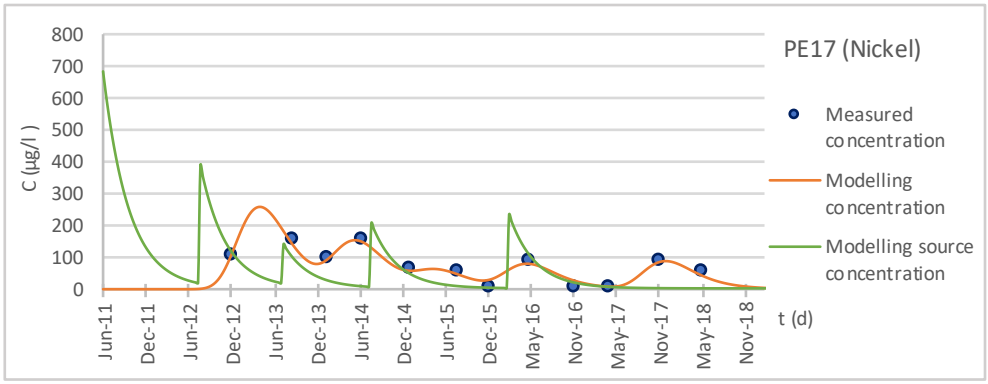

Figure 7.8:Well PE17- Analytical model.

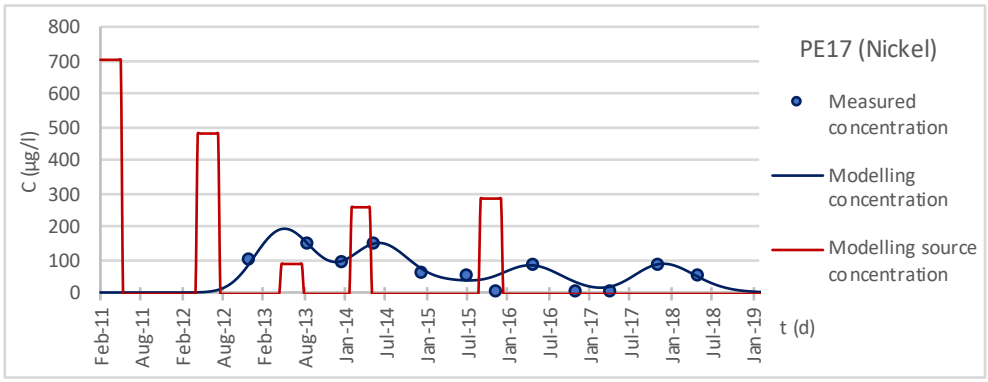

Figure 7.9: Well PE17-Numerical model.

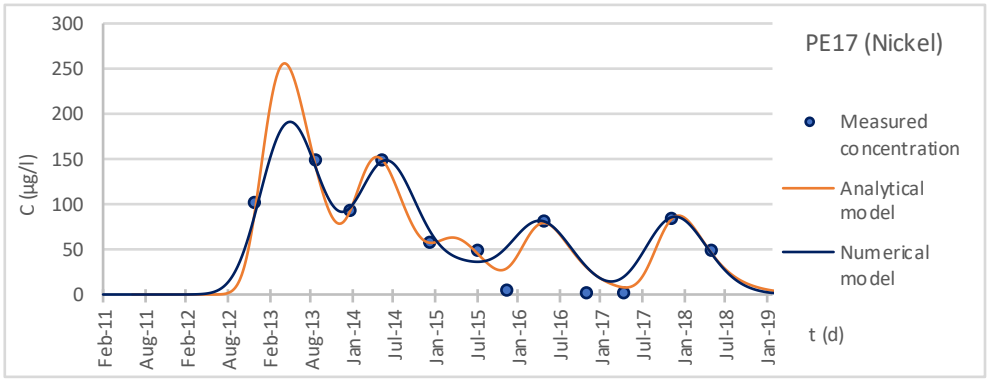

Figure 7.10: Well PE17-Comparison between analytical and numerical models.

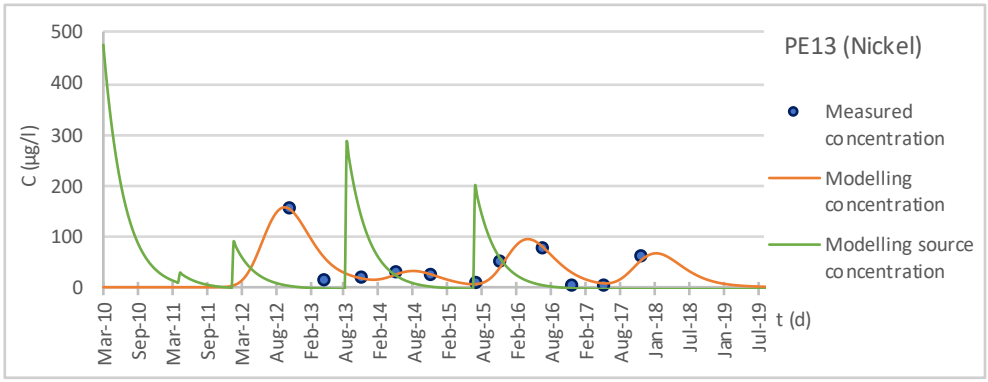

Figure 7.11: Well PE13- Analytical model.

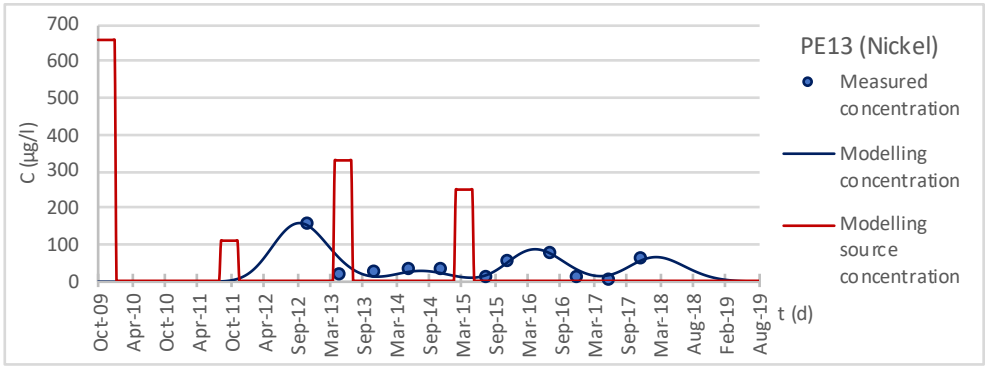

Figure 7.12: Well PE13- Numerical model.

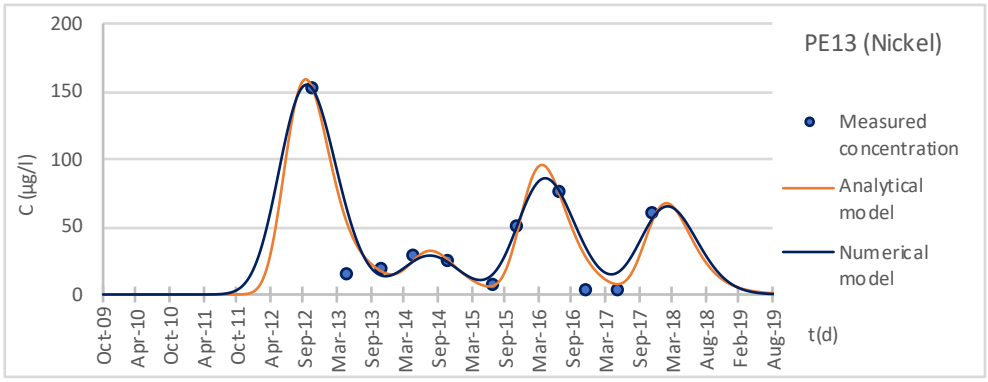

Figure 7.13: Well PE13- Comparison between analytical and numerical models.

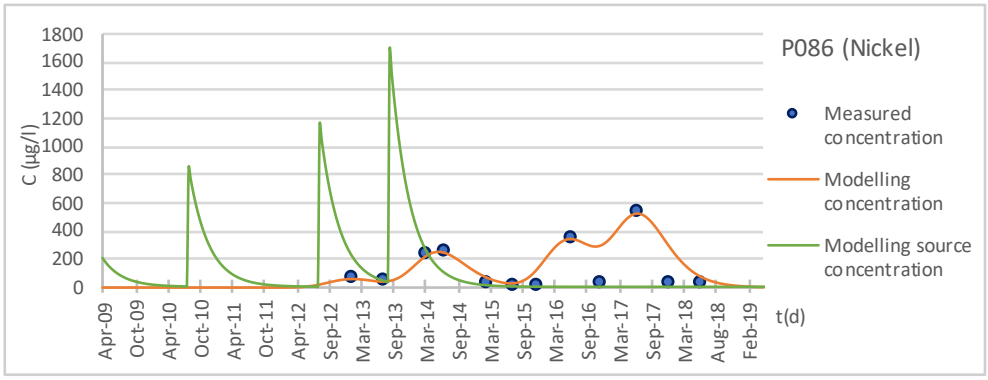

Figure 7.14: Well P086- Analytical model.

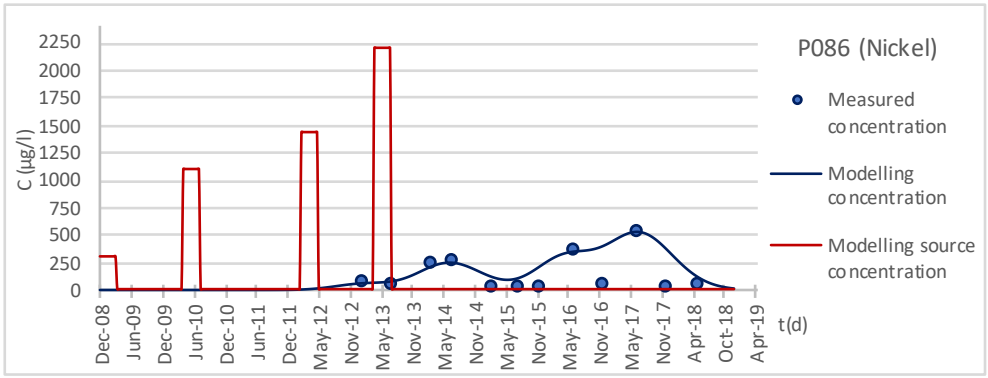

Figure 7.15: Well P086- Numerical model.

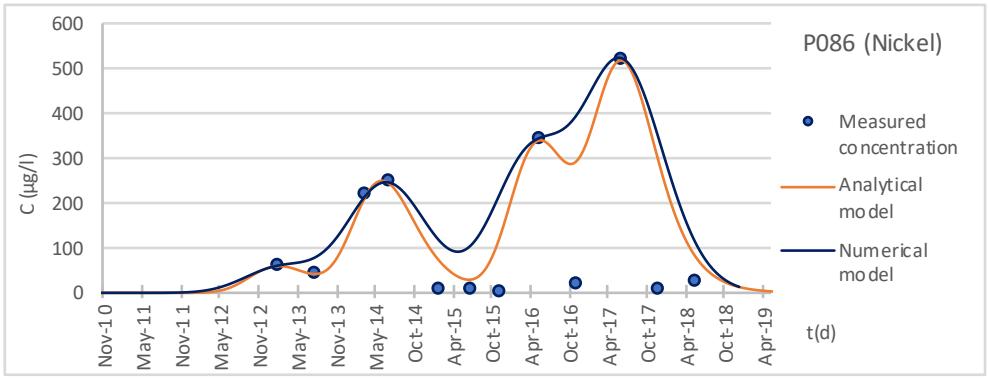

Figure 7.16: Well P086- Comparison between analytical and numerical models.

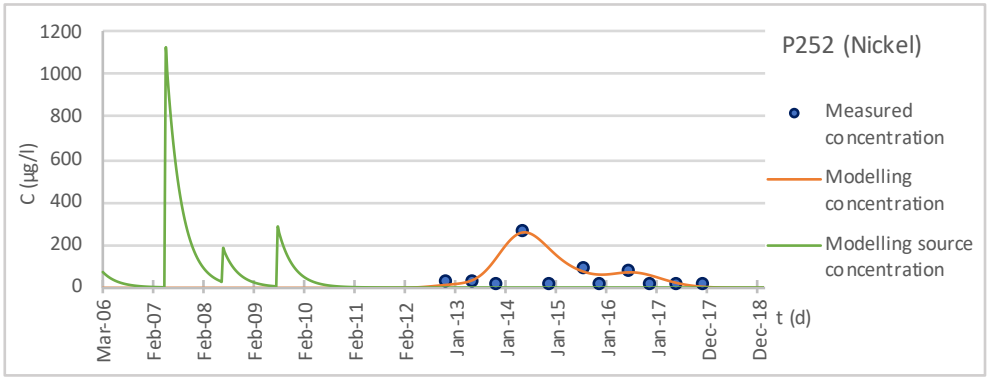

Figure 7.17: Well P252- Analytical model.

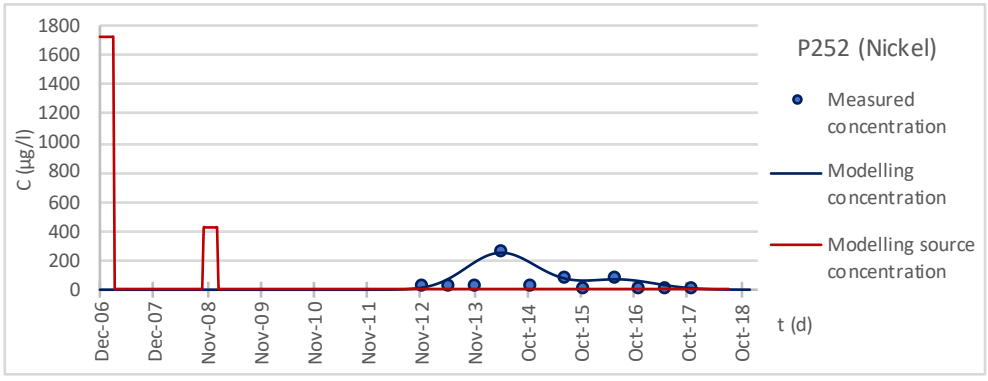

Figure 7.18: Well P252- Numerical model.

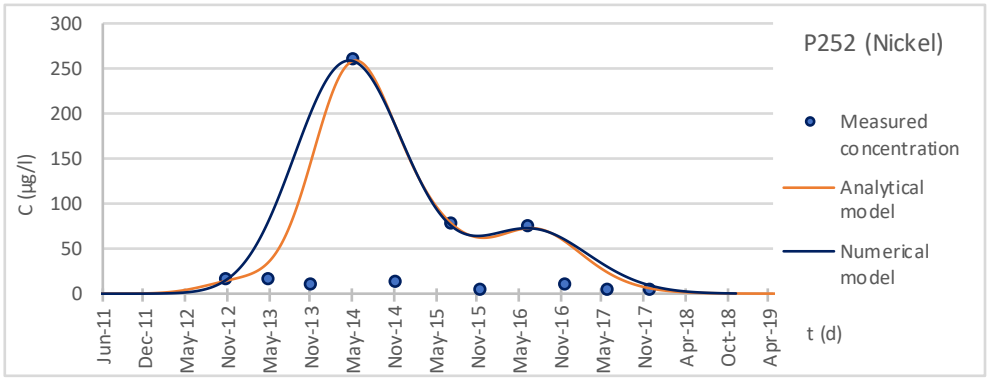

Figure 7.19: Well P252- Comparison between analytical and numerical models.

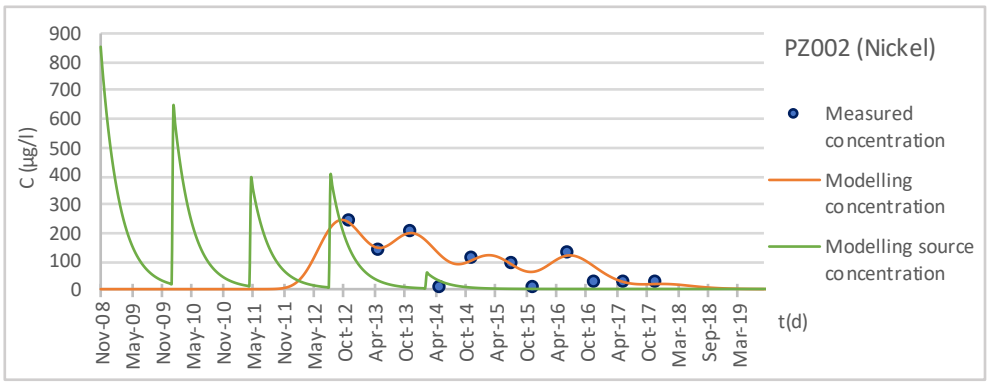

Figure 7.20: Well PZ002- Analytical model.

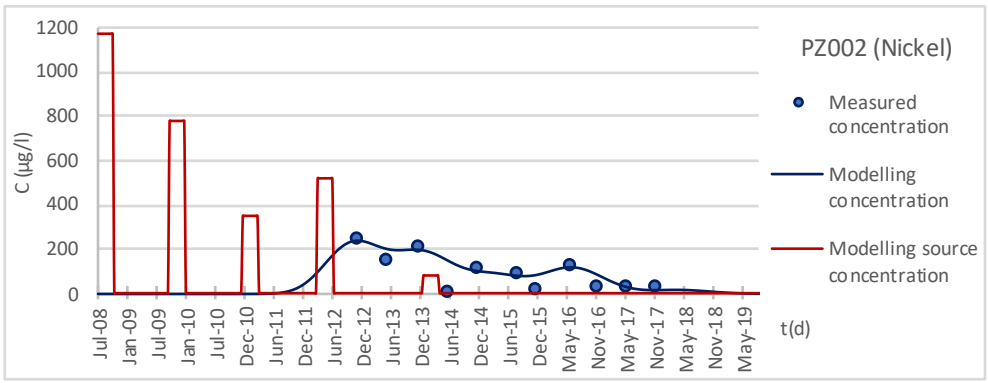

Figure 7.21: Well PZ002- Numerical model.

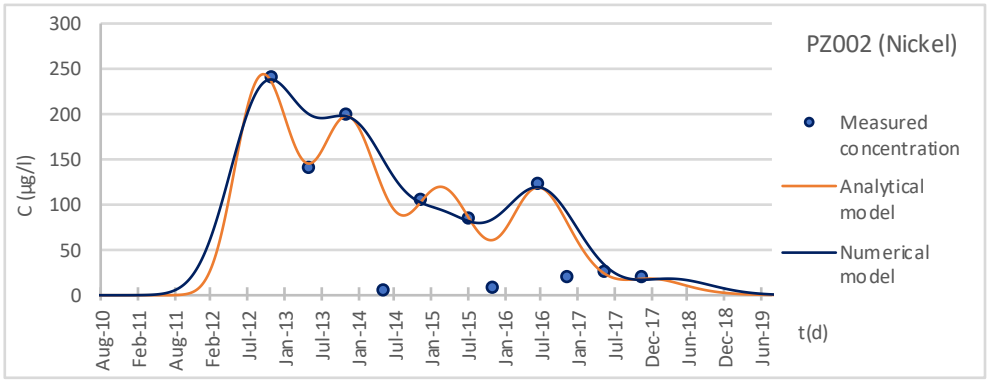

Figure 7.22: Well PZ002- Comparison between analytical and numerical models.

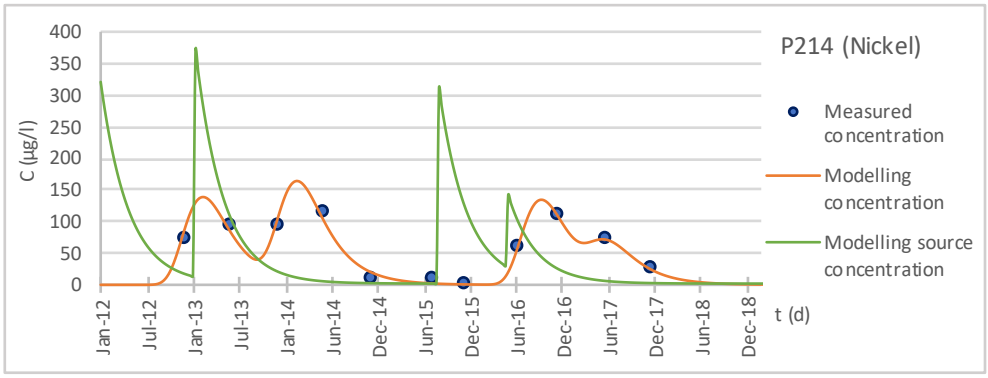

Figure 7.23: Well P214- Analytical model.

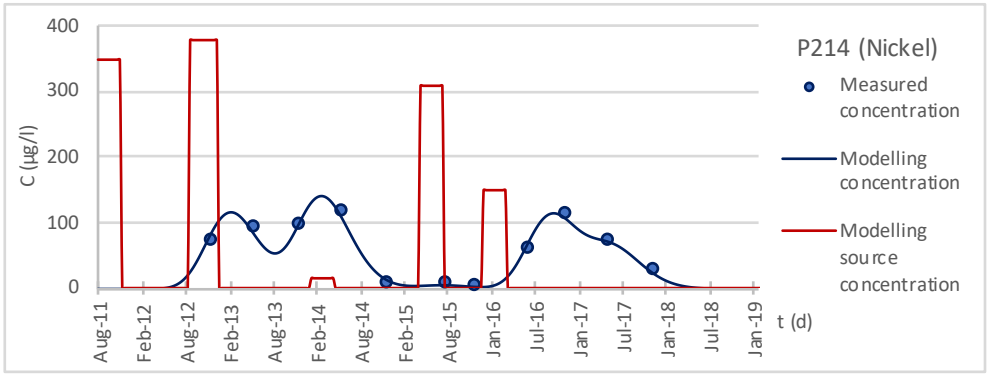

Figure 7.24: Well P214- Numerical model.

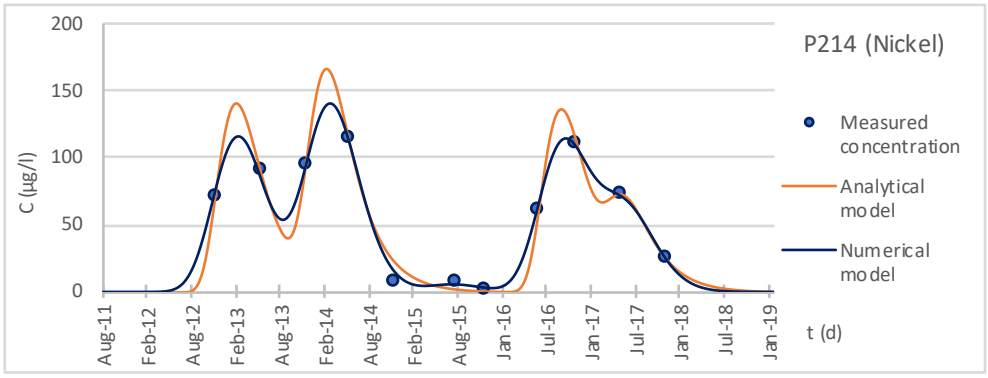

Figure 7.25: Well P214- Comparison between analytical and numerical models.

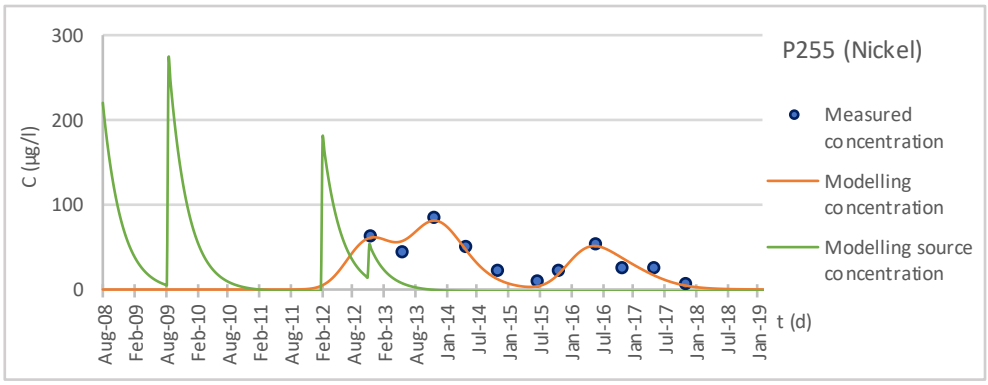

Figure 7.26: Well P255- Analytical model.

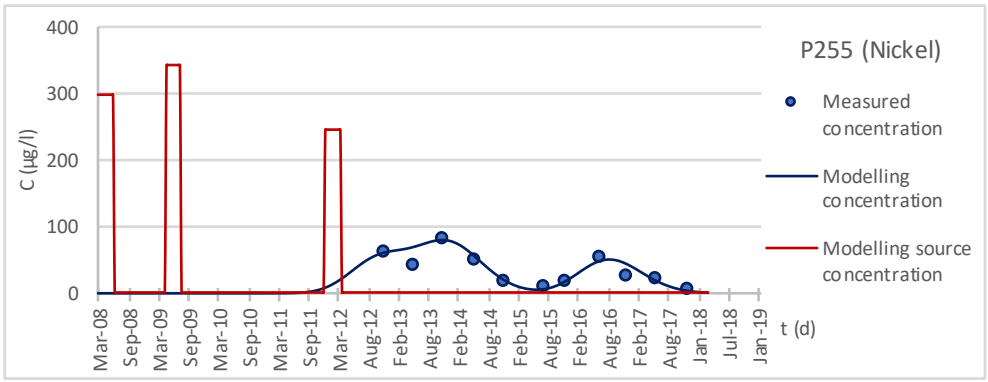

Figure 7.27: Well P255- Numerical model.

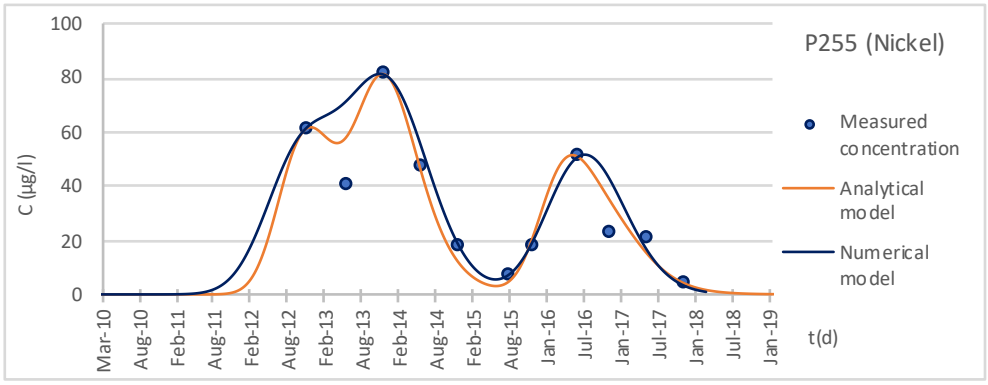

Figure 7.28: Well P255- Comparison between analytical and numerical models.

The modelling results seem to reproduce the measured contaminant concentrations, the best results have been obtained for the wells PE17, PE13, P214 which are the wells where the depth of the water table from the ground surface is lower than 2 m. In the wells where the water table is more distant from the ground surface worse results are achieved. Analytical concentrations seem exhibit a less smoothed trend than numerical ones.
The obtained contamination scenarios have been found plausible and consistent with the solubility of the analysed contaminant.

7.2.5 Results on MTBE modelling

For the two points (P245, P227) analytical and numerical models have been applied to reproduce the measured concentrations, furthermore contaminant source has been assessed for each models by means of back analysis. In Table 7.4 the depth from the ground surface of the modelling points is reported. The results of analytical and numerical have been compared. Results are shown in Figures from 7.29 to 7.34.

Table 7.4: Depth from the ground surface (m)of the modelling points

Monitoring well	Depth from the ground surface (m)
P245	4.31
P227	3.36

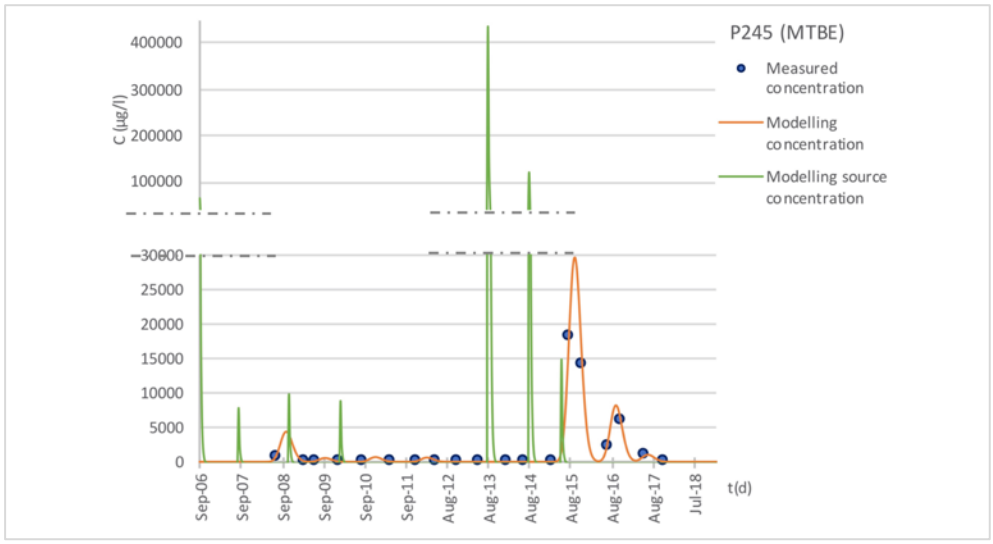

Figure 7.29: Well P245- Analytical model.

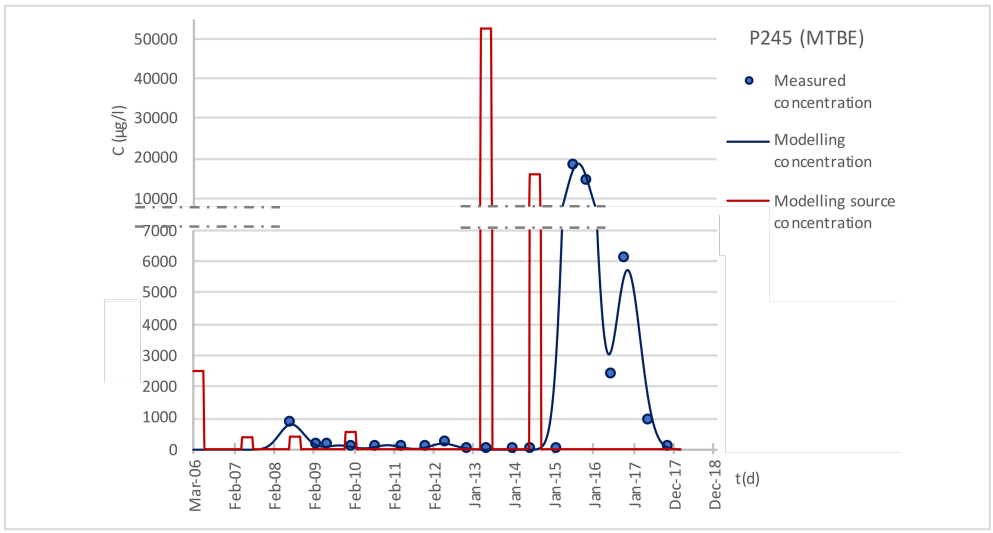

Figure 7.30: Well P245- Numerical model.

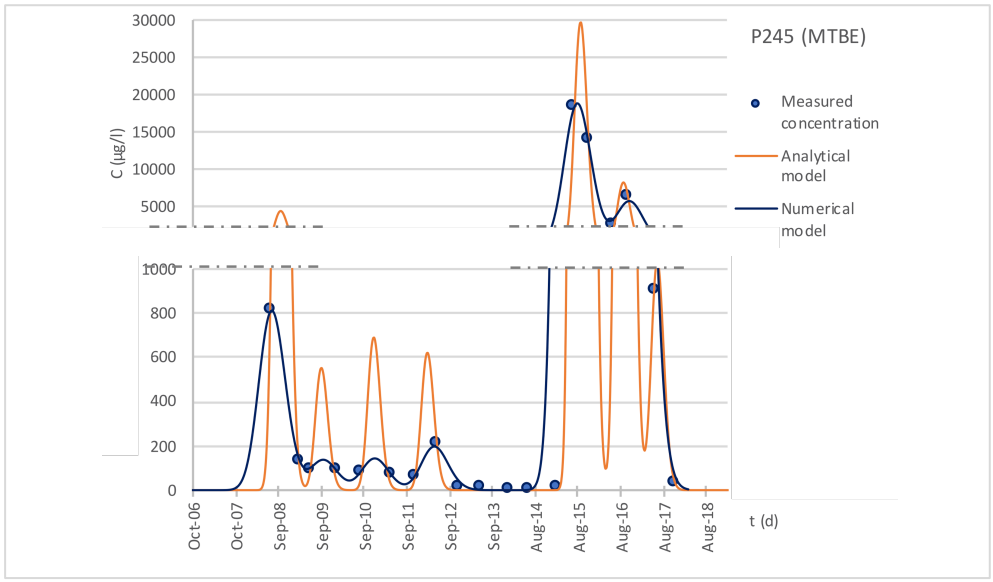

Figure 7.31: Well P245- Comparison between analytical and numerical models.

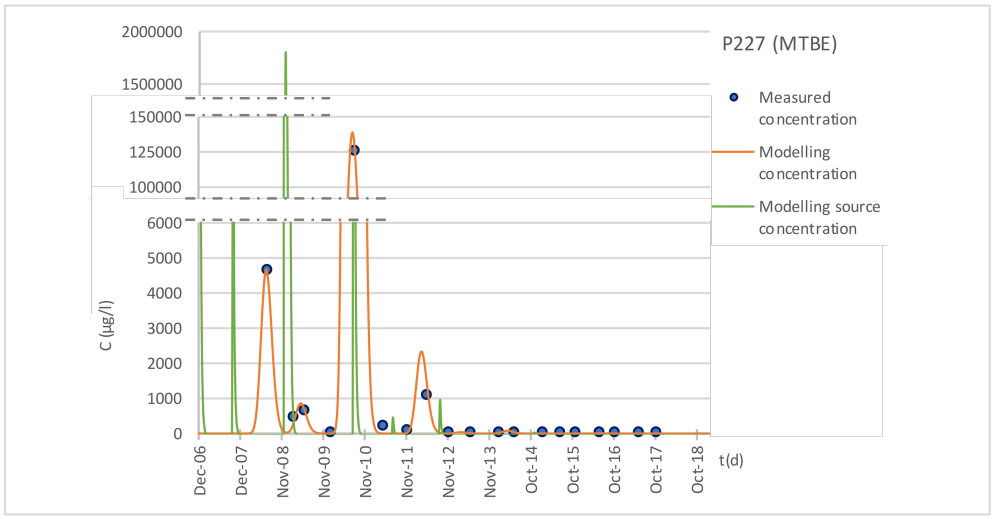

Figure 7.32: Well P227- Analytical model.

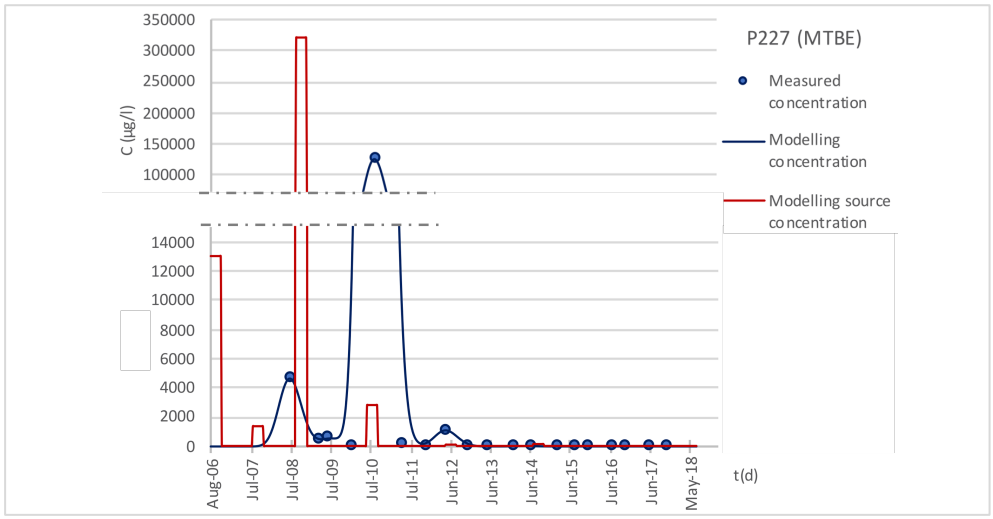

Figure 7.33: Well P227- Numerical model.

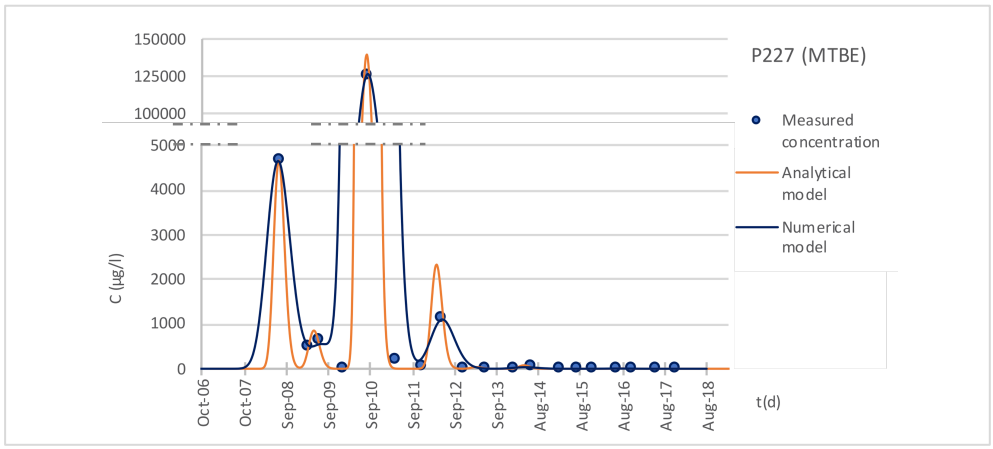

Figure 7.34: Well P227- Comparison between analytical and numerical models.

For the two MTBE monitoring points results similar to the previous wells have been obtained: the models are able to reproduce the measured contaminant concentrations and the analytical concentrations have a less smoothed trend than numerical ones. The obtained contamination scenarios are plausible and consistent with the solubility of the analysed contaminant.

7.2.6 Effects of the hydraulic gradient of groundwater

Figure 7.35: Developed section in the study area.

In the proposed approach, the horizontal driving forces of the flow have been neglected. In order to test this hypothesis, an indicator of the effectiveness of the results has been compared to the hydraulic gradients of the underlying groundwater. The hydraulic gradient of groundwater in some monitoring wells has been evaluated in simplified way through the creation of hydraulic profiles along these wells. The considered sections and their reference wells are show in Figure 7.35.

The modelling results for each wells have been evaluated by calculating the normalized root-mean square deviation, reported in Equation (7.1):

$$NRMSE = \sqrt{\frac{\sum(x_i - \hat{x}_i)^2}{\bar{x}^2} \cdot \frac{1}{n}} \tag{7.1}$$

where x_i is the predicted value, $\hat{x}_i$ is the observed value and $\bar{x}$ is the mean of the observed values and n is the number of observation. The NRMSE expresses the spread of the modelling results around the measurements (Tiktak et al., 1998).

The modelling wells with reference to the Nickel are: PE17, P086, P214, P255, PE13, P252, PZ002 and they are arranged along sections 1, 2, 3, 4, 5. These sections are shown in Figures from 7.36 to 7.40, the well data and the NMSE are reported in Tables from 7.5 to 7.11.

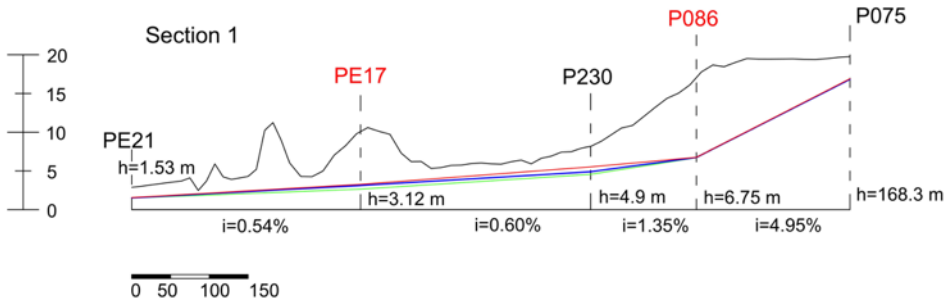

Figure 7.36: Section 1, in red the monitoring wells, with the blue line the average hydraulic profile, with the green line the minimum hydraulic profile and with the red line the maximum hydraulic profile.

Table 7.5:NRMSE – Well PE17

Monitoring well	PE17
Depth from the ground surface (m)	1.32
NRMSE	0.44

The monitoring and measured concentrations are reported in Figure 7.9.

Table 7.6:NRMSE – Well PE086

Monitoring well	P086
Depth from the ground surface (m)	2.68
NRMSE	1.34

The monitoring and measured concentrations are reported in Figure 7.15.

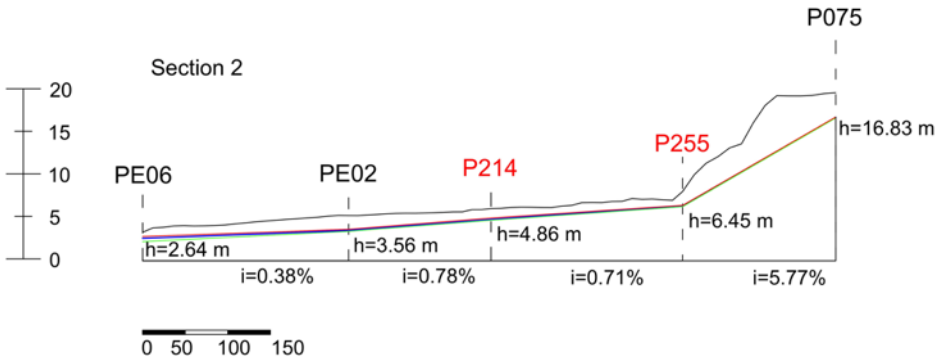

Figure 7.37: Section 2, in red the monitoring wells, with the blue line the average hydraulic profile, with the green line the minimum hydraulic profile and with the red line the maximum hydraulic profile.

Table 7.7:NRMSE – Well P214

Monitoring well	P214
Depth from the ground surface (m)	0.85
NRMSE	0.13

The monitoring and measured concentrations are reported in Figure 7.24.

Table 7.8:NRMSE – Well P255

Monitoring well	P255
Depth from the ground surface (m)	2.96
NRMSE	0.31

The monitoring and measured concentrations are reported in Figure 7.27.

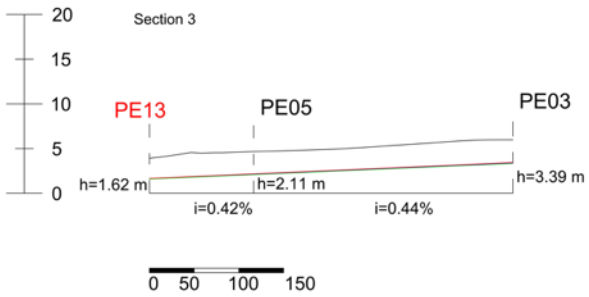

Figure 7.38: Section 3, in red the monitoring wells, with the blue line the average hydraulic profile, with the green line the minimum hydraulic profile and with the red line the maximum hydraulic profile.

Table 7.9:NRMSE – Well PE13

Monitoring well	PE13
Depth from the ground surface (m)	1.84
NRMSE	0.54

The monitoring and measured concentrations are reported in Figure 7.12.

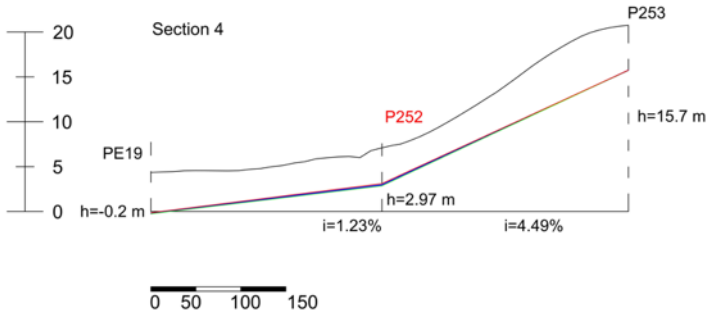

Figure 7.39: Section 4, in red the monitoring wells, with the blue line the average hydraulic profile, with the green line the minimum hydraulic profile and with the red line the maximum hydraulic profile.

Table 7.10:NRMSE – Well P252

Monitoring well	P252
Depth from the ground surface (m)	4.81
NRMSE	1.95

The monitoring and measured concentrations are reported in Figure 7.18.

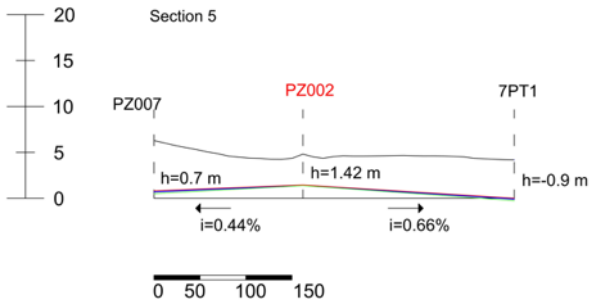

Figure 7.40: Section 5, in red the monitoring wells, with the blue line the average hydraulic profile, with the green line the minimum hydraulic profile and with the red line the maximum hydraulic profile.

Table 7.11:NRMSE – Well PZ002

Monitoring well	PZ002
Depth from the ground surface (m)	2.72
NRMSE	0.78

The monitoring and measured concentrations are reported in Figure 7.21.

The modelling wells with reference to the n-hexane are: P232, P052, P214, P225, P222, P243 and they are arrange along sections 6 and 7. The modelling results for these wells are shown in Figures from 7.43 to 7.47. The sections are shown in Figures 7.41 and 7.42, the data on the well and the NMSE are reported in Tables from 7.12 to 7.16.

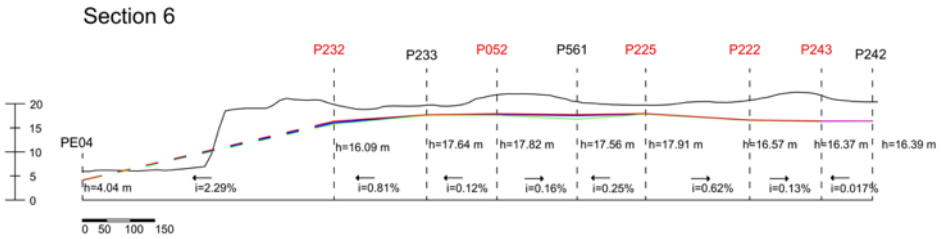

Figure 7.41: Section 6 in red the monitoring wells, with the blue line the average hydraulic profile, with the green line the minimum hydraulic profile and with the red line the maximum hydraulic profile.

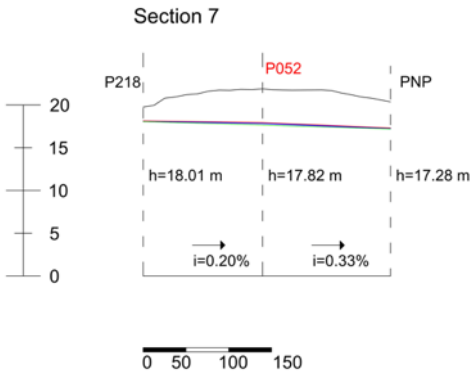

Figure 7.42: Section 7 in red the monitoring wells, with the blue line the average hydraulic profile, with the green line the minimum hydraulic profile and with the red line the maximum hydraulic profile.

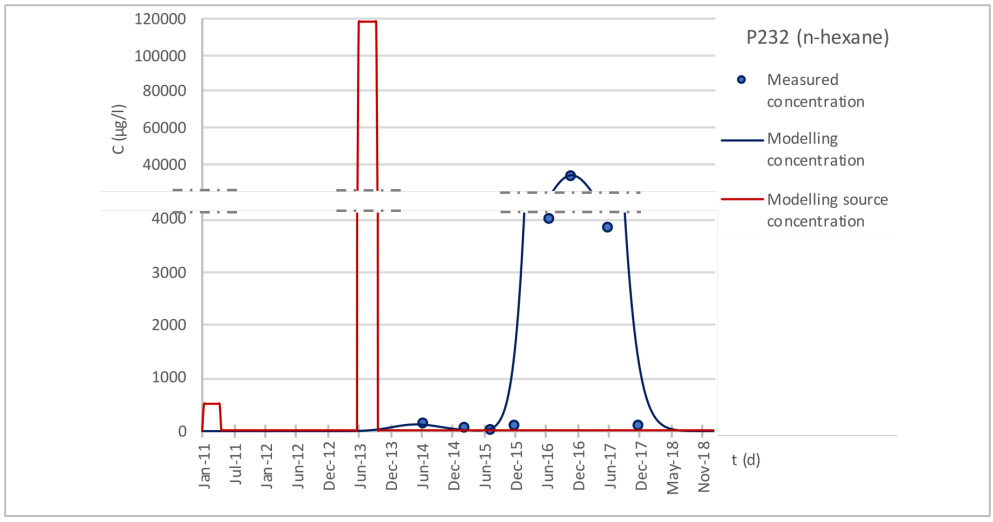

Figure 7.43: Well P232- Numerical model.

Table 7.12:NRMSE – Well P232

Monitoring well	P232
Depth from the ground surface (m)	3.89
NRMSE	1.35

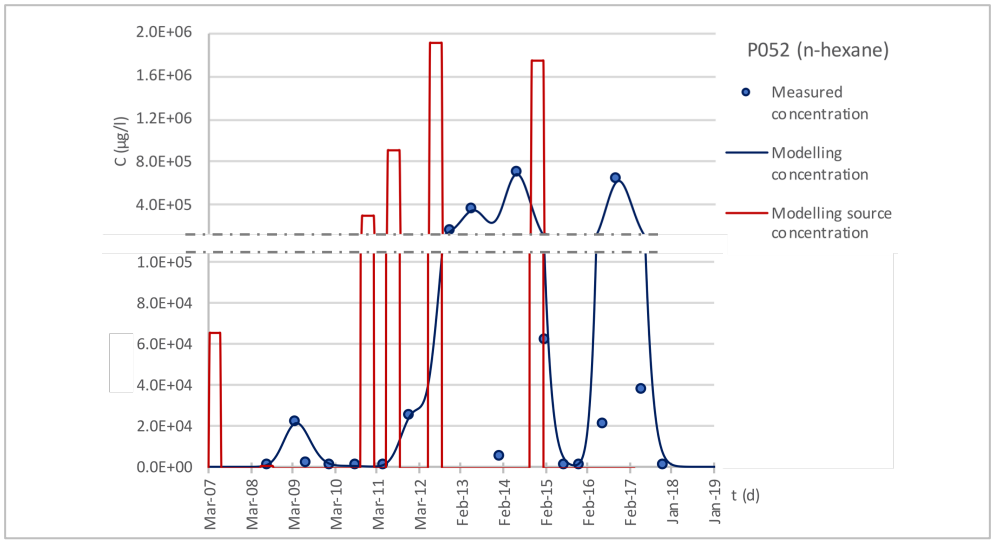

Figure 7.44: Well P052- Numerical model.

Table 7.13:NRMSE – Well P052

Monitoring well	P052
Depth from the ground surface (m)	2.22
NRMSE	0.99

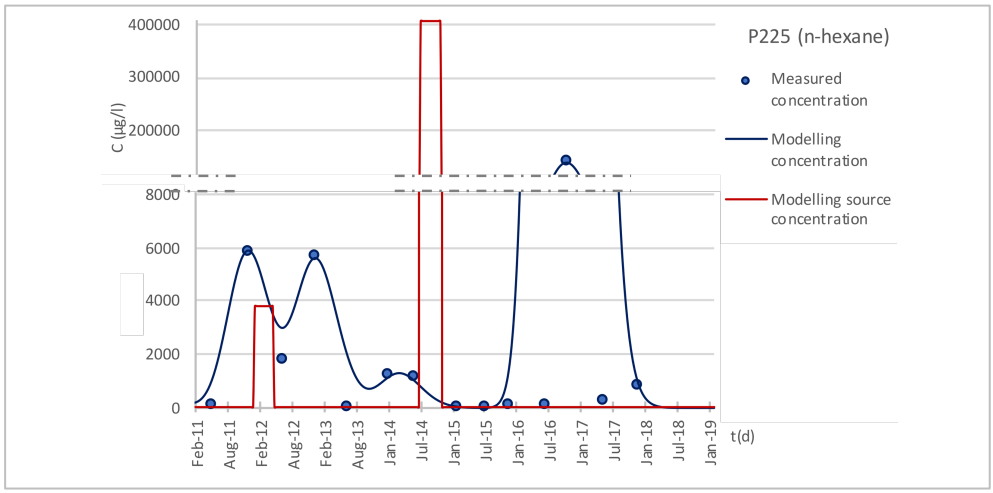

Figure 7.45: Well P225- Numerical model.

Table 7.14:NRMSE – Well P225

Monitoring well	P225
Depth from the ground surface (m)	2.45
NRMSE	2.42

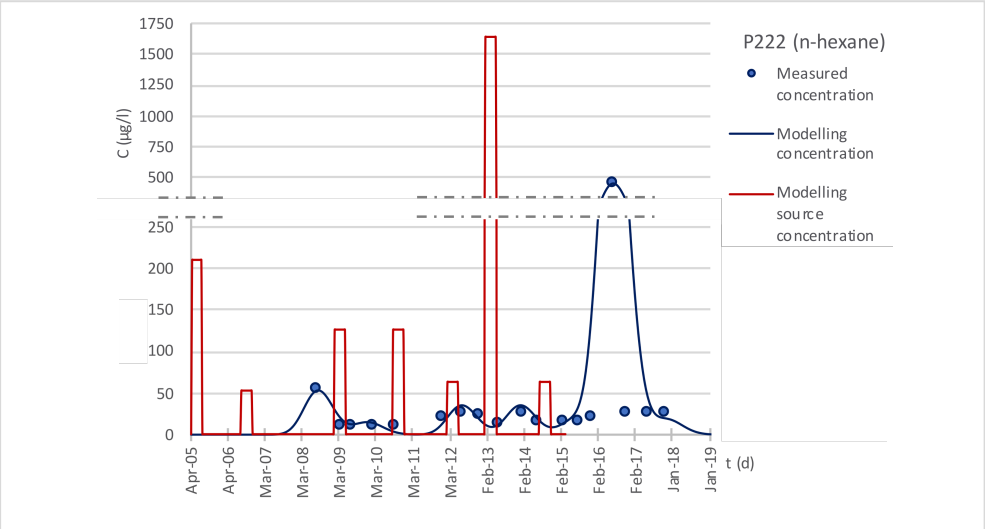

Figure 7.46: Well P222- Numerical model.

Table 7.15:NRMSE – Well P222

Monitoring well	P222
Depth from the ground surface (m)	3.89
NRMSE	1.73

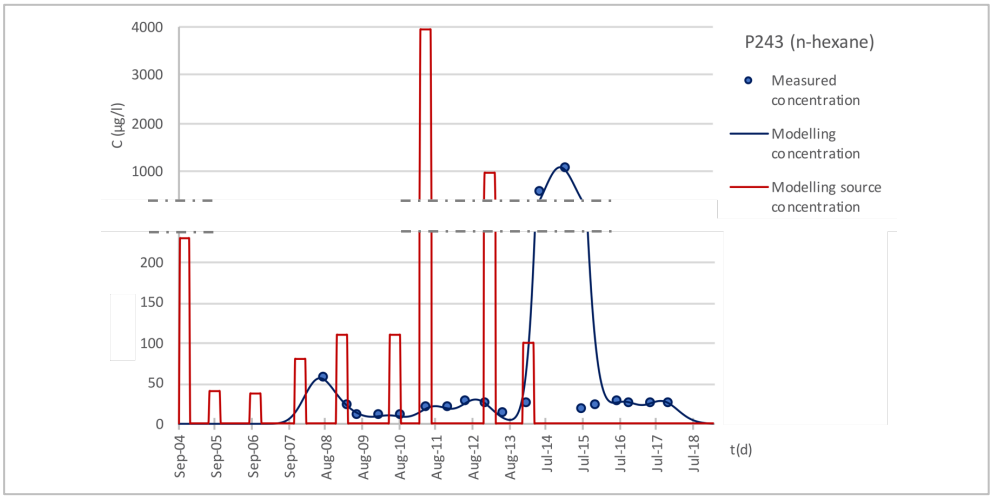

Figure 7.47: Well P243- Numerical model.

Table 7.16:NRMSE – Well P243

Monitoring well	P243
Depth from the ground surface (m)	4.38
NRMSE	0.85

For the wells with nickel contamination, P086, P252 e P255 are the wells with the higher hydraulic gradient (between 0.78% and 5.77%), these wells are located on the morphological scarp. P086 and P252 are the wells with the less accurate modelling, in fact for these two wells the NRMSE is a high value and the model is not able to simulate different measurement points. On the other hand, the well P255 return results comparable to the wells with a lower gradient. The effectiveness of modeling for wells PE17, P214, PE13, PZ002 (i <0.78%) is almost similar and it is not directly related to the gradient. These results would seem to confirm the hypothesis of an effect of the hydraulic gradients on modelling effectiveness.
The wells with n-hexane contamination have lower hydraulic gradients than nickels wells. The measured n-hexane concentrations vary, in the single well, by several orders of magnitude. These outliers could be caused by exceptional contaminant discharge in groundwater. The phenomenon has not been described by the developed conceptual model, hence it could lead to a lower effectiveness of the modelling. Nevertheless, it should be noted that wells P052 and P243, characterized by the lowest hydraulic gradients (between 0.017% and 0.33%), have the best results. This confirm the previous results.

8. Conclusions and remarks

Groundwater resources are increasingly threatened by contamination from different sources (contaminated sites, urbanization, industrial development and agricultural activities). One of the main and most concerning contamination pathways is the unsaturated zone transport of chemicals from shallow source zones to groundwater. Consequently, fate and transport models reproducing leaching in the unsaturated zone are increasingly considered in the risk assessment and the management of remediation practices. Many models reproducing these processes exist in scientific literature, ranging from simple to very complex mathematical formulations. However, their application to field scale in contaminated sites presents some critical issues, e.g. complexity of the involved natural processes, influence of co-contaminants, lack of an adequate dataset.

This PhD thesis wished to give a contribution to this topic. Therefore, the available models have been investigated to analyse their characteristics and the potential problems in the application to the field scale and a modelling approach has been proposed and applied to a field case study.

A quantitative comparison between analytical models with common characteristics has been developed to identify pros and cons as well as to point out any difference in the final output.

The comparison highlights a significant variability of the results with respect to the variation of the considered parameters. The analysis of the models makes it possible to identify three groups, according to the assumptions on contaminant source and chemical-physical mechanisms occurring during the transport. Each group appears suitable for a different contamination scenario. Furthermore, it should be noted that the more advanced are the models, the lower are the predicted concentrations, highlighting that simplified approaches could lead to outcomes some orders of magnitude greater than the advanced approaches.

Future research could be addressed to either enhance the existing analytical solutions or to propose new advanced ones, while preserving their suitability for engineering applications, in order to obtain a more realistic representation of contaminant fate and transport in the unsaturated zone.

A modelling approach has been proposed in order to reproduce the measured concentrations in a contaminated site and to provide a physically based

contamination scenario that could help in the identification of primary sources. The conceptual model behind the approach reproduces the downward vertical transport occurring as a result of water infiltration through the source at a constant rate and identify as the most important and dominant processes advection, longitudinal dispersion and sorption mechanisms. Two different mathematical models (analytical and numerical) have been used and the results compared.

The modelling results have been able to reproduce the measured contaminant concentrations, although analytical concentrations have exhibited a less smoothed trend than numerical ones. The obtained contamination scenarios have been found plausible and consistent with the solubility of the analysed contaminant.

In the proposed approach, the horizontal driving forces of the flow have been neglected. In order to test this hypothesis, an indicator of the effectiveness of the results has been compared to the hydraulic gradients of the underlying groundwater. The best modelling results have been obtained with low hydraulic gradients, probably because of the effects of the horizontal components of the flow on contaminant transport. This may represent a limitation which has to be considered in the model application and further deepened.

The developed modelling in this PhD thesis presents some elements related to the Taranto site that should be the subject of further research and investigations.

First, it would be worthwhile to carry out further field investigations to collect data of concentration measurements in surface soils of the monitoring points because these soils constitute secondary contaminant sources. The comparison of these measurements with the modelling contaminant sources would enable the validation of the obtained results.

Second, the influence of the horizontal driving forces on the results should be further analysed. A three-dimensional numerical modelling of the study area could be implemented and these results could be compared with the results of the approach presented in this thesis in order to give a further validation of this approach and to evaluate the effects of the hypothesis of the one-dimensional flow in the unsaturated medium.

Finally, the analysis of the modelling secondary sources could be used in the identification of the primary sources. Their identification is an important step to address the remediation management of the site and to identify the responsibilities of the involved economic subjects.

References

Addiscott, T. M., & Wagenet, R. J. (1985). Concepts of solute leaching in soils: a review of modelling approaches. Journal of soil science, 36(3), 411-424. https://doi.org/10.1111/j.1365-2389.1985.tb00347.x

Alastal, K., & Ababou, R. (2019). Moving Multi-Front (MMF): A generalized Green-Ampt approach for vertical unsaturated flows. Journal of Hydrology, 579, 124184. https://doi.org/10.1016/j.jhydrol.2019.124184

Alfnes, E., Kinzelbach, W., & Aagaard, P. (2004). Investigation of hydrogeologic processes in a dipping layer structure: 1. The flow barrier effect. Journal of contaminant hydrology, 69(3-4), 157-172. https://doi.org/10.1016/j.jconhyd.2003.08.005

Allam, A., Helal, E., & Mansour, M. (2019). Retarding contaminant migration through porous media using inclined barrier walls. Journal of Hydrology and Hydromechanics, 67(4), 339-348. DOI:10.2478/johh-2019-0020

Allen-King, R. M., Grathwohl, P., & Ball, W. P. (2002). New modeling paradigms for the sorption of hydrophobic organic chemicals to heterogeneous carbonaceous matter in soils, sediments, and rocks. Advances in Water resources, 25(8-12), 985-1016. https://doi.org/10.1016/S0309-1708(02)00045-3

Allaire-Leung, S. E., Wu, L., Mitchell, J. P., & Sanden, B. L. (2001). Nitrate leaching and soil nitrate content as affected by irrigation uniformity in a carrot field. Agricultural Water Management, 48(1), 37-50. https://doi.org/10.1016/S0378-3774(00)00112-8

Alloway, B. J. (Ed.). (2012). Heavy metals in soils: trace metals and metalloids in soils and their bioavailability (Vol. 22). Springer Science & Business Media. ISBN 9400744706

Anderson, M. P., Woessner, W. W., & Hunt, R. J. (2015). Applied groundwater modeling: simulation of flow and advective transport. Academic press. ISBN: 9780120581030

Aşçı, Y., Nurbaş, M., & Açıkel, Y. S. (2008). A comparative study for the sorption of Cd (II) by soils with different clay contents and mineralogy and the recovery of Cd (II) using rhamnolipid biosurfactant. Journal of Hazardous Materials, 154(1-3), 663-673. https://doi.org/10.1016/j.jhazmat.2007.10.078

ASTM, 2000. Standard Guide for Risk-Based Corrective Action. E2081, West Conshocken, PA.

Ataie-Ashtiani, B., & Hosseini, S. A. (2005). Error analysis of finite difference methods for two-dimensional advection–dispersion–reaction equation. Advances in water Resources, 28(8), 793-806. https://doi.org/10.1016/j.advwatres.2005.02.003

Balseiro-Romero, M., Monterroso, C., & Casares, J. J. (2018). Environmental fate of petroleum hydrocarbons in soil: Review of multiphase transport, mass transfer, and natural attenuation processes. Pedosphere, 28(6), 833-847. https://doi.org/10.1016/S1002-0160(18)60046-3

Baran, N., Richert, J., & Mouvet, C. (2007). Field data and modelling of water and nitrate movement through deep unsaturated loess. Journal of Hydrology, 345(1-2), 27-37. https://doi.org/10.1016/j.jhydrol.2007.07.006

Batu, V. (2005). Applied flow and solute transport modeling in aquifers: fundamental principles and analytical and numerical methods. CRC Press.

Bear, J. (1979). Hydraulics of Groundwater. McGraw-Hill ISBN-10: 0070041709

Bear, J., & Cheng, A. H. D. (2010). Modeling groundwater flow and contaminant transport (Vol. 23). Springer Science & Business Media. DOI 10.1007/978-1-4020-6682-5

Bear, J. (2013). Dynamics of fluids in porous media. Courier Corporation. ISBN 0486131807

Becker, S., Soukup, J. M., Sioutas, C., & Cassee, F. R. (2003). Response of human alveolar macrophages to ultrafine, fine, and coarse urban air pollution particles. Experimental lung research, 29(1), 29-44. https://doi.org/10.1080/01902140303762

Berkowitz, B., Dror, I., & Yaron, B. (2014). Contaminant geochemistry. Springer. https://doi.org/10.1007/978-3-642-54777-5

Berlin, M., Vasudevan, M., Kumar, G. S., & Nambi, I. M. (2015). Numerical modelling on fate and transport of petroleum hydrocarbons in an unsaturated subsurface system for varying source scenario. Journal of Earth System Science, 124(3), 655-674. https://doi.org/10.1007/s12040-015-0562-0

Beven, K. J., Henderson, D. E., & Reeves, A. D. (1993). Dispersion parameters for undisturbed partially saturated soil. Journal of hydrology, 143(1-2), 19-43. https://doi.org/10.1016/0022-1694(93)90087-P

Biggar, J. W., & Nielsen, D. R. (1976). Spatial variability of the leaching characteristics of a field soil. Water Resources Research, 12(1), 78-84. https://doi.org/10.1029/WR012i001p00078

Borch, T., Kretzschmar, R., Kappler, A., Cappellen, P. V., Ginder-Vogel, M., Voegelin, A., & Campbell, K. (2010). Biogeochemical redox processes and their impact on contaminant dynamics. Environmental science & technology, 44(1), 15-23. https://doi.org/10.1021/es9026248

Botros, F. E., Onsoy, Y. S., Ginn, T. R., & Harter, T. (2012). Richards equation–based modeling to estimate flow and nitrate transport in a deep alluvial vadose zone. Vadose Zone Journal, 11(4). https://doi.org/10.2136/vzj2011.0145

Boulding, J. R., & Ginn, J. S. (2016). Practical handbook of soil, vadose zone, and ground-water contamination: assessment, prevention, and remediation. CRC Press. ISBN : 0566706106

Brooks, R., & Corey, T. (1964). Hydraulic properties of porous media. Hydrology Papers, Colorado State University, 24, 37.

Brouyère, S. (2006). Modelling the migration of contaminants through variably saturated dual-porosity, dual-permeability chalk. Journal of contaminant hydrology, 82(3-4), 195-219. https://doi.org/10.1016/j.jconhyd.2005.10.004

Brusseau, M. L. (2019). Physical processes affecting contaminant transport and fate. In Environmental and Pollution Science (pp. 113-130). Academic Press. https://doi.org/10.1016/B978-0-12-814719-1.00007-0

Brusseau, M. L., & Chorover, J. (2019). Chemical processes affecting contaminant transport and fate. In Environmental and Pollution Science (pp. 113-130). Academic Press. https://doi.org/10.1016/B978-0-12-814719-1.00008-2

Butler, B. J., & Barker, J. F. (1996). Chemical and microbiological transformations and degradation of chlorinated solvent compounds. Dense Chlorinated Solvents, 267-312.

Cardellicchio, N., & Costiero, M. (2013). L'area di Taranto, sito contaminato di interesse nazionale: problematiche e riflessioni.

Carey, G. R., McBean, E. A., & Feenstra, S. (2018). Estimating transverse dispersivity based on hydraulic conductivity. Environmental technology & innovation, 10, 36-45. https://doi.org/10.1016/j.eti.2018.01.008

Carsel, R. F., & Parrish, R. S. (1988). Developing joint probability distributions of soil water retention characteristics. Water resources research, 24(5), 755-769. https://doi.org/10.1029/WR024i005p00755

Chen, H., Teng, Y., Lu, S., Wang, Y., & Wang, J. (2015). Contamination features and health risk of soil heavy metals in China. Science of the total environment, 512, 143-153. https://doi.org/10.1016/j.scitotenv.2015.01.025

Cherry, J. A., Parker, B. L., Bradbury, K. R., Eaton, T. T., Gotkowitz, M. B., Hart, D. J., & Borchardt, M. A. (2006). Contaminant transport through aquitards: a state-of-the-science review. Denver, Colorado: American Water Works Association Research Foundation.

Chibuike, G. U., & Obiora, S. C. (2014). Heavy metal polluted soils: effect on plants and bioremediation methods. Applied and environmental soil science, 2014. https://doi.org/10.1155/2014/752708

China Environment Chamber of Commerce (CECC), 2014. Strengthening environmental management of contaminated sites is an extremely urgent matter. CECC, http://www.cecc-china.org/detail/19702.html (last accessed on 09/08/19 - Chinese language).

Chiogna, G., Eberhardt, C., Grathwohl, P., Cirpka, O. A., & Rolle, M. (2010). Evidence of compound-dependent hydrodynamic and mechanical transverse dispersion by multitracer laboratory experiments. Environmental science & technology, 44(2), 688-693. https://doi.org/10.1021/es9023964

Christophersen, M., Broholm, M. M., Mosbæk, H., Karapanagioti, H. K., Burganos, V. N., & Kjeldsen, P. (2005). Transport of hydrocarbons from an emplaced fuel source experiment in the vadose zone at Airbase Værløse, Denmark. Journal of contaminant hydrology, 81(1-4), 1-33. https://doi.org/10.1016/j.jconhyd.2005.06.011

COMSOL Multiphysics,2010.http://www.comsol.com/

Connell, L. D. (2002). A simple analytical solution for unsaturated solute migration under dynamic water movement conditions and root zone effects. Geological Society, London, Special Publications, 193(1), 255-264. https://doi.org/10.1144/GSL.SP.2002.193.01.19

Connor, J. A., Newell, C. J., & Malander, M. W. (1996, November). Parameter estimation guidelines for risk-based corrective action (RBCA) modeling. In National Ground Water Association (ed.), Proceedings of the Petroleum Hydrocarbons and Organic Chemicals in Groundwater Conference, Houston, TX, USA (pp. 13-15)

Connor, J., Bowers, R., McHugh, T., & Spexet, A. (2007). Software guidance manual RBCA tool kit for chemical releases. Houston, Texas, USA: GSI Environmental Inc, 1-120.

Connor, J. A., Bowers, R. L., Paquette, S. M., & Newell, C. J. (1997). Soil attenuation model for derivation of risk-based soil remediation standards. Groundwater Services Inc., Houston, Texas, 1-34.

Cowan-Ellsberry, C. E., McLachlan, M. S., Arnot, J. A., MacLeod, M., McKone, T. E., & Wania, F. (2009). Modeling exposure to persistent chemicals in hazard and risk assessment. Integrated Environmental Assessment and Management: An International Journal, 5(4), 662-679. https://doi.org/10.1897/IEAM_2008-084.1

Cox, E., Austins, C., Spain, J., Shin, K., Nishino, S., Gossett, J., ... & Duhamel, M. (2010). The Truth is Out There: Unraveling the Mystery of the Missing DCE, Vinyl Chloride, and Ethene. In Proceedings of the Seventh International Conference, Remediation of Chlorinated and Recalcitrant Compounds (pp. 24-27).

CRCCARE, 2013. Global Contamination Initiative e a Proposal for a New Global Initiative Addressing One of the Most Serious Threats to Our Planet and Our Future. Cooperative Research Centre for Contamination Assessment and Remediation of Environment (CRC CARE), Australia, pp. 1e5.

Cronkite-Ratcliff, C., Phelps, G. A., & Boucher, A. (2012). A multiple-point geostatistical method for characterizing uncertainty of subsurface alluvial units and its effects on flow and transport. US Department of the Interior, US Geological Survey. https://doi.org/10.3133/ofr20121065

Cryer, S. A., Havens, P. L., Hillger, D. E., & van Wesenbeeck, I. J. (2015). An improved indirect procedure for estimating pesticide volatility from field trials. Journal of environmental quality, 44(5), 1513-1522. doi:10.2134/jeq2015.03.0125

Daus, A. D., Frind, E. O., & Sudicky, E. A. (1985). Comparative error analysis in finite element formulations of the advection-dispersion equation. Advances in Water Resources, 8(2), 86-95. https://doi.org/10.1016/0309-1708(85)90005-3

Day, M. J., Reinke, R. F., & Thomson, J. A. (2001). Fate and Transport of Fuel Components Below Slightly Leaking Underground Storage TanksTechnical Note. Environmental Forensics, 2(1), 21-28. doi:10.1006/enfo.2000.0036

DeNovio, N. M., Saiers, J. E., & Ryan, J. N. (2004). Colloid movement in unsaturated porous media. Vadose Zone Journal, 3(2), 338-351. DOI:10.2136/vzj2004.0338

Di Gianfilippo, M., Verginelli, I., Costa, G., Spagnuolo, R., Gavasci, R., & Lombardi, F. (2018). A risk-based approach for assessing the recycling potential of an alkaline waste material as road sub-base filler material. Waste Management, 71, 440-453. https://doi.org/10.1016/j.wasman.2017.10.006

Di Molfetta, A., & Sethi, R. (2012). Ingegneria degli acquiferi. Springer Science & Business Media. DOI 10.1007/978-88-470-1851-8

Di Sante, M., Mazzieri, F., Fratalocchi, E., Brianzoni, V., & Pasqualini, E. (2014). A possible approach for Tier 2 risk assessments of polluted sites: Framework, computer spreadsheet and application. Computers and Geotechnics, 56, 16-27. https://doi.org/10.1016/j.compgeo.2013.10.006

Di Sante, M., Fratalocchi, E., Mazzieri, F., Pasqualini, E. (2019). The role of geotechnics in the risk assessment procedure for polluted sites. RIVISTA ITALIANA DI GEOTECNICA, 3/2019. http://dx.doi.org/10.19199/2019.3.0557-1405.030

Dubinin, M. M. & Radushkevich L.V., The equation of the characteristic curve of the activated charcoal, Proc. Acad. Sci. USSR Phys. Chem. Sect. 55 (1947) 331–337.

Dupuis, J., & Knoepfel, P. (2016). Politics of Contaminated Sites Management. Springer International Pu. DOI: 10.1007/978-3-319-11307-4

Durães, N., Novo, L. A., Candeias, C., & da Silva, E. F. (2018). Distribution, Transport and Fate of Pollutants. In Soil Pollution (pp. 29-57). Academic Press. https://doi.org/10.1016/B978-0-12-849873-6.00002-9

Enfield, C. G., Carsel, R. F., Cohen, S. Z., Phan, T., & Walters, D. M. (1982). Approximating Pollutant Transport to Ground Water a. Groundwater, 20(6), 711-722. https://doi.org/10.1111/j.1745-6584.1982.tb01391.x

Espana, V. A. A., Pinilla, A. R. R., Bardos, P., & Naidu, R. (2018). Contaminated land in Colombia: a critical review of current status and future approach for the management of contaminated sites. Science of the Total Environment, 618, 199-209. https://doi.org/10.1016/j.scitotenv.2017.10.245

European Chemical Agency (2017) Guidance on Information Requirements and Chemical Safety Assessment Chapter R.11: PBT/vPvB Assessment, ECHA-17-G-12-EN. https://doi.org/10.2823/128621

Farlin, J., Gallé, T., Bayerle, M., Pittois, D., Braun, C., El Khabbaz, H., ... & Weihermueller, L. (2013). Using the long-term memory effect of pesticide and metabolite soil residues to estimate field degradation half-life and test leaching predictions. Geoderma, 207, 15-24. https://doi.org/10.1016/j.geoderma.2013.04.028

Feng, X., Simpson, A. J., & Simpson, M. J. (2005). Chemical and mineralogical controls on humic acid sorption to clay mineral surfaces. Organic Geochemistry, 36(11), 1553-1566. https://doi.org/10.1016/j.orggeochem.2005.06.008

Ferguson, C., Darmendrail, D., Freier, K., Jensen, B. K., Jensen, J., Kasamas, H., & Urzelai, A. (1998). Risk Assessment for Contaminated Sites in Europe: Vol 1: Scientific Basis.

Ferrey, M. L., Wilkin, R. T., Ford, R. G., & Wilson, J. T. (2004). Nonbiological removal of cis-dichloroethylene and 1, 1-dichloroethylene in aquifer sediment containing magnetite. Environmental science & technology, 38(6), 1746-1752. https://doi.org/10.1021/es0305609

Fetter, C. W., Boving, T., & Kreamer, D. (2017). Contaminant hydrogeology. Waveland Press. ISBN 1478636505

Flury, M., & Qiu, H. (2008). Modeling colloid-facilitated contaminant transport in the vadose zone. Vadose Zone Journal, 7(2), 682-697. DOI:10.2136/vzj2007.0066

Flury, M., & Wai, N. N. (2003). Dyes as tracers for vadose zone hydrology. Reviews of Geophysics, 41(1). https://doi.org/10.1029/2001RG000109

Foo, K. Y., & Hameed, B. H. (2010). Insights into the modeling of adsorption isotherm systems. Chemical engineering journal, 156(1), 2-10. https://doi.org/10.1016/j.cej.2009.09.013

Forrer, I., Kasteel, R., Flury, M., & Flühler, H. (1999). Longitudinal and lateral dispersion in an unsaturated field soil. Water resources research, 35(10), 3049-3060. https://doi.org/10.1029/1999WR900185

Foster, S., Hirata, R., Gomes, D., D'Elia, M., & Paris, M. (2002). Groundwater quality protection: a guide for water service companies, municipal authorities and environment agencies. The World Bank. https://doi.org/10.1596/0-8213-4951-1

Francisca, F. M., Carro Pérez, M. E., Glatstein, D. A., & Montoro, M. A. (2012). Contaminant transport and fluid flow in soils. Horizons in earth research, 6, 97-131. ISBN: 978-1-61470-462-1

František, K., Zbyněk, B., Pavel, M., Miloslava, K., & Irena, S. (2003). Contamination of soils and groundwater by petroleum hydrocarbons and volatile organic compounds–Case study: ELSLAV BRNO. Bulletin of Geosciences, 78(3), 225-239.

Fredlund, D. G., & Rahardjo, H. (1993). Soil mechanics for unsaturated soils. John Wiley & Sons.

Fredlund, D. G., Wilson, G. W., & Barbour, S. L. (2001). Unsaturated soil mechanics and property assessment. In Geotechnical and geoenvironmental engineering handbook (pp. 107-146). Springer, Boston, MA. https://doi.org/10.1007/978-1-4615-1729-0_5

Fredlund, D. G. (2006). Unsaturated soil mechanics in engineering practice. Journal of geotechnical and geoenvironmental engineering, 132(3), 286-321. https://doi.org/10.1061/(ASCE)1090-0241(2006)132:3(286)

Freundlich, H. M. F. (1906). Over the adsorption in solution. J. Phys. Chem, 57(385471), 1100-1107.

Frey, S. K., Hwang, H. T., Park, Y. J., Hussain, S. I., Gottschall, N., Edwards, M., & Lapen, D. R. (2016). Dual permeability modeling of tile drain management influences on hydrologic and nutrient transport characteristics in macroporous soil. Journal of Hydrology, 535, 392-406. https://doi.org/10.1016/j.jhydrol.2016.01.073

Gao, Y., Pu, S., Zheng, C., & Yi, S. (2019). An improved method for the calculation of unsaturated–saturated water flow by coupling the FEM and FDM. Scientific reports, 9(1), 1-9. https://doi.org/10.1038/s41598-019-51405-4

Garakani, A. A., Haeri, S. M., Cherati, D. Y., Givi, F. A., Tadi, M. K., Hashemi, A. H., ... & Qahremani, F. (2018). Effect of road salts on the hydro-mechanical behavior of unsaturated collapsible soils. Transportation Geotechnics, 17, 77-90. https://doi.org/10.1016/j.trgeo.2018.09.005

Garré, S., Koestel, J., Günther, T., Javaux, M., Vanderborght, J., & Vereecken, H. (2010). Comparison of heterogeneous transport processes observed with electrical resistivity tomography in two soils. Vadose Zone Journal, 9(2), 336-349. doi:10.2136/vzj2009.0086

Gelhar, L. W. (1985). A review of field-scale physical solute transport processes in saturated and unsaturated porous media. EPRI EA-4190, Project 2485-5, Final Report.

Gelhar, L. W., Welty, C., & Rehfeldt, K. R. (1992). A critical review of data on field-scale dispersion in aquifers. Water resources research, 28(7), 1955-1974. https://doi.org/10.1029/92WR00607

GEOSLOPE International Ltd., 2017. Heat and Mass Transfer Modeling with GeoStudio 2018. 2nd Ed. Calgary, Alberta, Canada.

Gerba, C. P. (2019). Environmental Toxicology. In Environmental and Pollution Science (pp. 511-540). Academic Press. https://doi.org/10.1016/B978-0-12-814719-1.00028-8

Gerke, H. H., & Van Genuchten, M. T. (1993). A dual-porosity model for simulating the preferential movement of water and solutes in structured porous media. Water resources research, 29(2), 305-319. https://doi.org/10.1029/92WR02339

Goldscheider, N. (2010). Delineation of spring protection zones. In Groundwater hydrology of springs (pp. 305-338). Butterworth-Heinemann. https://doi.org/10.1016/B978-1-85617-502-9.00008-6

Goyne, K. W., Jun, H. J., Anderson, S. H., & Motavalli, P. P. (2008). Phosphorus and nitrogen sorption to soils in the presence of poultry litter-derived dissolved organic matter. Journal of environmental quality, 37(1), 154-163. doi:10.2134/jeq2007.0141

Green, W. H., & Ampt, G. A. (1911). Studies on Soil Phyics. The Journal of Agricultural Science, 4(1), 1-24. https://doi.org/10.1017/S0021859600001441

Greskowiak, J., Hamann, E., Burke, V., & Massmann, G. (2017). The uncertainty of biodegradation rate constants of emerging organic compounds in soil and groundwater–A compilation of literature values for 82 substances. Water research, 126, 122-133. https://doi.org/10.1016/j.watres.2017.09.017

Grim, R. E. (1962). Applied Clay Mineralogy. Mc-Graw-Hill Book Company Inc. New York.

Gwo, J. P., Jardine, P. M., Wilson, G. V., & Yeh, G. T. (1995). A multiple-pore-region concept to modeling mass transfer in subsurface media. Journal of Hydrology, 164(1-4), 217-237. https://doi.org/10.1016/0022-1694(94)02555-P

Haggerty, R., Harvey, C. F., Freiherr von Schwerin, C., & Meigs, L. C. (2004). What controls the apparent timescale of solute mass transfer in aquifers and soils? A comparison of experimental results. Water Resources Research, 40(1). https://doi.org/10.1029/2002WR001716

Hallberg, G. R. (1989). Pesticides pollution of groundwater in the humid United States. Agriculture, ecosystems & environment, 26(3-4), 299-367. https://doi.org/10.1016/0167-8809(89)90017-0Get

Hemond, H. F., & Fechner, E. J. (2015). Chapter 3-The subsurface environment. Chemical Fate and Transport In The Environment, 219-230. https://doi.org/10.1016/B978-0-12-398256-8.00003-7

Hendrickx, J. M., & Flury, M. (2001). Uniform and preferential flow mechanisms in the vadose zone. Conceptual models of flow and transport in the fractured vadose zone, 149-187. ISBN 0309170990

Hillel, D. (2003). Introduction to environmental soil physics. Elsevier. https://doi.org/10.1016/B978-0-12-348655-4.X5000-X

Holden, P. A., & Fierer, N. (2005). VADOSE ZONE| Microbial Ecology. In Encyclopedia of Soils in the Environment. Elsevier. https://doi.org/10.1016/B0-12-348530-4/00172-7

Höhener, P., Dakhel, N., Christophersen, M., Broholm, M., & Kjeldsen, P. (2006). Biodegradation of hydrocarbons vapors: Comparison of laboratory studies and field investigations in the vadose zone at the emplaced fuel source experiment, Airbase Værløse, Denmark. Journal of Contaminant Hydrology, 88(3-4), 337-358. https://doi.org/10.1016/j.jconhyd.2006.07.007

Hopmans, J. W. (2011). Infiltration and Unsaturated Zone. In Treatise on Water Science (pp. 103 -114) Elsevier. https://doi.org/10.1016/B978-0-444-53199-5.00031-2

Howard, P. H. (2017). Handbook of environmental degradation rates. CRC Press. 776 pages. ISBN: 9780873713580

Huang, P. M., Li, Y., & Sumner, M. E. (Eds.). (2011). Handbook of soil sciences: properties and processes. CRC Press. ISBN 1439803064

Hunt, B. (1978). Dispersive sources in uniform ground-water flow. Journal of the Hydraulics Division, 104(ASCE 13467 Proceeding).

Hussein, M., Jin, M., & Weaver, J. W. (2002). Development and verification of a screening model for surface spreading of petroleum. Journal of contaminant hydrology, 57(3-4), 281-302. https://doi.org/10.1016/S0169-7722(01)00220-0

Huyakorn, P. S., Thomas, S. D., & Thompson, B. M. (1984). Techniques for making finite elements competitve in modeling flow in variably saturated porous media. Water Resources Research, 20(8), 1099-1115. https://doi.org/10.1029/WR020i008p01099

HydroGeoLogic. (1998). MODFLOW-SURFACT v. 3.0: A Comprehensive MODFLOW-based Flow and Transport Simulator. Code Documentation Report.

Ite, A. E., Ibok, U. J., Ite, M. U., & Petters, S. W. (2013). Petroleum exploration and production: Past and present environmental issues in the Nigeria's Niger Delta. American Journal of Environmental Protection, 1(4), 78-90. DOI:10.12691/env-1-4-2

Jarvis, N. J. (1998). Modeling the impact of preferential flow on nonpoint source pollution. Physical nonequilibrium in soils: modeling and application, 195-221. ISBN 1575040492

Javaux, M., & Vanclooster, M. (2004). In situ long-term chloride transport through a layered, nonsaturated subsoil. 1. Data set, interpolation methodology, and results. Vadose zone journal, 3(4), 1322-1330. doi:10.2136/vzj2004.1322

Javaux, M., Kasteel, R., Vanderborght, J., & Vanclooster, M. (2006). Interpretation of dye transport in a macroscopically heterogeneous, unsaturated subsoil with a one-dimensional model. doi:10.2136/vzj2005.0085

Jing, F., Chen, X., Yang, Z., & Guo, B. (2018). Heavy metals status, transport mechanisms, sources, and factors affecting their mobility in Chinese agricultural soils. Environmental earth sciences, 77(3), 104. https://doi.org/10.1007/s12665-018-7299-4

Jury, W. A., Spencer, W. F., & Farmer, W. (1983). Behavior assessment model for trace organics in soil: I. Model description 1. Journal of environmental quality, 12(4), 558-564. doi:10.2134/jeq1983.00472425001200040025x

Jury, W. A., Spencer, W. F., & Farmer, W. J. (1984). Behavior assessment model for trace organics in soil: III. Application of screening model. Journal of Environmental Quality, 13(4), 573-579. https://doi.org/10.2134/jeq1984.00472425001300040013x

Jury, W. A., Russo, D., Streile, G., & El Abd, H. (1990). Evaluation of volatilization by organic chemicals residing below the soil surface. Water Resources Research, 26(1), 13-20. https://doi.org/10.1029/WR026i001p00013

Karapanagioti, H. K., Gaganis, P., & Burganos, V. N. (2003). Modeling attenuation of volatile organic mixtures in the unsaturated zone: codes and usage. Environmental modelling & software, 18(4), 329-337. https://doi.org/10.1016/S1364-8152(02)00108-1

Karkush, M. O., & Altaher, T. A. (2016). Risk assessment of AL-Nassyriah oil refinery soil. Journal of Civil Engineering Research, 6(1), 16-21. DOI: 10.5923/j.jce.20160601.03

Kavetski, D., Binning, P., & Sloan, S. W. (2001). Adaptive time stepping and error control in a mass conservative numerical solution of the mixed form of Richards equation. Advances in water resources, 24(6), 595-605. https://doi.org/10.1016/S0309-1708(00)00076-2

Khamehchiyan, M., Charkhabi, A. H., & Tajik, M. (2007). Effects of crude oil contamination on geotechnical properties of clayey and sandy soils. Engineering geology, 89(3-4), 220-229. https://doi.org/10.1016/j.enggeo.2006.10.009

Khan, M. A. Q., Khan, S. F., & Shattari, F. (2008). Halogenated hydrocarbons. https://doi.org/10.1016/B978-008045405-4.00399-2

Klenk, I. D., & Grathwohl, P. (2002). Transverse vertical dispersion in groundwater and the capillary fringe. Journal of Contaminant Hydrology, 58(1-2), 111-128. https://doi.org/10.1016/S0169-7722(02)00011-6

Kocman, D., Horvat, M., Pirrone, N., & Cinnirella, S. (2013). Contribution of contaminated sites to the global mercury budget. Environmental research, 125, 160-170. https://doi.org/10.1016/j.envres.2012.12.011

Kogovšek, J., & Šebela, S. (2004). Water tracing through the vadose zone above Postojnska Jama, Slovenia. Environmental Geology, 45(7), 992-1001. https://doi.org/10.1007/s00254-003-0958-z

Kosugi K, Hopmans JW, and Dane JH (2002) Water retention and storage – parametric models. In: Dane JH and Topp GC (eds.) Methods of Soil Analysis. Part 4. Physical Methods, pp. 739--758. Madison, WI: Soil Science Society of America. ISBN-13 978-0891188414

Kovalick Jr, W. W., & Montgomery, R. H. (2014). Developing a Program for Contaminated Site Management in Low and Middle Income Countries.

Kresic, N. (2006). Hydrogeology and groundwater modeling. CRC press. ISBN 0849333482

Kuppusamy, S., Venkateswarlu, K., Megharaj, M., Mayilswami, S., & Lee, Y. B. (2017). Risk-based remediation of polluted sites: A critical perspective. Chemosphere, 186, 607-615. https://doi.org/10.1016/j.chemosphere.2017.08.043

Kuzmin, D., & Hämäläinen, J. (2015). Finite element methods for computational fluid dynamics: a practical guide. SIAM Rev, 57(4), 642. ISBN 1611973600

Lahvis, M. A., & Baehr, A. L. (1997). Documentation of R-UNSAT, a computer model for the simulation of reactive, multispecies transport in the unsaturated zone. US Department of the Interior, US Geological Survey.

Lahvis, M. A., & Rehmann, L. C. (1999). Simulation of methyl tert-butyl ether (MTBE) transport to ground water from immobile sources of gasoline in the vadose zone. In 2000 Petroleum Hydrocarbons abd Organic Chemicals in Ground Water: Prevention, Detection, and Remediation (Vol. 1, pp. 247-259).

Lai, A., Panfilo, S., & Stacchezzini, R. (2019). The governmentality of corporate (un) sustainability: the case of the ILVA steel plant in Taranto (Italy). Journal of Management and Governance, 23(1), 67-109. https://doi.org/10.1007/s10997-019-09457-1

Langmuir, I. (1916). The constitution and fundamental properties of solids and liquids. Part I. Solids. Journal of the American chemical society, 38(11), 2221-2295. https://doi.org/10.1021/ja02268a002

Lehosmaa, K., Jyväsjärvi, J., Ilmonen, J., Rossi, P. M., Paasivirta, L., & Muotka, T. (2018). Groundwater contamination and land drainage induce divergent responses in boreal spring ecosystems. Science of The Total Environment, 639, 100-109. https://doi.org/10.1016/j.scitotenv.2018.05.126

Leij, F. J., Toride, N., & Van Genuchten, M. T. (1993). Analytical solutions for non-equilibrium solute transport in three-dimensional porous media. Journal of Hydrology, 151(2-4), 193-228. https://doi.org/10.1016/0022-1694(93)90236-3

Leij, F. J., & Bradford, S. A. (1994). 3DADE: A computer program for evaluating three-dimensional equilibrium solute transport in porous media. US Salinity Laboratory, Agricultural Research Service, US Department of Agriculture.

Leij, F. J., & Toride, N. (1997). N3DADE: A computer program for evaluating nonequilibrium three-dimensional equilibrium solute transport in porous media. US Salinity Laboratory Research Report No. 143.

Li, N., Yue, X., & Ren, L. (2016). Numerical homogenization of the Richards equation for unsaturated water flow through heterogeneous soils. Water Resources Research, 52(11), 8500-8525. https://doi.org/10.1002/2015WR018508

Li, X., Li, D., Xu, Y., & Feng, X. (2020). A DFN based 3D numerical approach for modeling coupled groundwater flow and solute transport in fractured rock mass. International Journal of Heat and Mass Transfer, 149, 119179. https://doi.org/10.1016/j.ijheatmasstransfer.2019.119179

Liu, H. H., & Bodvarsson, G. S. (2001). Constitutive relations for unsaturated flow in a fracture network. Journal of Hydrology, 252(1-4), 116-125. https://doi.org/10.1016/S0022-1694(01)00449-8

Liu, J. L., & Wong, M. H. (2013). Pharmaceuticals and personal care products (PPCPs): a review on environmental contamination in China. Environment international, 59, 208-224. https://doi.org/10.1016/j.envint.2013.06.012

Liu, W., Xu, S., Xing, B., Pan, B., & Tao, S. (2010). Nonlinear binding of phenanthrene to the extracted fulvic acid fraction in soil in comparison with other organic matter fractions and to the whole soil sample. Environmental pollution, 158(2), 566-575. https://doi.org/10.1016/j.envpol.2009.08.035

Locatelli, L., Binning, P. J., Sanchez-Vila, X., Søndergaard, G. L., Rosenberg, L., & Bjerg, P. L. (2019). A simple contaminant fate and transport modelling tool for management and risk assessment of groundwater pollution from contaminated sites. Journal of contaminant hydrology, 221, 35-49. https://doi.org/10.1016/j.jconhyd.2018.11.002

Ma, L., Liu, Y., Zhang, J., Yang, Q., Li, G., & Zhang, D. (2018). Impacts of irrigation water sources and geochemical conditions on vertical distribution of pharmaceutical and personal care products (PPCPs) in the vadose zone soils. Science of the Total Environment, 626, 1148-1156. https://doi.org/10.1016/j.scitotenv.2018.01.168

Maier, R. M. (2019). Biological Processes Affecting Contaminants Transport and Fate. In Environmental and Pollution Science (pp. 131-146). Academic Press. https://doi.org/10.1016/B978-0-12-814719-1.00009-4

Mallants, D., Tseng, P. H., Toride, N., Tinunerman, A., & Feyen, J. (1997). Evaluation of multimodal hydraulic functions in characterizing a heterogeneous field soil. Journal of hydrology, 195(1-4), 172-199. https://doi.org/10.1016/S0022-1694(96)03251-9

Mallants, D., Van Genuchten, M. T., Šimůnek, J., Jacques, D., & Seetharam, S. (2011). Leaching of contaminants to groundwater. In Dealing with Contaminated Sites (pp. 787-850). Springer, Dordrecht. https://doi.org/10.1007/978-90-481-9757-6_18

Massoudieh, A., & Ginn, T. R. (2010). Colloid-facilitated contaminant transport in unsaturated porous media. Modelling of pollutants in complex environmental systems, 2, 263-286. ISBN : 9781906799014

MARTINIS B. & ROBBA E. (1971) - Note illustrative della Carta Geologica d'Italia alla scala 1: 100.000 - Foglio 202, Taranto Serv. Geol. d'It. .

Mazzieri, F., Di Sante, M., Fratalocchi, E., & Pasqualini, E. (2016). Modeling contaminant leaching and transport to groundwater in Tier 2 risk assessment procedures of contaminated sites. Environmental Earth Sciences, 75(18), 1247. https://doi.org/10.1007/s12665-016-6043-1

McDonald, M. G., & Harbaugh, A. W. (1988). A modular three-dimensional finite-difference ground-water flow model. US Geological Survey. https://doi.org/10.3133/ofr83875

McLachlan, M. S., Zou, H., & Gouin, T. (2017). Using benchmarking to strengthen the assessment of persistence. Environ. Sci. Technol. 2017, 51 (1), 4-11. DOI: 10.1021/acs.est.6b03786

Mechlińska, A., Gdaniec-Pietryka, M., Wolska, L., & Namieśnik, J. (2009). Evolution of models for sorption of PAHs and PCBs on geosorbents. TrAC Trends in Analytical Chemistry, 28(4), 466-482. https://doi.org/10.1016/j.trac.2009.01.005

Mendoza, C. A., & Frind, E. O. (1990). Advective-dispersive transport of dense organic vapors in the unsaturated zone: 2. Sensitivity analysis. Water Resources Research, 26(3), 388-398. https://doi.org/10.1029/WR026i003p00388

Meza, J. C. S., Perez, P. A., Salin, M. B., Salazar, V. F. P., & Lapoint, T. (2010). Inhibition of cholinesterase activity by soil extracts and predicted environmental concentrations (PEC) to select relevant pesticides in polluted soils. Journal of Environmental Science and Health Part B, 45(3), 214-221. https://doi.org/10.1080/03601231003613575

Min, J. E., Kim, M., Kim, J. Y., Park, I. S., & Park, J. W. (2010). Leachate modeling for a municipal solid waste landfill for upper expansion. KSCE Journal of Civil Engineering, 14(4), 473-480. https://doi.org/10.1007/s12205-010-0473-1

Ministry of Environmental Protection of P.R. China (MEP), Ministry of Land Resources of People's Republic of China (MLR), 2014. Public report of the National Soil Pollution Survey. MEP, MLR,

Ministry for the Environment, 2019. Factsheets for Estimate 2019/2020 https://www.mfe.govt.nz/sites/default/files/media/About/contaminated-land.pdf

Molins, S., Mayer, K. U., Amos, R. T., & Bekins, B. A. (2010). Vadose zone attenuation of organic compounds at a crude oil spill site—Interactions between biogeochemical reactions and

multicomponent gas transport. Journal of Contaminant Hydrology, 112(1-4), 15-29. https://doi.org/10.1016/j.jconhyd.2009.09.002

Moldrup, P., Olesen, T., Komatsu, T., Schjønning, P., & Rolston, D. E. (2001). Tortuosity, diffusivity, and permeability in the soil liquid and gaseous phases. Soil Science Society of America Journal, 65(3), 613-623. DOI:10.2136/sssaj2001.653613x

Molins, S., Mayer, K. U., Amos, R. T., & Bekins, B. A. (2010). Vadose zone attenuation of organic compounds at a crude oil spill site—Interactions between biogeochemical reactions and multicomponent gas transport. Journal of Contaminant Hydrology, 112(1-4), 15-29. https://doi.org/10.1016/j.jconhyd.2009.09.002

Morbidelli, R., Corradini, C., Saltalippi, C., Flammini, A., Dari, J., & Govindaraju, R. S. (2018). Rainfall infiltration modeling: a review. Water, 10(12), 1873. https://doi.org/10.3390/w10121873

Mulligan, C. N., & Yong, R. N. (2004). Natural attenuation of contaminated soils. Environment international, 30(4), 587-601. https://doi.org/10.1016/j.envint.2003.11.001

Nachtegaal, M., & Sparks, D. L. (2003). Nickel sequestration in a kaolinite-humic acid complex. Environmental science & technology, 37(3), 529-534. https://doi.org/10.1021/es025803w

Nham, H. T. T., Greskowiak, J., Nödler, K., Rahman, M. A., Spachos, T., Rusteberg, B., ... & Licha, T. (2015). Modeling the transport behavior of 16 emerging organic contaminants during soil aquifer treatment. Science of the Total Environment, 514, 450-458. https://doi.org/10.1016/j.scitotenv.2015.01.096

Naidu, R., Bolan, N. S., Megharaj, M., Juhasz, A. L., Gupta, S. K., Clothier, B. E., & Schulin, R. (2008). Chemical bioavailability in terrestrial environments. Developments in soil science, 32, 1-6. https://doi.org/10.1016/S0166-2481(07)32001-1

Naidu, R., & Birke, V. (Eds.). (2014). Permeable reactive barrier: sustainable groundwater remediation (Vol. 1). CRC Press. ISBN : 9781482224474

Nasehi, S. A., Uromeihy, A., Nikudel, M. R., & Morsali, A. (2016). Influence of gas oil contamination on geotechnical properties of fine and coarse-grained soils. Geotechnical and Geological Engineering, 34(1), 333-345. https://doi.org/10.1007/s10706-015-9948-7

Nelson, Y. M., & Jewell, W. J. (1993). Vinyl chloride biodegradation with methanotrophic attached films. Journal of Environmental Engineering, 119(5), 890-907. https://doi.org/10.1061/(ASCE)0733-9372(1993)119:5(890)

Neuman, S. P. (1990). Universal scaling of hydraulic conductivities and dispersivities in geologic media. Water resources research, 26(8), 1749-1758. https://doi.org/10.1029/WR026i008p01749

Nezhad, M. M., Rezania, M., & Baioni, E. (2019). Transport in porous media with nonlinear flow condition. Transport in Porous Media, 126(1), 5-22. https://doi.org/10.1007/s11242-018-1173-4

Nimmo, J. R. (2006). Unsaturated zone flow processes. Encyclopedia of hydrological sciences. https://doi.org/10.1002/0470848944.hsa161

Nimmo, J. R. (2009). Vadose water. In Biogeochemistry of inland waters. Academic Press. ISBN 0123819970

Nofziger, D. L., Williams, J. R., & Short, T. E. (1988). Interactive simulation of the fate of hazardous chemicals during land treatment of oily wastes: RITZ user's guide (Vol. 1). Robert S. Kerr Environmental Research Laboratory, Office of Research and Development, US Environmental Protection Agency.

Ogata, A., & Banks, R.B. (1961). A solution of the differential equation of longitudinal dispersion in porous media, US Geol. Surv. Prof. Paper 411-A, Washington, DC.

Ohio, Environmental Protection Agency (EPA). (2007). Ground Water Flow and Fate and Transport Modeling. Division of Drinking and Ground Waters State of Ohio Environmental Protection Agency.

Olsson, Å., & Grathwohl, P. (2007). Transverse dispersion of non-reactive tracers in porous media: a new nonlinear relationship to predict dispersion coefficients. Journal of contaminant hydrology, 92(3-4), 149-161. https://doi.org/10.1016/j.jconhyd.2006.09.008

Ouhadi, V. R., Yong, R. N., & Sedighi, M. (2006). Influence of heavy metal contaminants at variable pH regimes on rheological behaviour of bentonite. Applied Clay Science, 32(3-4), 217-231. https://doi.org/10.1016/j.clay.2006.02.003

Paladino, O., Moranda, A., Massabò, M., & Robbins, G. A. (2018). Analytical Solutions of Three-Dimensional Contaminant Transport Models with Exponential Source Decay. Groundwater, 56(1), 96-108. https://doi.org/10.1111/gwat.12564

Panagos, P., Van Liedekerke, M., Yigini, Y., & Montanarella, L. (2013). Contaminated sites in Europe: review of the current situation based on data collected through a European network. Journal of Environmental and Public Health, 2013. https://doi.org/10.1155/2013/158764

Pankow, J. F., & Cherry, J. A. (1996). Dense chlorinated solvents and other DNAPLs in groundwater: History, behavior, and remediation. ISBN-13: 978-0964801417

Pérez, A. P., & Eugenio, N. R. (2018). Status of Local Soil Contamination in Europe: Revision of the Indicator “Progress in the Management Contaminated Sites in Europe”. EUR 29124 EN, Publications Office of the European Union. Luxembourg 978-92-79-80072-6 https://doi.org/10.2760/093804

Perkins, T. K., & Johnston, O. C. (1963). A review of diffusion and dispersion in porous media. Society of Petroleum Engineers Journal, 3(01), 70-84. https://doi.org/10.2118/480-PA

Pepper, I. L., & Brusseau, M. L. (2019). Physical-chemical characteristics of soils and the subsurface. In Environmental and Pollution Science (pp. 9-22). Academic Press. https://doi.org/10.1016/B978-0-12-814719-1.00002-1

Peterson, D. M., Singletary, M. A., Studer, J. E., & Miller, D. R. (2000). Natural attenuation assessment of multiple VOCs in a deep vadose zone (No. SAND--2000-0600C). Sandia National Labs..

Plant, R., Wilmot, K. and Ege, C. (2014) Contaminated Soil Wastes in Australia. [Prepared for the Australian Department of the Environment]. Institute for Sustainable Futures, University of Technology, Sydney.

Polichetti, G., Cocco, S., Spinali, A., Trimarco, V., & Nunziata, A. (2009). Effects of particulate matter (PM10, PM2. 5 and PM1) on the cardiovascular system. Toxicology, 261(1-2), 1-8. https://doi.org/10.1016/j.tox.2009.04.035

Pop, I. S. (2002). Error estimates for a time discretization method for the Richards' equation. Computational geosciences, 6(2), 141-160. https://doi.org/10.1023/A:1019936917350

Pratt, D. L., & Fonstad, T. A. (2017). Geochemical modelling of livestock mortality leachate transport through the subsurface. Biosystems Engineering, 162, 67-80. https://doi.org/10.1016/j.biosystemseng.2017.08.002

Qafoku, N. P., Ainsworth, C. C., Szecsody, J. E., & Qafoku, O. S. (2004). Transport-controlled kinetics of dissolution and precipitation in the sediments under alkaline and saline conditions. Geochimica et Cosmochimica Acta, 68(14), 2981-2995. https://doi.org/10.1016/j.gca.2003.12.017

Ramírez-García, R., Gohil, N., & Singh, V. (2019). Recent advances, challenges, and opportunities in bioremediation of hazardous materials. In Phytomanagement of Polluted Sites (pp. 517-568). Elsevier. https://doi.org/10.1016/B978-0-12-813912-7.00021-1

Ravi, V., & Johnson, J. A. (1993) Pesticide Analytical Model Version 4.0.

Redlich, O. J. D. L., & Peterson, D. L. (1959). A useful adsorption isotherm. Journal of Physical Chemistry, 63(6), 1024-1024. https://doi.org/10.1021/j150576a611

Ren, X., Zeng, G., Tang, L., Wang, J., Wan, J., Liu, Y., ... & Deng, R. (2018). Sorption, transport and biodegradation–an insight into bioavailability of persistent organic pollutants in soil. Science of the total environment, 610, 1154-1163. https://doi.org/10.1016/j.scitotenv.2017.08.089

Richards, L.A., 1931. Capillary conduction of liquids through porous mediums. Physics 1, 318–333. https://doi.org/10.1063/1.1745010

Richards, B. (1967). Moisture flow and equilibria in unsaturated soils for shallow foundations. In Permeability and Capillarity of Soils. ASTM International. DOI: 10.1520/STP47257S

Rivett, M. O., Wealthall, G. P., Dearden, R. A., & McAlary, T. A. (2011). Review of unsaturated-zone transport and attenuation of volatile organic compound (VOC) plumes leached from shallow source zones. Journal of contaminant hydrology, 123(3-4), 130-156. https://doi.org/10.1016/j.jconhyd.2010.12.013

Roels, S., Carmeliet, J., & Hens, H. (2003). Modelling unsaturated moisture transport in heterogeneous limestone. Transport in porous media, 52(3), 333-350.

Roque, A. J., & Didier, G. (2006). Calculating hydraulic conductivity of fine-grained soils to leachates using linear expressions. Engineering geology, 85(1-2), 147-157. https://doi.org/10.1016/j.enggeo.2005.09.034

Sagar, B. (1982). Dispersion in three dimensions: approximate analytic solutions. Journal of the Hydraulics Division, 108(1), 47-62.

Sander, T., & Gerke, H. H. (2007). Preferential flow patterns in paddy fields using a dye tracer. Vadose Zone Journal, 6(1), 105-115. doi:10.2136/vzj2006.0035

Scanlon, B. R., Tyler, S. W., & Wierenga, P. J. (1997). Hydrologic issues in arid, unsaturated systems and implications for contaminant transport. Reviews of Geophysics, 35(4), 461-490. https://doi.org/10.1029/97RG01172

Schaider, L. A., Rudel, R. A., Ackerman, J. M., Dunagan, S. C., & Brody, J. G. (2014). Pharmaceuticals, perfluorosurfactants, and other organic wastewater compounds in public drinking water wells in a

shallow sand and gravel aquifer. Science of the Total Environment, 468, 384-393. https://doi.org/10.1016/j.scitotenv.2013.08.067

Shao, Y., Wang, Y., Xu, X., Wu, X., Jiang, Z., He, S., & Qian, K. (2014). Occurrence and source apportionment of PAHs in highly vulnerable karst system. Science of the Total Environment, 490, 153-160. https://doi.org/10.1016/j.scitotenv.2014.04.128

Schiefler, A. A., Tobler, D. J., Overheu, N. D., & Tuxen, N. (2018). Extent of natural attenuation of chlorinated ethenes at a contaminated site in Denmark. Energy Procedia, 146, 188-193. https://doi.org/10.1016/j.egypro.2018.07.024

Schwab, A. P., Splichal, P. A., & Banks, M. K. (2006). Persistence of atrazine and alachlor in ground water aquifers and soil. Water, Air, & Soil Pollution, 171(1-4), 203-235. https://doi.org/10.1007/s11270-005-9037-2

Schwarzenbach, R. P., Gschwend, P. M., & Imboden, D. M. (2016). Environmental organic chemistry. John Wiley & Sons. ISBN 1118767233

Sen, T. K., & Khilar, K. C. (2006). Review on subsurface colloids and colloid-associated contaminant transport in saturated porous media. Advances in colloid and interface science, 119(2-3), 71-96. https://doi.org/10.1016/j.cis.2005.09.001

Selim, H. M. (Ed.). (2012). Competitive sorption and transport of heavy metals in soils and geological media. CRC Press. ISBN 143988014X

Shan, C., & Stephens, D. B. (1995). An analytical solution for vertical transport of volatile chemicals in the vadose zone. Journal of contaminant hydrology, 18(4), 259-277. https://doi.org/10.1016/0169-7722(95)00011-J

Sherene, T. (2010). Mobility and transport of heavy metals in polluted soil environment. In Biological Forum—An International Journal (Vol. 2, No. 2, pp. 112-121). ISSN 0975-1130

Shenker, M., Seitelbach, S., Brand, S., Haim, A., & Litaor, M. I. (2005). Redox reactions and phosphorus release in re-flooded soils of an altered wetland. European Journal of Soil Science, 56(4), 515-525. https://doi.org/10.1111/j.1365-2389.2004.00692.x

Shukla, A. K., Upadhyay, S. N., & Dubey, S. K. (2014). Current trends in trichloroethylene biodegradation: a review. Critical reviews in biotechnology, 34(2), 101-114. https://doi.org/10.3109/07388551.2012.727080

Singh, R., Gautam, N., Mishra, A., & Gupta, R. (2011). Heavy metals and living systems: An overview. Indian journal of pharmacology, 43(3), 246. doi: 10.4103/0253-7613.81505

Šimůnek, J., & van Genuchten, M. T. (2016). Contaminant transport in the unsaturated zone: Theory and modeling. In The Handbook of Groundwater Engineering, Third Edition (pp. 221-254). CRC Press. ISBN: 9781498703055

Sipos, P., Németh, T., Kis, V. K., & Mohai, I. (2008). Sorption of copper, zinc and lead on soil mineral phases. Chemosphere, 73(4), 461-469. https://doi.org/10.1016/j.chemosphere.2008.06.046

Sipos, P., Kis, V. K., Balázs, R., Tóth, A., Kovács, I., & Németh, T. (2018). Contribution of individual pure or mixed-phase mineral particles to metal sorption in soils. Geoderma, 324, 1-8. https://doi.org/10.1016/j.geoderma.2018.03.008

Sips, R. (1948). On the structure of a catalyst surface. The Journal of Chemical Physics, 16(5), 490-495. https://doi.org/10.1063/1.1746922

Smiles, D. E., Perroux, K. M., Zegelin, S. J., & Raats, P. A. C. (1981). Hydrodynamic Dispersion During Constant Rate Absorption of Water by Soil 1. Soil Science Society of America Journal, 45(3), 453-458. doi:10.2136/sssaj1981.03615995004500030001x

Sollecito, F., Vitone, C., Miccoli, D., Plötze, M., Puzrin, A. M., & Cotecchia, F. (2019). Marine Sediments from a Contaminated Site: Geotechnical Properties and Chemo-Mechanical Coupling Processes. Geosciences, 9(8), 333. https://doi.org/10.3390/geosciences9080333

Song, X. Y., Li, H. Y., & Shi, W. J. (2013). The Development of a One-Parameter Model for the Soil-Water Characteristic Curve in Loess Gully Regions. In Applied Mechanics and Materials (Vol. 256, pp. 488-493). Trans Tech Publications Ltd. https://doi.org/10.4028/www.scientific.net/AMM.256-259.488

Song, X., & Borja, R. I. (2014). Mathematical framework for unsaturated flow in the finite deformation range. International Journal for Numerical Methods in Engineering, 97(9), 658-682. https://doi.org/10.1002/nme.4605

Soule, N. M., & Burns, S. E. (2001). Effects of organic cation structure on behavior of organobentonites. Journal of Geotechnical and Geoenvironmental Engineering, 127(4), 363-370. https://doi.org/10.1061/(ASCE)1090-0241(2001)127:4(363)

Søvik, A. K., Alfnes, E., Breedveld, G. D., French, H. K., Pedersen, T. S., & Aagaard, P. (2002). Transport and degradation of toluene and o-xylene in an unsaturated soil with dipping sedimentary layers. Journal of environmental quality, 31(6), 1809-1823. doi:10.2134/jeq2002.1809

Spence, L. R., & Walden, T. (2001). RISC4 User's Manual. Pleasanton, California: Spence Engineering and Sunbury: BP Oil International.

Stefanakis, A. I., & Becker, J. A. (2016). A review of emerging contaminants in water: classification, sources, and potential risks. In Impact of Water Pollution on Human Health and Environmental Sustainability (pp. 55-80). IGI Global. DOI: 10.4018/978-1-4666-9559-7.ch003

Stenger, R., Priesack, E., & Beese, F. (2002). Spatial variation of nitrate–N and related soil properties at the plot-scale. Geoderma, 105(3-4), 259-275. https://doi.org/10.1016/S0016-7061(01)00107-0

Stoppiello, M.G.; Lofrano, G.; Carotenuto, M.; Viccione, G.; Guarnaccia, C.; Cascini, L. (2020). A Comparative Assessment of Analytical Fate and Transport Models of Organic Contaminants in Unsaturated Soils. Sustainability 2020, 12, 2949 https://doi.org/10.3390/su12072949

Suter II, G. W., Efroymson, R. A., Sample, B. E., & Jones, D. S. (2000). Ecological risk assessment for contaminated sites. CRC Press. https://doi.org/10.1201/9780367802707

Sunil, B. M., Nayak, S., & Shrihari, S. (2006). Effect of pH on the geotechnical properties of laterite. Engineering geology, 85(1-2), 197-203. https://doi.org/10.1016/j.enggeo.2005.09.039

Swift, R. S., & McLaren, R. G. (1991). Micronutrient adsorption by soils and soil colloids. In Interactions at the soil colloid—soil solution interface (pp. 257-292). Springer, Dordrecht. https://doi.org/10.1007/978-94-017-1909-4_9

Tardiff, M. F., & Katzman, D. (2007). Estimating contaminant attenuation half-lives in alluvial groundwater systems. Journal of Environmental Monitoring, 9(3), 266-274. https://doi.org/10.1039/B700494J

Tempkin, M. I., & Pyzhev, V. (1940). Kinetics of ammonia synthesis on promoted iron catalyst. Acta Phys. Chim. USSR, 12(1), 327.

Thomé, A., Reginatto, C., Vanzetto, G., & Braun, A. B. (2018, October). Remediation Technologies Applied in Polluted Soils: New Perspectives in This Field. In The International Congress on Environmental Geotechnics (pp. 186-203). Springer, Singapore. ISBN 978-981-13-2221-1

Thomsen, N. I., Binning, P. J., McKnight, U. S., Tuxen, N., Bjerg, P. L., & Troldborg, M. (2016). A Bayesian belief network approach for assessing uncertainty in conceptual site models at contaminated sites. Journal of contaminant hydrology, 188, 12-28. https://doi.org/10.1016/j.jconhyd.2016.02.003

Tiktak, A., van der Linden, A. M., & van der Pas, L. J. (1998). Application of the pesticide transport assessment model to a field study in a humic sandy soil in Vredepeel, The Netherlands. Pesticide science, 52(4), 321-336. https://doi.org/10.1002/(SICI)1096-9063(199804)52:4<321::AID-PS734>3.0.CO;2-T

Toride, N., Leij, F. J., & van Genuchten, M. T. (1993). A comprehensive set of analytical solutions for nonequilibrium solute transport with first-order decay and zero-order production. Water Resources Research, 29(7), 2167-2182. https://doi.org/10.1029/93WR00496

Toth, J. (1971). State equation of the solid-gas interface layers. Acta chim. hung., 69, 311-328.

Troldborg, M., Binning, P. J., Nielsen, S., Kjeldsen, P., & Christensen, A. G. (2009). Unsaturated zone leaching models for assessing risk to groundwater of contaminated sites. Journal of contaminant hydrology, 105(1-2), 28-37. https://doi.org/10.1016/j.jconhyd.2008.11.002

Troldborg, M., Lemming, G., Binning, P. J., Tuxen, N., & Bjerg, P. L. (2008). Risk assessment and prioritisation of contaminated sites on the catchment scale. Journal of Contaminant Hydrology, 101(1-4), 14-28. https://doi.org/10.1016/j.jconhyd.2008.07.006

Troldborg, M. (2010). Risk assessment models and uncertainty estimation of groundwater contamination from point sources. PhD Thesis

Tsanis, I. K. (2006). Modeling leachate contamination and remediation of groundwater at a landfill site. Water resources management, 20(1), 109-132. https://doi.org/10.1007/s11269-006-4634-4

Tufenkji, N. (2007). Modeling microbial transport in porous media: Traditional approaches and recent developments. Advances in water resources, 30(6-7), 1455-1469. https://doi.org/10.1016/j.advwatres.2006.05.014

Uddin, M. K. (2017). A review on the adsorption of heavy metals by clay minerals, with special focus on the past decade. Chemical Engineering Journal, 308, 438-462. https://doi.org/10.1016/j.cej.2016.09.029

Ünlü, K., Kemblowski, M. W., Parker, J. C., Stevens, D., Chong, P. K., & Kamil, I. (1992). A screening model for effects of land-disposed wastes on groundwater quality. Journal of contaminant hydrology, 11(1-2), 27-49. https://doi.org/10.1016/0169-7722(92)90032-A

USEPA, 1996. Soil screening guidance technical background document, office of solid waste and emergency response, s.l.: s.n.

US Environmental Protection Agency (USEPA), 2004. Cleaning up the Nation's Waste Sites: Markets and Technology Trends, 2004 Edition. Technology Innovation office, Cincinnati. https://nepis.epa.gov/Exe/ZyPURL.cgi?Dockey=30006II3.txt

Vanclooster, M., Javaux, M., & Vanderborght, J. (2006). Solute transport in soil at the core and field scale. Encyclopedia of hydrological sciences. https://doi.org/10.1002/0470848944.hsa073

Vanderborght, J., Kasteel, R., Herbst, M., Javaux, M., Thiéry, D., Vanclooster, M., Mouvet, C. & Vereecken, H. (2005). A set of analytical benchmarks to test numerical models of flow and transport in soils. Vadose Zone Journal, 4(1), 206-221. doi:10.2136/vzj2005.0206

Vanderborght, J., Kasteel, R., & Vereecken, H. (2006). Stochastic continuum transport equations for field-scale solute transport. Vadose Zone Journal, 5(1), 184-203. doi:10.2136/vzj2005.0024

Vanderborght, J., & Vereecken, H. (2007). Review of dispersivities for transport modeling in soils. Vadose Zone Journal, 6(1), 29-52. doi:10.2136/vzj2006.0096

Van Genuchten, M. T. (1980). A closed-form equation for predicting the hydraulic conductivity of unsaturated soils 1. Soil science society of America journal, 44(5), 892-898. doi:10.2136/sssaj1980.03615995004400050002x

Van Genuchten, M. T. (1981). Analytical solutions for chemical transport with simultaneous adsorption, zero-order production and first-order decay. Journal of hydrology, 49(3-4), 213-233. https://doi.org/10.1016/0022-1694(81)90214-6

Venkateshan, S. P., & Swaminathan, P. (2013). Computational methods in engineering. Elsevier. ISBN 0124167039

Verginelli, I., & Baciocchi, R. (2013). Role of natural attenuation in modeling the leaching of contaminants in the risk analysis framework. Journal of environmental management, 114, 395-403. https://doi.org/10.1016/j.jenvman.2012.10.035

Vijayaraghavan, K., Padmesh, T. V. N., Palanivelu, K., & Velan, M. (2006). Biosorption of nickel (II) ions onto Sargassum wightii: application of two-parameter and three-parameter isotherm models. Journal of hazardous materials, 133(1-3), 304-308. https://doi.org/10.1016/j.jhazmat.2005.10.016

Violante, A., Cozzolino, V., Perelomov, L., Caporale, A. G., & Pigna, M. (2010). Mobility and bioavailability of heavy metals and metalloids in soil environments. Journal of soil science and plant nutrition, 10(3), 268-292. http://dx.doi.org/10.4067/S0718-95162010000100005

Vitone, C., Federico, A., Puzrin, A. M., Ploetze, M., Carrassi, E., & Todaro, F. (2016). On the geotechnical characterisation of the polluted submarine sediments from Taranto. Environmental Science and Pollution Research, 23(13), 12535-12553. https://doi.org/10.1007/s11356-016-6317-x

Vogel, T. M., Criddle, C. S., & McCarty, P. L. (1987). ES&T critical reviews: transformations of halogenated aliphatic compounds. Environmental science & technology, 21(8), 722-736. https://doi.org/10.1021/es00162a001

Vorhees, D. J., Weisman, W. H., & Gustafson, J. B. (1999). Total Petroleum Hydrocarbon Criteria Working Group Series. Volume 5: Human health risk-based evaluation of petroleum release sites: Implementing the Working Group Approach. ISBN 1884940129

Voss, C. I. (1984). A finite-element simulation model for saturated-unsaturated, fluid-density-dependent ground-water flow with energy transport or chemically-reactive single-species solute transport. Water Resources Investigation Report, 84, 4369.

Voss, C. I., & Provost, A. M. (2002). SUTRA: A model for 2D or 3D saturated-unsaturated, variable-density ground-water flow with solute or energy transport (No. 2002-4231). https://doi.org/10.3133/wri024231

Wang, Q., & Kelly, B. C. (2018). Assessing bioaccumulation behaviour of hydrophobic organic contaminants in a tropical urban catchment. Journal of hazardous materials, 358, 366-375. https://doi.org/10.1016/j.jhazmat.2018.06.070

Washington, J. W. (1995). Hydrolysis rates of dissolved volatile organic compounds: principles, temperature effects and literature review. Groundwater, 33(3), 415-424. https://doi.org/10.1111/j.1745-6584.1995.tb00298.x

Wauchope, R. D., Yeh, S., Linders, J. B. H. J., Kloskowski, R., Tanaka, K., Rubin, B., ... & Unsworth, J. B. (2002). Pesticide soil sorption parameters: theory, measurement, uses, limitations and reliability. Pest management science, 58(5), 419-445. https://doi.org/10.1002/ps.489

Weaver, J. W., Lien, B. K., Charbeneau, R. J., Tauxe, J. D., & Provost, J. B. (1994). Hydrocarbon Spill Screening Model (HSSM). Volume 1. User's guide. Research report (No. PB-94-189487/XAB; EPA--600/R-94/039A). Environmental Protection Agency, Ada, OK (United States). Robert S. Kerr Environmental Research Lab..

Weaver, J. W., & Charbeneau, R. J. (2001). Screening approach to simulation of aquifer contamination by fuel hydrocarbons(BTEX and MTBE). MAN REP ENG PRACT ASCE,, (100), 41-78. https://doi.org/10.1061/9780784405277

Weber Jr, W. J., McGinley, P. M., & Katz, L. E. (1991). Sorption phenomena in subsurface systems: concepts, models and effects on contaminant fate and transport. Water Research, 25(5), 499-528. https://doi.org/10.1016/0043-1354(91)90125-A

Wen, B., Zhang, J. J., Zhang, S. Z., Shan, X. Q., Khan, S. U., & Xing, B. (2007). Phenanthrene sorption to soil humic acid and different humin fractions. Environmental science & technology, 41(9), 3165-3171. https://doi.org/10.1021/es062262s

Wexler, E. J. (1989). Analytical solutions for one-, two-, and three-dimensional solute transport in ground-water systems with uniform flow (No. 89-56). US Geological Survey. https://doi.org/10.3133/ofr8956

Wexler, E. J. (1992). Analytical solutions for one-, two-, and three-dimensional solute transport in ground-water systems with uniform flow. US Government Printing Office. ISSN 0565-596X

Withers, P. J., Jordan, P., May, L., Jarvie, H. P., & Deal, N. E. (2014). Do septic tank systems pose a hidden threat to water quality?. Frontiers in Ecology and the Environment, 12(2), 123-130. https://doi.org/10.1890/130131

Wilson, J. L., & Gelhar, L. W. (1981). Analysis of longitudinal dispersion in unsaturated flow: 1. The analytical method. Water Resources Research, 17(1), 122-130. https://doi.org/10.1029/WR017i001p00122

Wilson, L. G., Everett, L. G., & Cullen, S. J. (2018). Handbook of vadose zone characterization & monitoring. Routledge. ISBN 1351441949

Wissmeier, L., & Barry, D. A. (2011). Simulation tool for variably saturated flow with comprehensive geochemical reactions in two-and three-dimensional domains. Environmental Modelling & Software, 26(2), 210-218. https://doi.org/10.1016/j.envsoft.2010.07.005

Wu, Y. S. (2015). Multiphase fluid flow in porous and fractured reservoirs. Gulf Professional Publishing. ISBN 0128039116

Yaghi, N., & Hartikainen, H. (2013). Enhancement of phosphorus sorption onto light expanded clay aggregates by means of aluminum and iron oxide coatings. Chemosphere, 93(9), 1879-1886. https://doi.org/10.1016/j.chemosphere.2013.06.059

Yan, J. M., Vairavamoorthy, K., & Gorantiwar, S. D. (2006). Contaminant transport model for unsaturated soil using fuzzy approach. Journal of Environmental Engineering, 132(11), 1489-1497. https://doi.org/10.1061/(ASCE)0733-9372(2006)132:11(1489)

Yang, J. C., & Hsu, E. L. (1990). Time-line interpolation for solution of the dispersion equation. Journal of Hydraulic Research, 28(4), 503-520 https://doi.org/10.1080/00221689009499063

Yaron, B., Calvet, R., Prost, R., & Prost, R. (1996). Soil pollution: processes and dynamics. Springer Science & Business Media. ISBN 354060927X

Yaron, B., Dror, I., & Berkowitz, B. (2008). Contaminant-induced irreversible changes in properties of the soil–vadose–aquifer zone: an overview. Chemosphere, 71(8), 1409-1421. https://doi.org/10.1016/j.chemosphere.2007.11.045

Yaron, B., Dror, I., & Berkowitz, B. (2010). Contaminant geochemistry—a new perspective. Naturwissenschaften, 97(1), 1-17. https://doi.org/10.1007/s00114-009-0592-z

Yeh, G. T. (1981). AT123D: Analytical transient one-, two-, and three-dimensional simulation of waste transport in the aquifer system (No. ORNL-5602). Oak Ridge National Lab., TN (USA). DOI: 10.2172/6531241

Ye, J., Chen, X., Chen, C., & Bate, B. (2019). Emerging sustainable technologies for remediation of soils and groundwater in a municipal solid waste landfill site--A review. Chemosphere, 227, 681-702. https://doi.org/10.1016/j.chemosphere.2019.04.053

Yuan, G. D., Theng, B. K. G., Churchman, G. J., & Gates, W. P. (2013). Clays and clay minerals for pollution control. In Developments in clay science (Vol. 5, pp. 587-644). Elsevier. https://doi.org/10.1016/B978-0-08-098259-5.00021-4

Zamani, K., & Bombardelli, F. A. (2014). Analytical solutions of nonlinear and variable-parameter transport equations for verification of numerical solvers. Environmental Fluid Mechanics, 14(4), 711-742. https://doi.org/10.1007/s10652-013-9325-0

Zentner, E., Gerstl, Z., Weisbrod, N., Lev, O., Pankratov, I., Russo, D., ... & Ronen, D. (2015). Deep penetration of pharmaceuticals and personal care products through the vadose zone of effluent-irrigated land. Vadose Zone Journal, 14(1). https://doi.org/10.2136/vzj2014.09.0115

Zhang, D. (2001). Stochastic methods for flow in porous media: coping with uncertainties. Elsevier. https://doi.org/10.1016/B978-012779621-5/50006-1

Zhang, Z. F., Ward, A. L., & Gee, G. W. (2003). A tensorial connectivity–tortuosity concept to describe the unsaturated hydraulic properties of anisotropic soils. Vadose Zone Journal, 2(3), 313-321. doi:10.2136/vzj2003.3130

Zuffianò, L. E., Basso, A., Casarano, D., Dragone, V., Limoni, P. P., Romanazzi, A., Santaloia, F. & Polemio, M. (2016). Coastal hydrogeological system of mar Piccolo (Taranto, Italy). Environmental Science and Pollution Research, 23(13), 12502-12514. https://doi.org/10.1007/s11356-015-4932-6